

Design optimisation and commissioning of the Delft rotating heat pipe setup

Stefan van Leeuwen

Technische universiteit Delft

Design optimisation and commissioning of the Delft Rotating Heat Pipe Setup

For the

Heat pipe Assisted Annealing Project

By

S.J.M. van Leeuwen

in partial fulfilment of the requirements for the degree of

Master of Science
in Mechanical Engineering

at the Delft University of Technology,
to be defended publicly on Thursday April 12, 2018 at 15:00.

Student number:	4215877	
P&E report number:	P&E-2891	
Thesis committee:	Prof. dr. ir. W. de Jong,	TU Delft, supervisor
	Prof.dr.ir. B.J. Boersma,	TU Delft
	Dr. ir C.A. Infante Ferreira,	TU Delft
	Ir. M. Celik,	TU Delft, daily supervisor
	BSc. G. Paulussen,	Tata Steel

This thesis is confidential and cannot be made public until April 12, 2021.

An electronic version of this thesis is available at <http://repository.tudelft.nl/>.

Abstract

The heat pipe assisted annealing project is a project in which Tata Steel, TU Delft and Drever International work together to develop a continuous annealing line with heat pipes. In an annealing line cold rolled steel is heated to 973 K and cooled down again to change the properties of the steel. In the heat pipe assisted annealing project the cooling line is thermally connected to the heating line via heat pipes. A heat pipe is a closed cylinder which is partly filled with a liquid. Heat pipes are very effective heat transfer devices, due to evaporation of the liquid at one side of the heat pipe and condensation of the vapour at the other side of the heat pipe. Due to rotation and a head, liquid will return to the evaporator side of the heat pipe. Applying heat pipes in a continuous annealing line could lead to energy savings up to 70%.

The TU Delft rotating heat pipe setup is in development for testing the performance of organic working fluids in heat pipes and validation of models, for the temperature range from 423 K to 723 K. The goal of this thesis is described as: finishing the development of the TU Delft rotating heat pipe setup and use this test setup to validate the developed model. This goal was divided into several objectives.

An investigation was made of what has to be done before the commissioning of the setup. It was discovered that the heat input calculation is overestimated, because insulation is not taken into account. Therefore, a new calculation was made. It is concluded that in the worst case scenario 1155 W of heat input is needed. Also, the available band heaters could not be used, therefore IR heating with quartz lamps has been considered. A calculation was made to confirm if they will provide enough power to meet the requirements of the setup. It is concluded that six quartz lamps with an effective heating length of 165 mm will provide enough power. In the fill ratio calculation, it is learned that non-annular flow is beneficial for the heat transfer compared to annular flow. Also, it was decided to fill the heat pipe with 35 grams of Dowtherm A as a start. With this amount of fluid, it is possible to operate the heat in both flow patterns over the whole temperature range. Last, it is concluded that bearing cooling is needed.

Another objective was to select the required data acquisition hardware and program the required software for control and data acquisition. A compactRIO from National Instruments is selected together with several modules. This configuration is able to process all the signals and has extra capacity to handle more signals in the future. A LabVIEW program was designed to control the Delft setup. This program meets all the requirements. It has been tested with dummy signals and during a leakage test with the actual heat pipe.

A model which represents the actual Delft rotating heat pipe setup has been made. The same inputs as in the Delft setup can be adjusted. This model has been developed as a network model. These types of models are often used because of their reasonably accurate and practically simple way to model transient heat pipe analysis. This model was validated with two different papers. In the first paper, an experiment is performed with a stainless steel ammonia heat pipe, which operates in non-annular flow. The data of this paper is only useful for steady state. At the steady state part, the maximum deviation is 0.96 K. In the second paper, a copper-water heat pipe is used. This heat pipe is not rotating, but has a wick. This means its behaviour is similar to a rotating heat pipe with annular flow. The data of this paper is very precise and shown in tabular form at three different points at 4 time stamps. The root-mean-square error between the experiment and the model at all data points is 0.36 K.

The commissioning of the heat pipe is in progress now. When all the safety procedures are checked, the experiments can be conducted.

Preface

This thesis is the final part of my study at the TU Delft. It is written to obtain the degree of Master of Science in Mechanical Engineering. The work conducted during this thesis is part of a collaboration project between TU Delft, Tata Steel and Drever International. My goal during this thesis was to finish the development of the TU Delft rotating heat pipe setup and perform some initial experiments as part of the commissioning of the setup. I hope my work during this thesis will help everybody that will work with the Delft rotating heat pipe setup in the future.

I would like to thank some people who helped me during this thesis. First of all, Metin Celik, my daily supervisor. You helped me a lot during this thesis and you always had time and answers for my questions. I hope my work on the setup will help you a lot for the rest of your PhD. Also, I would like to thank Prof. Wiebren de Jong, who introduced me to this project and gave me very useful feedback on my work. Furthermore, I would like to thank the people from DEMO for their time and assistance during this thesis. Also, I would like to thank Bendiks Jan Boersma, Carlos Infante Ferreira and Geert Paulussen for being part of my graduation committee.

Finally, I would like to thank my friends and family, especially my parents, for their support during my whole education. Many things would not have been possible without you.

*Stefan van Leeuwen
Delft, March 2018*

Contents

1	Introduction.....	1
1.1	Continuous Annealing Line.....	1
1.2	Heat pipe	2
1.3	Heat pipe assisted annealing.....	3
1.4	Existing Tata Steel test setup.....	5
1.5	Problem statement.....	6
1.6	Outline	6
2	Design calculations for Delft Setup	7
2.1	Changes in design	9
2.2	Thermal heat transfer to evaporator section.....	13
2.3	IR Heating	17
2.3.1	Analytical calculation.....	17
2.3.2	Thermal simulations with Solidworks	22
2.4	Thermal heat transfer from condenser section	27
2.5	Flow pattern and fill ratio.....	29
2.6	Slip ring error.....	35
2.7	Bearing cooling.....	37
3	Measurement and control in Delft setup.....	41
3.1	Temperature measurements inside the heat pipe	41
3.2	Data acquisition hardware	41
3.3	LabVIEW	42
4	Model of the Delft setup	45
4.1	Rotating heat pipe model.....	45
4.2	Modelling approach	48
4.3	Literature based validation	52
4.3.1	Rotating ammonia heat pipe.....	52
4.3.2	Non rotating water-copper heat pipe	54
4.3.3	Conclusion	55
5	Commissioning of the Delft setup	57
6	Conclusion	59
6.1	Conclusive summary.....	59
6.2	Recommendations.....	60

6.2.1	Recommendations for the experiment	60
6.2.2	Recommendations for manufacturing a new heat pipe	60
	References.....	61
	List of symbols.....	65
	Appendix A	69
	Required heat input	69
	Appendix B	73
	Radiation calculation	73
	Appendix C.....	75
	Filling amount Dowtherm A	75
	Appendix D	79
	LabVIEW program.....	79
	Appendix E.....	83
	Head calculation	83
	Appendix F.....	84
	Network model.....	84

1 Introduction

The heat pipe assisted annealing project is a project in which Tata Steel, TU Delft and Drever International work together to develop a continuous annealing line. A heat pipe assisted annealing line can reduce the energy consumption significantly compared to a conventional annealing line. This is achieved by the use of rotating heat pipes. The concept of this project has been invented by Tata Steel R&D in 2009 and the research and development has been ongoing since then. In 2011, the concept of using heat pipes in an annealing line has been patented by Tata Steel [1]. After that, a test setup has been built at Tata Steel IJmuiden. Next, the development of a second test setup at TU Delft has started. This test rig will be used to test and validate the models for different working fluids at higher temperatures. Also the performance of organic working fluids will be tested with this setup. The main aim of this project is to finish the development of this second test setup and use this test setup to validate the behaviour with the developed models. The exact description of the aim of this thesis will be described later in the introduction. First, the concept of a continuous annealing line and a rotating heat pipe is given.

1.1 Continuous Annealing Line

In the steel industry there are two types of steel rolling: cold rolling and hot rolling. The rolling process is called hot rolling if the temperature of the steel is above the recrystallization temperature. This means that the grains in the steel can reorganise and there will be less internal stresses in the steel. The steel will thus remain ductile. However, the dimensions of hot rolled steel are less accurate than the dimensions of cold rolled steel [2]. When steel is cold rolled, the temperature of the steel is below the recrystallization temperature. During cold rolling of steel more dislocations are formed. This increases the yield strength of the steel, but also lowers the ductility of the steel. Annealing is a heat treatment that is usually applied after cold rolling of steel to change the mechanical properties of the steel.

An annealing process lets the steel benefit from the advantages of both processes. In an annealing line, cold rolled steel is processed through an oven. In this line the steel is heated up to the recrystallization temperature. At this temperature the grains reorganise and the steel gets the desired properties, in terms of ductility, yield strength and hardness. The properties can be varied by changing the temperature the steel is heated up to and by the time the steel is kept at that temperature. For certain properties, the cooling trajectory is also important [2]. In Figure 1.1, the temperature cycle of the conventional annealing line is shown, which is the reference for this project. This process takes place in an inert atmosphere to protect against oxidation. In a conventional annealing line, the heat is supplied through radiative gas furnaces fuelled by the combustion of natural gas. The cooling of the annealed steel is done with gas jet cooling. At the end of the cooling cycle, cooling water is used.

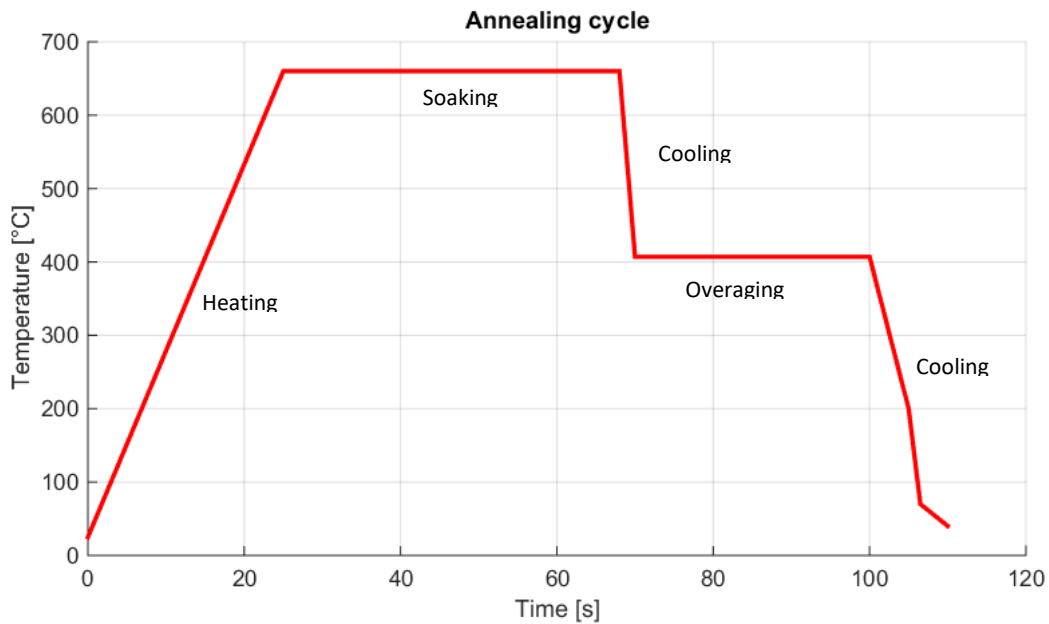


Figure 1.1: Temperature cycle of a conventional annealing line, figure adapted from [7]

1.2 Heat pipe

Although the concept of a heat pipe has been used back in the steam age, Grover was the first one to develop a capillary based heat pipe and patented it in 1963 [3]. In 1969, the rotating heat pipe was described for the first time by Gray [4]. A heat pipe is a heat transfer device that has a very high effective thermal conductivity. This is achieved through a combination of conductivity, phase transition and mass transfer. A heat pipe is basically a hollow pipe or channel, which is partly filled with liquid. A typical heat pipe consists of three sections: an evaporator section, an adiabatic section and a condenser section. At the evaporator, heat is supplied to the heat pipe and the liquid inside the heat pipe evaporates. The vapour flows via the adiabatic section to the condenser, because the temperature is slightly lower in the condenser section. The fluid inside the heat pipe is at saturated condition, so a lower temperature also means a lower pressure. This results in a vapour flow. In the condenser section of the heat pipe, heat is extracted. This causes the vapour in the condenser to condense. The liquid flows back to the evaporator via a wick, a taper or the liquid height difference. In Figure 1.2, a heat pipe is shown and the described process is illustrated. The high latent heat of certain fluids makes it possible to transport very large heat fluxes with a small amount of fluid and a small temperature gradient. The heat pipe is a closed system, so there is no direct contact between the liquid and the heat source. It is commonly used for cooling in space applications and in electronic components like processors, which generate a lot of heat [5].



Figure 1.2: Heat pipe [6]

1.3 Heat pipe assisted annealing

In the heat pipe assisted annealing project the idea is to replace the rolls over which the steel is transported through the oven by heat pipes. The heat pipes should be placed in such a way that heat is extracted from the strip that should be cooled and is used to heat the strip that needs to be heated. Figure 1.3 shows a schematic overview of how such a heat pipe assisted annealing line could be designed. It should be noted that there is a temperature difference between the heating strip and the cooling strip. This means it is always necessary to add conventional heating to reach the desired temperature and cooling to reach the ambient temperature again. Nevertheless, this technology is expected to lead to a 70% energy reduction in natural gas combustion [7].

In Figure 1.4, it can be seen that the heat pipes should cover a temperature range from ambient temperature up to 973 K. The pressure inside the tube may not exceed 5 bar [8], so a fluid can only cover a part of this temperature range. Besides safety, there are more reasons why the pressure inside the heat pipe is limited to 5 bar. At higher temperatures, the decomposition rate of the fluids become too high [8]. Also, the heat pipe will deform at high temperature and pressure after a long time, due to creep [7]. In [8], an investigation for the different fluids that could be used to cover the temperature range has been made. From ambient temperature up to 423 K water will be used. From 423 K to 623 K Biphenyl or Dowtherm A (a eutectic mixture of 26.5% biphenyl and 73.5% diphenyloxide) will be used. Phenanthrene will be used to cover the region from 623 K to 717 K. Unfortunately, there is no data available about the stability of phenanthrene at these temperatures for a long time. Therefore a lifetime test has to be performed to investigate this. For the last part of the temperature range, alkali metals will be used. Cesium or potassium are viable options. A choice has to be made regarding costs and thermodynamic properties.

It should also be noted that there will be much more heat pipes to be used than the six heat pipes shown in Figure 1.3. In reality there will be tens of heat pipes [9]. This can also be seen in Figure 1.4, where a simulation result with 70 heat pipes is shown. The number of heat pipes used in a heat pipe assisted annealing line will be decided after the technical and economic analysis are completed. More heat pipes will rise the capital costs, but will improve the energy savings.

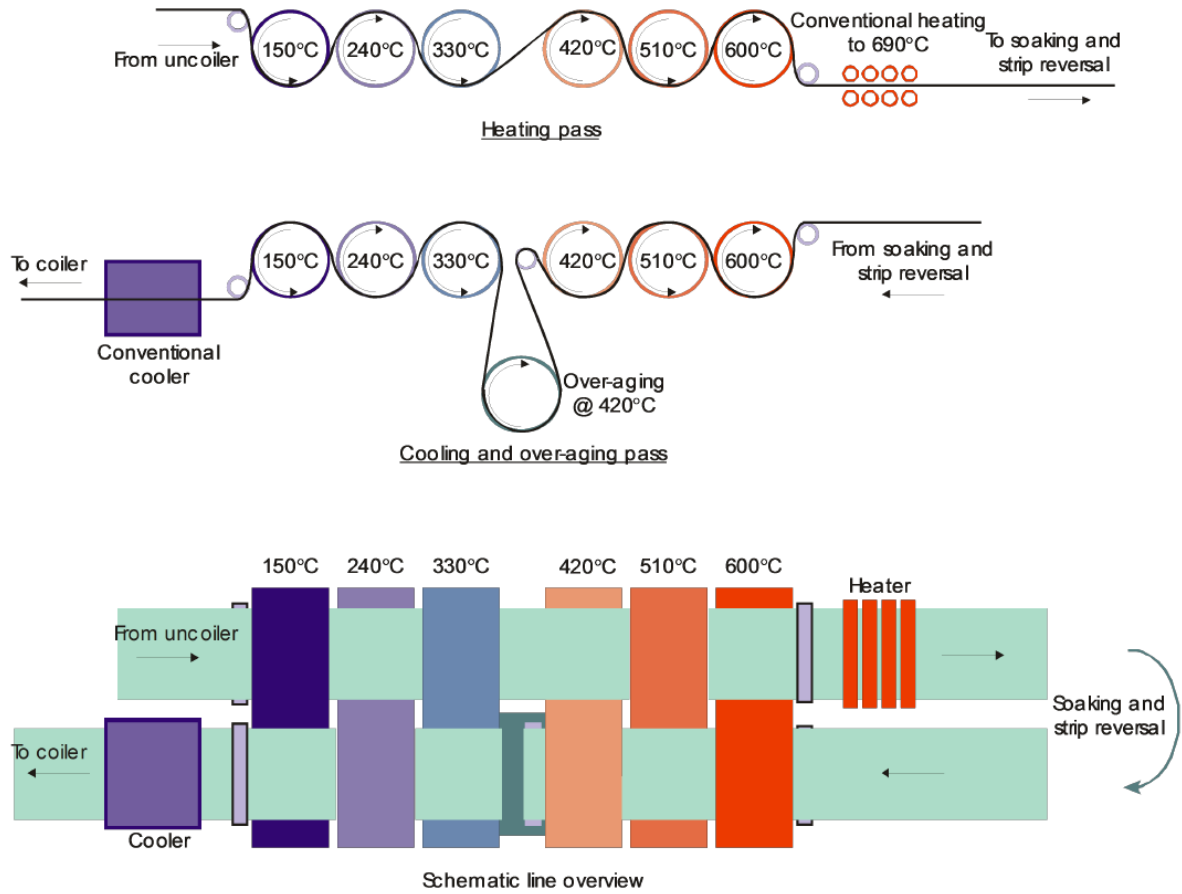


Figure 1.3: Schematic side and top view of a conceptual heat pipe assisted annealing line [7]

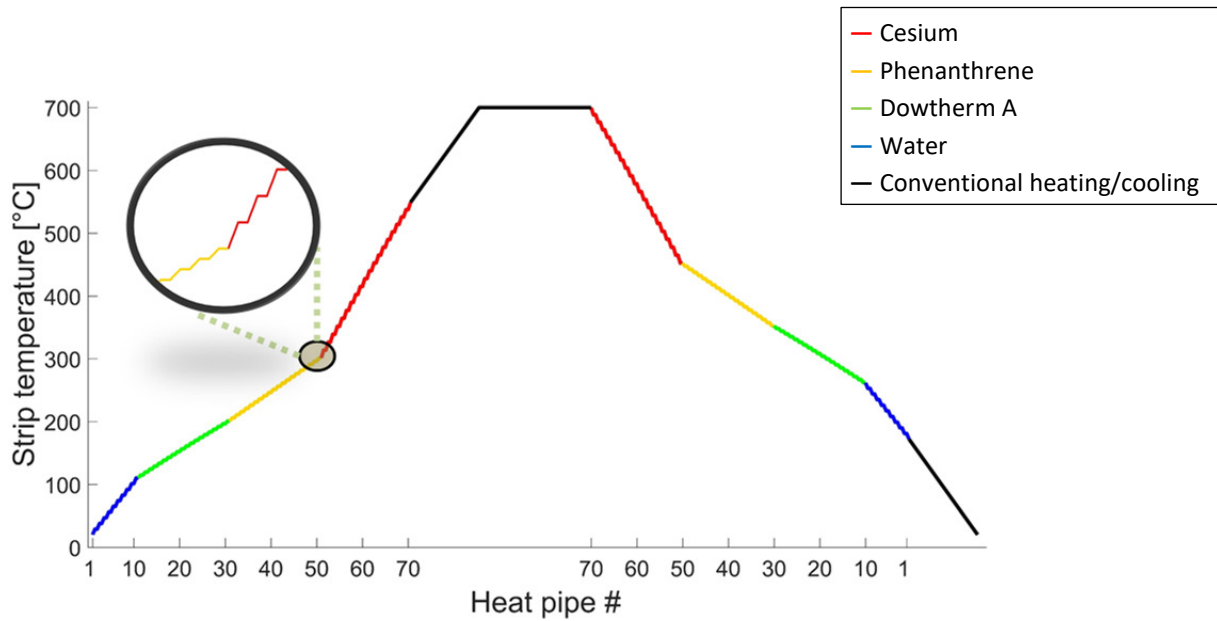


Figure 1.4: Heat pipe assisted annealing line simulation with 70 heat pipes [9]

1.4 Existing Tata Steel test setup

The Tata Steel test setup consists of one large heat pipe filled with water and connected with two strips. A CAD view of the setup can be seen in Figure 1.5. These strips represent the strip that is heated and the strip that is cooled. The strip which is cooled by the heat pipe is at the evaporator side of the heat pipe. This strip is heated by an induction coil, so there is a temperature difference between the strip and the heat pipe. This creates a heat flow and water inside the heat pipe evaporates. The vapour flows to the other side of the heat pipe, where it condenses. The energy is transferred to the other strip, which is the strip that is heating up. This arrangement of the setup represents a small part of the complete annealing line. The temperature of the strip at the condenser side is measured by an infrared camera and the temperature inside the heat pipe is measured at three axial locations by thermocouples. Because water is used as working fluid inside the heat pipe, the temperature range from ambient to 423 K can be covered. Above 423 K the pressure inside the heat pipe becomes too high. This setup has been used to prove the concept and get knowledge about the heat transfer between the strip and the heat pipe [10]. Because this is investigated with the Tata Steel setup, the Delft setup does not have heat transfer via a strip in contact with the heat pipe.

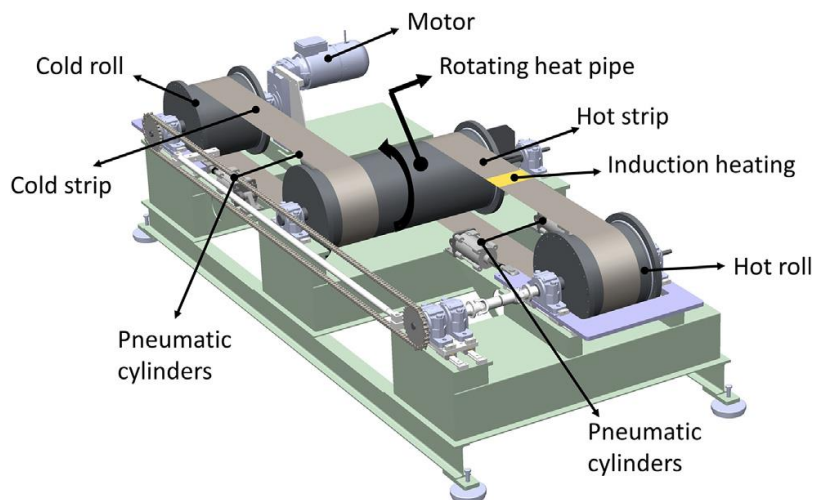


Figure 1.5: Tata Steel setup [10]

The development of a second test setup at TU Delft has started and the initial design is described in [8]. The Delft setup will be used to cover the temperature range of 423 K to 623 K with Dowtherm A as working fluid. After that, a heat pipe filled with phenanthrene can be placed inside the Delft setup to cover the temperature range from 623 K to 723 K. This setup will be used to test and validate the models for Dowtherm A and phenanthrene as working fluids. Also the performance of these working fluids will be tested with this setup.

1.5 Problem statement

As described before, the main goal of this project is to finish the development of the TU Delft rotating heat pipe setup and use this test setup to validate the developed model. The following objectives are described to finish the development of the test setup:

- Analyse and improve the design of the Delft setup compared to the design described in [8].
- Identify what has to be done before the heat pipe can be commissioned.
- Develop solutions for the encountered problems or missing parts.
- Select the required data acquisition hardware and program the required software for control and data acquisition.
- Create or adapt a model which has the same inputs and outputs as the actual setup and validate this model with literature.
- Commission the Delft setup in combination with some initial experiments and use these results for model validation.

After that, the Delft setup will be finished and ready for experiments.

1.6 Outline

In Chapter 2, the changes in the design described in [8] are reported along with the engineering calculations for these design changes and identified potential problems. Chapter 3 contains information regarding the measurements and the hardware and software used to process the measurements. Chapter 4 describes the transient model of the heat pipe and its validation with data from literature. In Chapter 5, the latest status of the commissioning of the Delft setup is described. Chapter 6 contains the conclusions of this thesis and some recommendations.

2 Design calculations for Delft Setup

This chapter gives an overview of the Delft heat pipe setup and the changes compared to the original design described in [8]. Also, several design calculations have been made to make the setup ready for experiments.

The Delft rotating heat pipe setup is a small scale heat pipe, that fits on a table top. The heat pipe has an outer diameter of 60 mm and a wall thickness of 8 mm. The effective working length of the heat pipe is 500 mm. However, the overall length of the heat pipe is longer, because there are end parts connected to the heat pipe for bearing support, motor connection and the electronic connections. An overview of the heat pipe with motor, motor coupling, bearings and slip ring can be seen in Figure 2.1. The space between the bearings is the effective working length of the heat pipe. In this space the heater unit and cooling channel are placed.

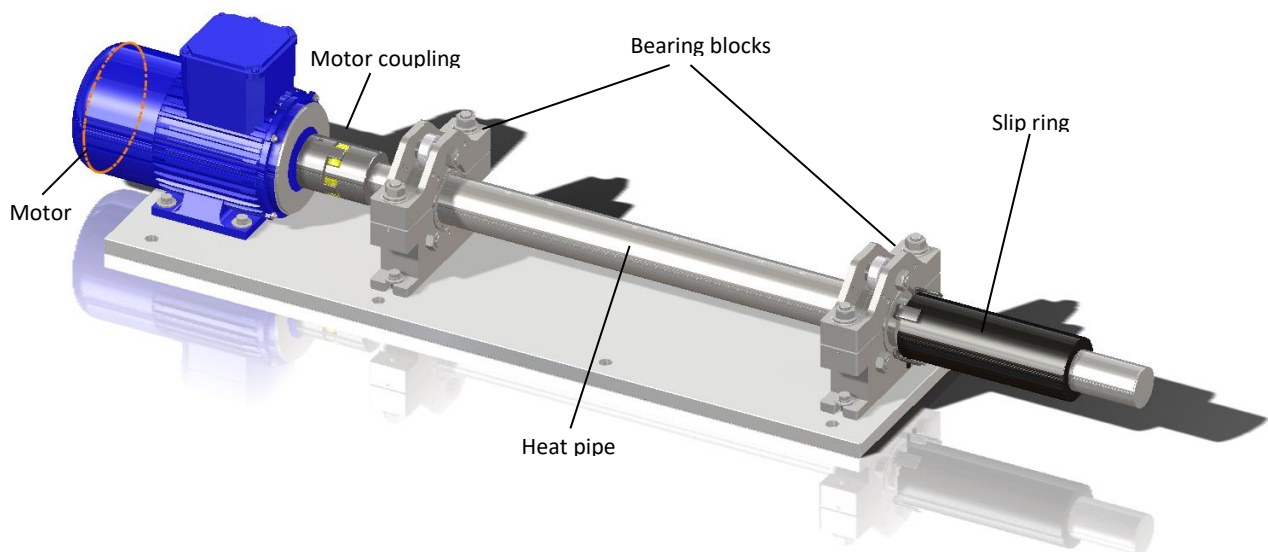


Figure 2.1: Rotating heat pipe with motor, bearings and slip ring

The setup in Figure 2.1 is placed inside a cabinet. This cabinet has been designed to ensure safe operation of the heat pipe. Also, it contains all the required equipment, like the fan for cooling, the heater unit and the electronics. In Figure 2.2 a drawing of the cabinet is shown.

The heat pipe will operate within certain limits. Most of limits have been set in [8], but some of the limits have been set in consultation with DEMO during this thesis. The limits are shown in a tabular form in Table 1. The 5 bar pressure limit is set because of safety, to prevent high decomposition rates of the fluid and deformation of the heat pipe at high temperature due to creep.

First, the heat pipe setup will be used with a heat pipe filled with Dowtherm A. However, in future it should be possible to swap the heat pipe with a different one, which is filled with Phenanthrene. Therefore, different temperature limits occur during this thesis.

The upper temperature limit for Dowtherm A and Phenanthrene shown in Table 1 corresponds to a slightly higher pressure inside the heat pipe than 5 bar. At the lower temperature limit the pressure inside the heat pipe will be 0.05 bar for Dowtherm A and 1.21 bar for Phenanthrene. The transition temperature from Dowtherm A to Phenanthrene could be lowered as well.

Table 1: Limits for Delft rotating heat pipe setup

Variable	Lower limit	Upper limit
Rotational speed [rpm]	150	1000
Pressure [bar]	0	5
Temperature Dowtherm A [K]	423	623
Temperature Phenanthrene [K]	623	723
Heat output at condenser [W]	0	900

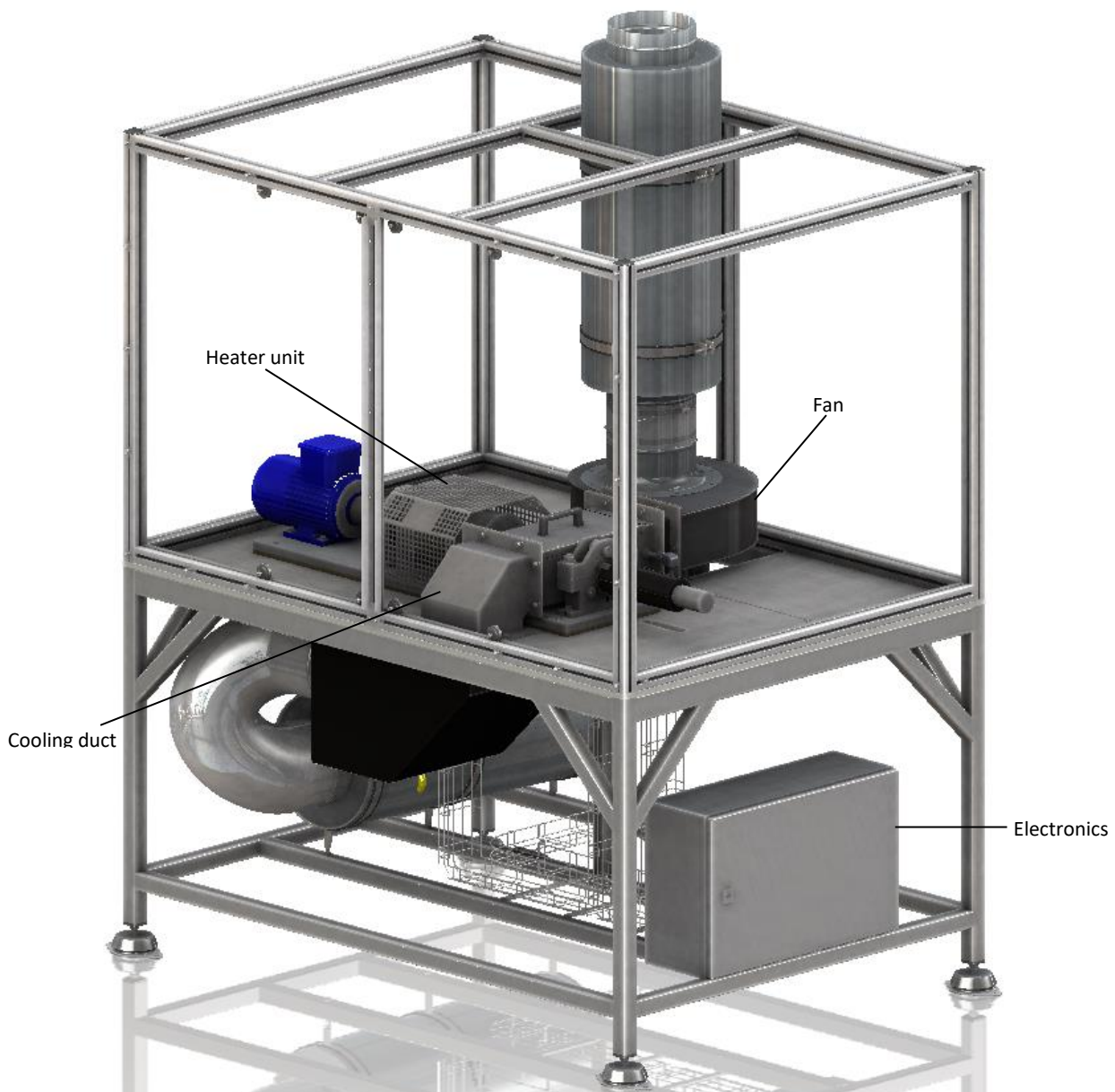


Figure 2.2: Drawing of the cabinet with all the equipment

2.1 Changes in design

The design described in [8] has been worked out further. The Dienst Elektronische en Mechanische Ontwikkeling (DEMO) of TU Delft has built the setup in the P&E laboratory in Delft. In this chapter, the procedure regarding the building of the test setup and the changes to the design relative to the design described in [8] is described. The company Cadans Engineering, located in Noordwijkerhout, has been involved in this project to make the drawings of the final design of the setup. The company Thermo-Electra, located in Pijnacker, manufactured the heat pipe. They were also involved in the design of the heat pipe, regarding the feasibility to manufacture the heat pipe.

In Figure 2.3, the schematic overview as described in [8] is given. Since the publication of this report, several changes have been made to the design. First, the band heater will not provide the heat anymore. The band heater has a clamp at one side of the band heater, so the centre of mass of the band heater is not on the axis of rotation of the heat pipe. So, when the heat pipe is rotating with 1000 rpm, this will cause large vibrations. To prevent problems with rotation, the best option would be to heat without the need of physical contact. To enable this, multiple options are available. As described before in [8], induction heating is too expensive, so this is not a feasible option. Another option would be placing an oven around the heating zone of the rotating heat pipe. This is also an expensive option, but it is cheaper than induction heating. The last option is heating with lamps. With quartz lamps which heat up to 1173 K, it is possible to reach the target working fluid temperature of this setup of 723 K. These lamps are placed around the heat pipe and enclosed by a reflector, so that ideally all of the radiation coming from the lamps reaches the heat pipe. In Chapter 2.3, a calculation is made to determine how many lamps would be needed to heat up to this temperature and keep the heat flux as specified. Another advantage of heating with quartz lamps relative to heating with a band heater is that the electric energy provided to the lamps does not go through the slip ring. This will prevent that there is interference from the band heater power to the thermocouple signals.

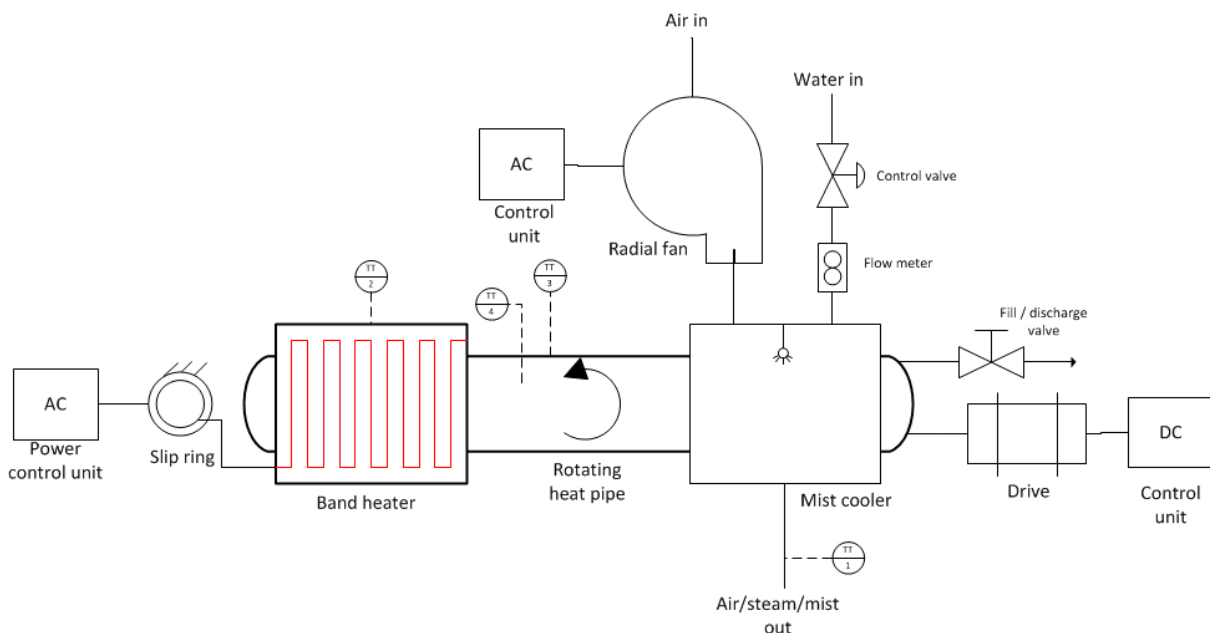


Figure 2.3: A schematic overview of the test setup as described in [8]

Also, it was decided to turn around the heat pipe, so that the slip ring is at the condenser side of the heat pipe and the motor drive at the evaporator side. Although the condenser side is also relatively hot, it is expected that it is better for the electronics to be at the cooler side of the heat pipe¹. This means that the coupling from the motor to the heat pipe should withstand high temperatures. For this, a ceramic coupling is used which can withstand temperatures up to 523 K [11]. However, due to a mistake in the drawings this change is not applied during manufacturing of the heat pipe. So, in the actual setup the electronics are still at the evaporator side. The consequence will potentially be a limited upper operating temperature. An extra thermocouple will monitor the temperature of the electronics.

Furthermore, the pressure relief system has been replaced by a pressure sensor. When the pressure inside the tube goes too high, the heating is turned off while keeping the mist cooler on. Then the temperature and pressure inside the tube will automatically drop. The heat pipe is subjected to a pressure test up to 25-30 bar to check for any leakages by Thermo Electra. This allows for a safety margin as the safety regulations prescribe that the maximum pressure should not exceed 5 bar. Nevertheless, it is advantageous to have a pressure sensor because it can also be used to measure the vacuum inside the tube and check if the heat pipe is still at vacuum after some heat cycles. The pressure sensor used for this is the Kulite ETL-GTS-X-312 (M) Series [12]. This pressure sensor has a pressure range from 0 bar to 10 bar.

In [8], the only specification about the valve is that it should be made of 316 stainless steel, like the rest of the heat pipe. A valve which could fit in a cylindrical space with a diameter of 32 mm and a length of 28 mm, can handle vacuum and is able to operate at a temperature of 623 K could not be found. Most common seals use plastics, which deteriorate or pyrolyse at 623 K. Pyrolysis produces non-condensable gases, which reduces the performance of the heat pipe. Therefore, metal seals should be used. To solve these problems, the valve is replaced by a 316 stainless steel tube with a diameter of 12 mm. The tube is squeezed to close the heat pipe. This technique is described in [13]. The same procedure as in the paper is followed. First, the squeeze tube is annealed to make the steel ductile. Next, the squeeze tube is welded to a plug with screw thread. The plug is screwed into the heat pipe and sealed with a copper ring between the heat pipe and the plug. Then, the tube is connected to the vacuum pump to get the heat pipe at vacuum. After that, the squeeze tube is squeezed to keep the vacuum inside the heat pipe. When the heat pipe is still being squeezed, the tube is cut and the squeezed part is welded together. This is done to secure a completely tight sealing.

Also, it was described in [8] that the wall thickness of the heat pipe will be thicker than 5 mm to guarantee accurate measurement of the heat flux through the wall of the heat pipe. For this, it is decided in collaboration with Thermo-Electra that the wall thickness is increased to 8 mm. With a wall thickness of 8 mm, it should be possible to make accurate heat flux measurements inside the wall.

Last, there is a connector placed between the heat pipe and the slip ring. This makes the heat pipe exchangeable with another heat pipe with the same dimensions and connector. This can be used when tests with another fluid inside the heat pipe will be performed in the future. To be able to handle enough connections in the available space, a custom made connector is used.

¹ Personal communication with M. Celik and DEMO

All these changes give an updated schematic overview of the Delft setup, which can be seen in Figure 2.4.

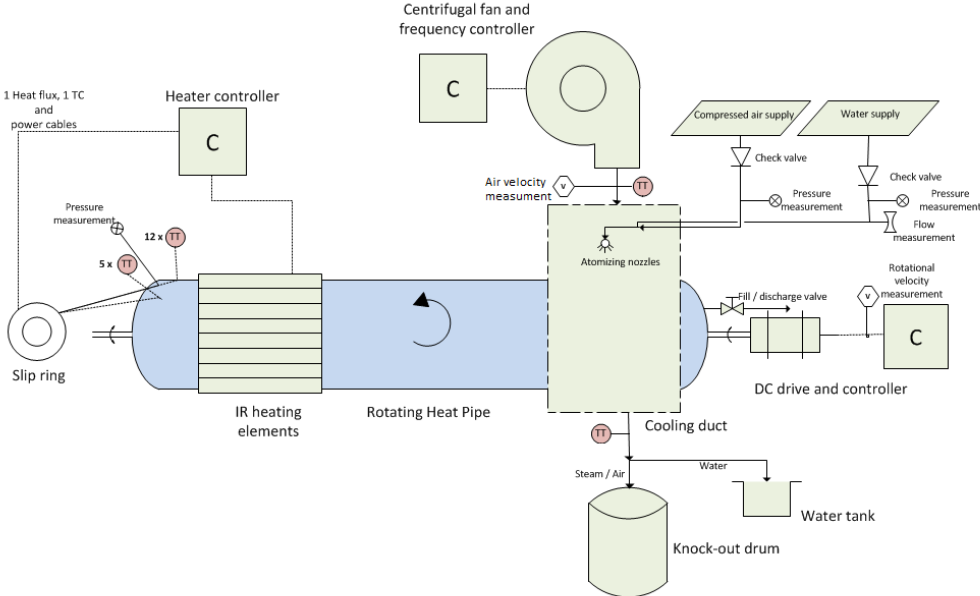


Figure 2.4: Updated schematic overview of the Delft setup design

2.2 Thermal heat transfer to evaporator section

In [8], a calculation of the heat losses and the required heat input has been made. This calculation does not take insulation into account. Therefore a new calculation is made, where insulation of the adiabatic zone and evaporator is applied. For the adiabatic zone a similar approach as in [8] is used. For the evaporator zone a temperature of the reflector is assumed based on the results in Chapter 2.3. An overview of all the heat flows can be seen in Figure 2.5.

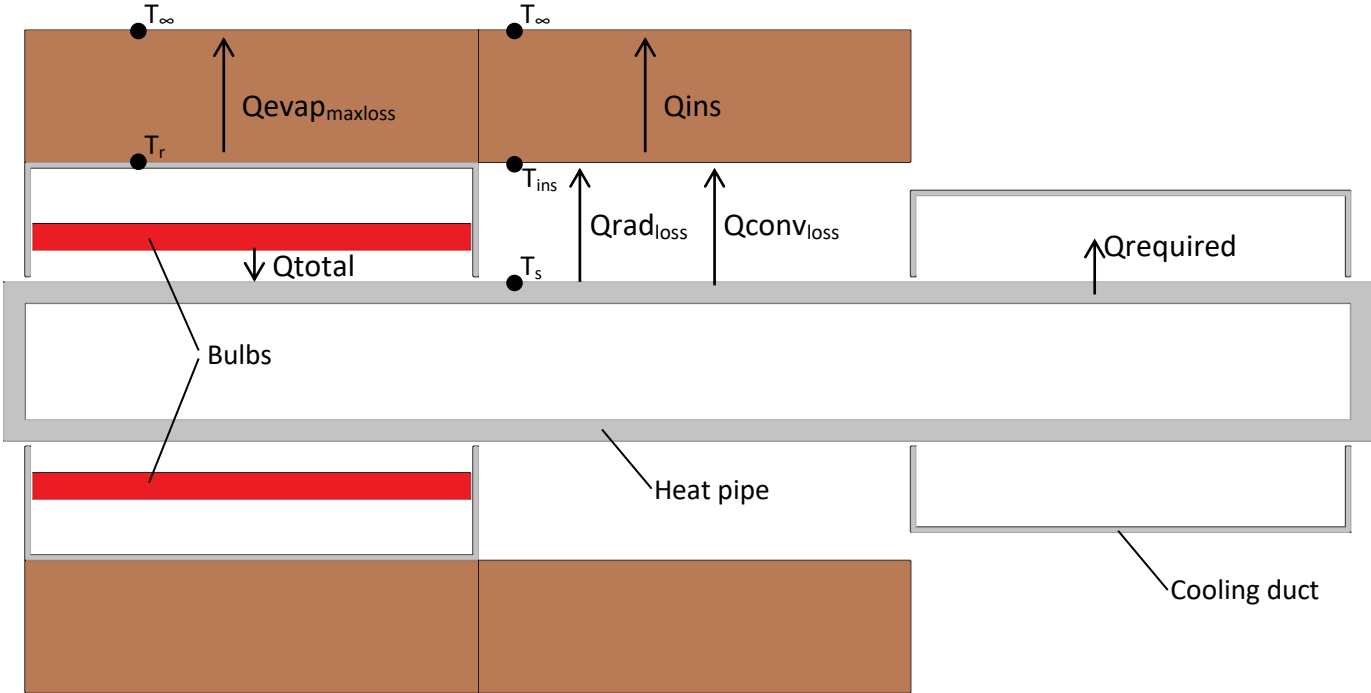


Figure 2.5: Overview of the heat losses, side section cut

First, the calculation in [8] is reproduced. This calculation is reproduced with a maximum deviation of 2%. From this point, the calculation is adapted to the new situation with insulation around the evaporator and adiabatic zone. For the adiabatic zone, this is a vermiculite scale with a thermal conductivity of 0.11 W/(m·K). This scale has an inner diameter of 150 mm and an outer diameter of 250 mm. An schematic overview of the situation can be seen in Figure 2.6.

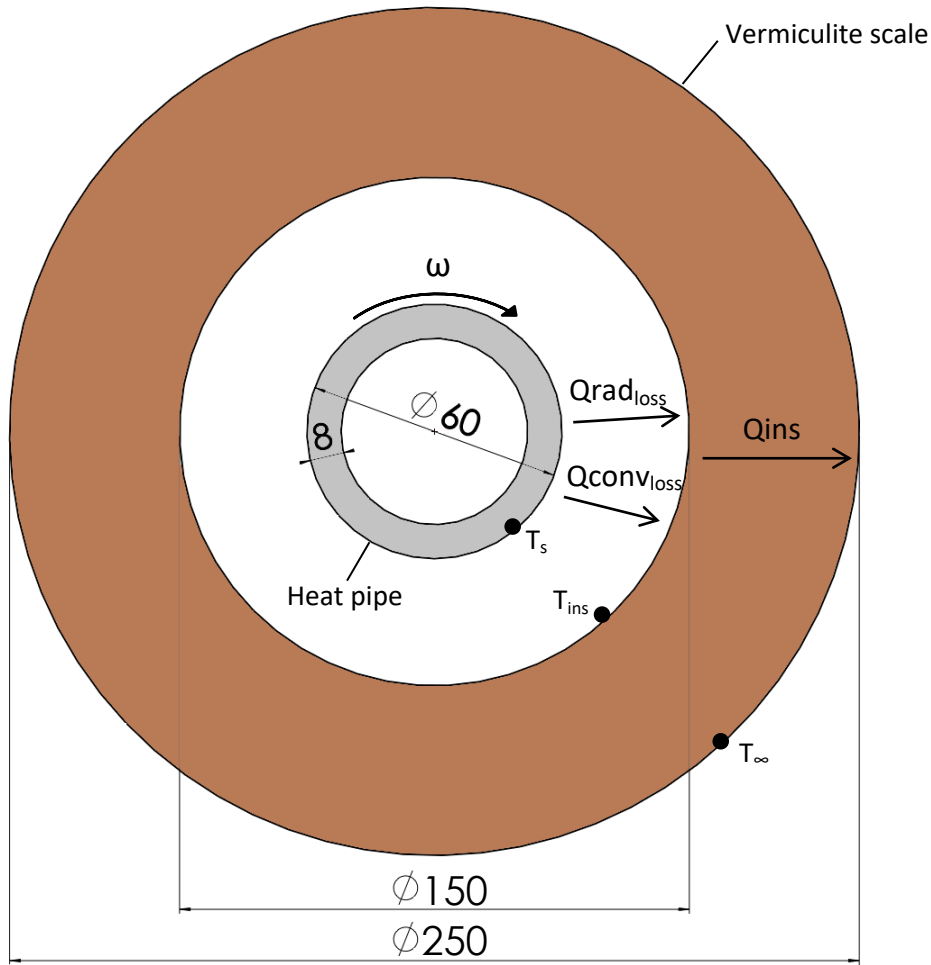


Figure 2.6: Overview of the heat losses

The heat loss in the adiabatic zone consists of a convective heat loss and a radiative heat loss. Because these two parallel heat losses are in series with the heat loss through the insulation, the sum of these two heat losses is equal to the heat loss through the insulation. It should be noted that the convective resistance at the outer surface of the insulation is neglected. Therefore, the temperature at the outer surface of the insulation is taken as the ambient temperature.

The equations for these individual heat losses are [14]:

$$Q_{rad_{loss}} = \epsilon \cdot \sigma \cdot A \cdot (T_s^4 - T_{ins}^4) \quad (2.1)$$

$$Q_{conv_{loss}} = h_{conv} \cdot A \cdot (T_s - T_{ins}) \quad (2.2)$$

$$Q_{ins} = k_{ins} \cdot 2\pi \cdot L_a \cdot \frac{T_{ins} - T_{\infty}}{\ln\left(\frac{r_o}{r_i}\right)} \quad (2.3)$$

In these equations, ϵ is the emissivity of the heat pipe, σ is the Stefan-Boltzmann constant, A is the area of the heat pipe, h_{conv} is the convective heat transfer coefficient and k_{ins} is the thermal conductivity of the insulation.

Solving the equation $Q_{rad_{loss}} + Q_{conv_{loss}} = Q_{ins}$ gives a value for T_{ins} , with T_s as a variable temperature. When T_{ins} is calculated, Eq. 2.1 and Eq. 2.2 can be used to calculate the radiative and convective heat loss in the adiabatic zone. For the adiabatic section of the heat pipe, an emissivity factor of 0.62 is used [15]. For the calculation of h_{conv} , the same correlation for the calculation of the Nusselt number as in [8] is used, which is:

$$Nu_d = 0.10 \cdot (Re_d)^{\frac{2}{3}} \quad (2.4)$$

This is a correlation for the convective heat transfer from a heated cylinder rotating along its longitudinal axis in air. It is derived by Anderson and Saunders [33]. This correlation is valid when the Reynolds number is above a critical Reynolds number described by:

$$Re_{d,c} = 0.93 \sqrt{\frac{Gr_d}{Pr}} \quad (2.5)$$

The Grashof number is defined as:

$$Gr_d = \frac{g\beta(T_s - T_{ins})d_o^3}{\nu^2} \quad (2.6)$$

The Prandtl number is defined as:

$$Pr = \frac{c_p\mu}{k} \quad (2.7)$$

The Reynolds number is defined as:

$$Re_d = \frac{\rho \cdot v \cdot d}{\mu} \quad (2.8)$$

In Figure 2.7 the Reynolds number and the critical Reynolds number can be seen. It can be seen that the Reynolds number is higher than the critical Reynolds number for every temperature. Therefore, it can be concluded that Eq. 2.4 is valid and can be used to calculate the convective heat loss at the adiabatic zone.

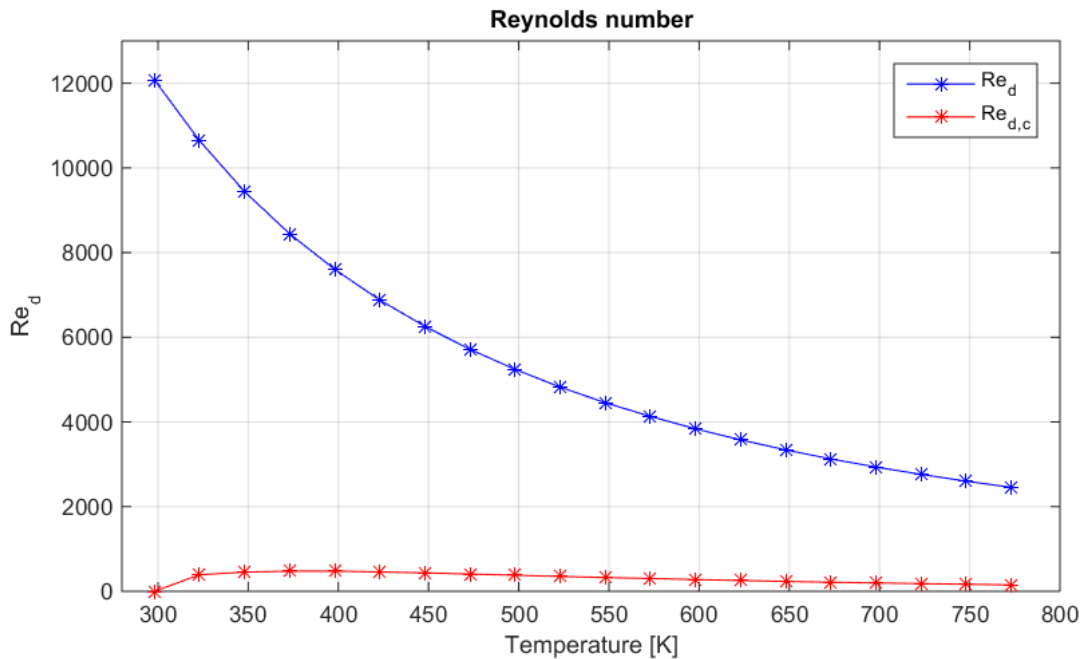


Figure 2.7: Reynolds number compared to the critical Reynolds number

In the evaporator section, also a vermiculite scale is placed around the reflector as insulation. Again, the vermiculite scale has an inner diameter of 150 mm and an outer diameter of 250 mm. The inner diameter is the same as the outer diameter of the reflector. So, the heat loss only consists of a conductive loss through the insulation. The calculation can be performed by using the temperature of the reflector. The temperature of the reflector is calculated with a thermal simulation, similar to the simulations in Chapter 2.3. When the reflector is perfectly insulated the temperature at the outside of the reflector wall reaches 1039 K. This temperature is used to calculate the heat loss at the evaporator. It should be noted that this temperature might be lower when operating at lower heat pipe temperatures. However, it is unknown how the reflector temperature will change with respect to the surface temperature of the heat pipe. Also, it is unknown how this temperature will change when operating at a lower temperature. Therefore, the temperature T_r is kept constant. The equation to calculate the maximum heat loss in the evaporator is:

$$Q_{evap_{maxloss}} = k_{ins} \cdot 2\pi \cdot L_e \cdot \frac{T_r - T_\infty}{\ln\left(\frac{r_o}{r_i}\right)} \quad (2.9)$$

The total heat loss is the sum of the losses in the adiabatic and evaporator zone and the required load for the heat pipe. The maximum required load for the heat pipe is 900 W. Based on the previous equations, the result is calculated with a Matlab script. The script can be found in Appendix A. The result of the calculation can be found in Figure 2.8. At the maximum heat pipe temperature of 723 K the required heat input is 1155 W.

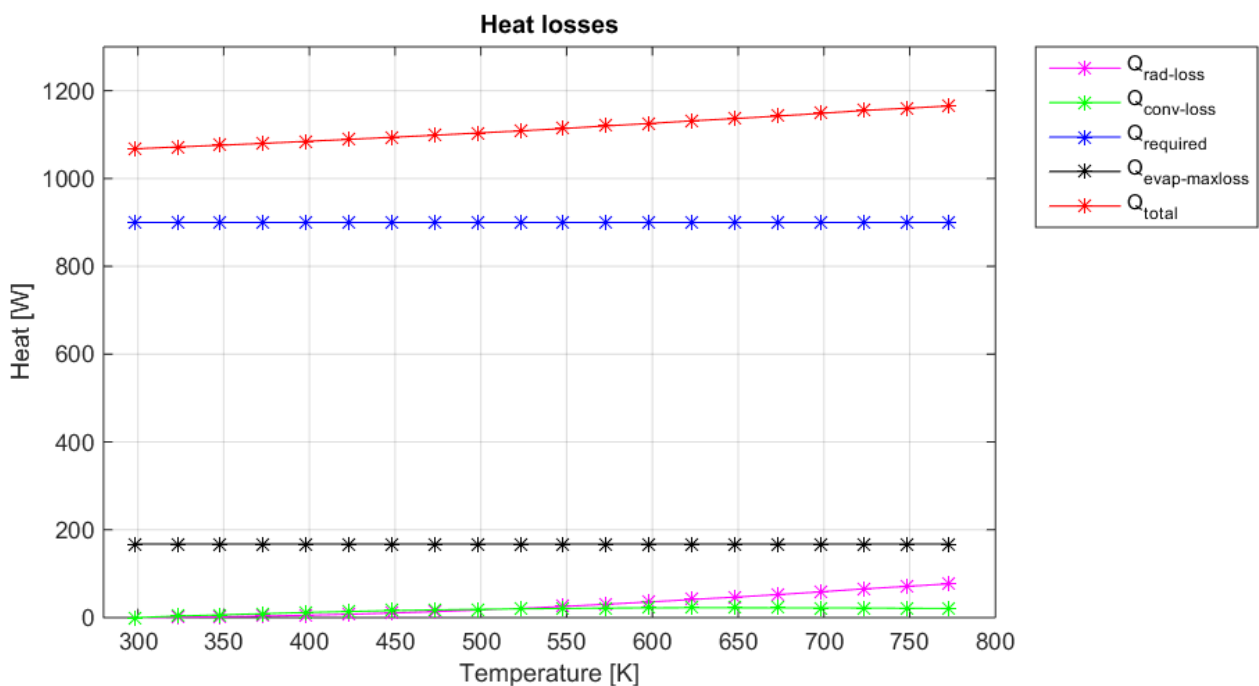


Figure 2.8: Plot of the radiative and convective losses at the adiabatic zone and the losses at the evaporator. Also the required heat load and the sum of all of these are plotted.

2.3 IR Heating

As described before, the heating part of the heat pipe has to be performed without direct contact. Because of possible vibrations, which can potentially break down the heat pipe and the bearings, heating by direct contact is not an option anymore. Therefore, the heat flux should be supplied without direct contact. Therefore, radiant heating with lamps is considered. The quartz lamps that are considered to be used have bulb temperatures up to 1173 K. These lamps have an effective heating length of 165 mm, which is almost equal to the evaporation zone of 167 mm. To know how many bulbs are necessary, following calculations are performed.

2.3.1 Analytical calculation

First, an analytical calculation is made with the basic radiation equations. From [14], it can be read that the equation for the radiation of two grey-body surfaces from one surface to another is equal to:

$$\dot{Q}_{12} = \frac{\sigma(T_1^4 - T_2^4)}{\frac{1 - \epsilon_1}{\epsilon_1 A_1} + \frac{1}{A_1 F_{12}} + \frac{1 - \epsilon_2}{\epsilon_2 A_2}} \quad (2.10)$$

In the first calculation, two concentric cylinders are assumed. The outer cylinder represents the bulbs and the inner cylinder represents the heat pipe. The heat pipe will be coated with a high temperature resistant black paint. Therefore, it is assumed that the heat pipe has an emissivity factor of 0.9 and the outer cylinder approaches blackbody radiation and also has an emissivity factor of 0.9. The radius of the heat pipe is 30 mm and the radius of the outer cylinder is 46 mm. The outer cylinder has a radius of 46mm because the quartz bulb has a diameter of 12 mm and a 10 mm safety margin is kept between the bulb shell and the heat pipe. Figure 2.9 illustrates the situation as described before. The bulb in Figure 2.9 is only to illustrate where the bulbs will be in the future design compared to the outer cylinder. So the outer cylinder is assumed to be at the centre of the bulbs.

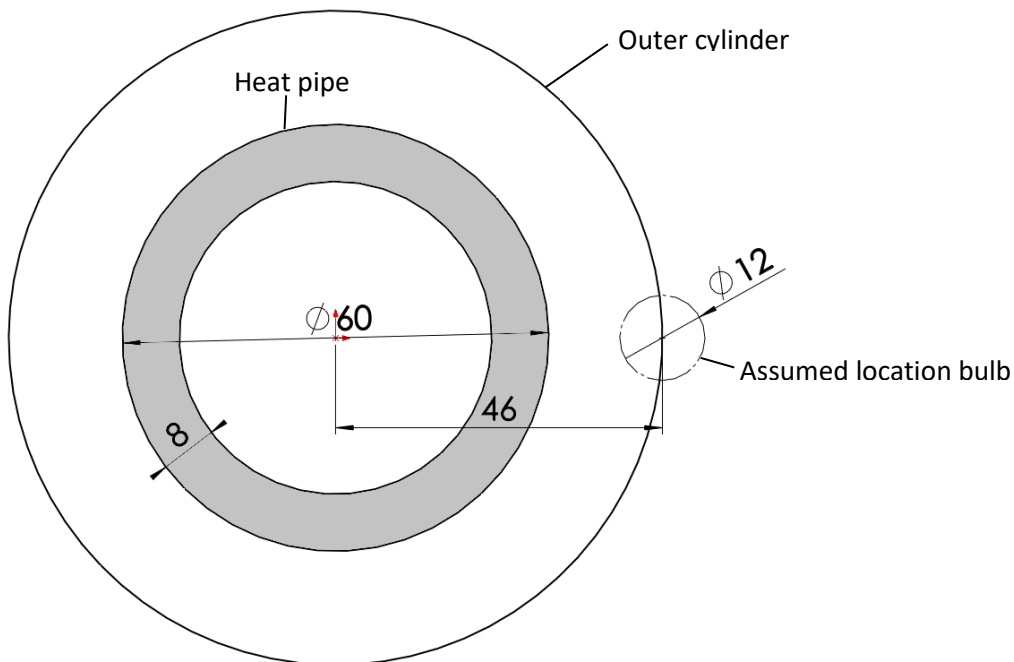


Figure 2.9: Position of the outer cylinder compared to where the bulbs will be

The view factor from the outer cylinder to the inner cylinder can be calculated by using the rule of reciprocity [14]:

$$A_1 \cdot F_{12} = A_2 \cdot F_{21} \quad (2.11)$$

For the view factor from the inner cylinder to the outer cylinder, the view factor for two infinitely long concentric cylinders is used. Then, the view factor F_{21} is equal to 1 [16]. By using the rule of reciprocity, the view factor from the outer cylinder to the inner cylinder is calculated to be 0.652.

When phenanthrene is used as working fluid, the working fluid temperature inside the heat pipe should reach a maximum value of 723 K. There will be a temperature gradient over the wall of the heat pipe. With a heat input of 1200 W the temperature drop over the wall of the heat pipe is 19.8 K. So the outer wall of the heat pipe should heat up to 743 K. The outer cylinder is assumed to have a temperature of 1173 K. As described in Chapter 2.2 the required heat input is 1155 W.

Now that every variable is described, the heat transfer from the outer cylinder to the inner cylinder can be calculated. This heat transfer is calculated with Eq. 2.10 and is equal to 2439 W. This is well above the maximum calculated heat input of 1155 W in Section 2.2. This means that only 47.5% of this area should provide heat at a temperature of 1173 K to have a heat input of 1155 W, the rest of the area can be a reflector material. This area is almost equal to the area of five bulbs with an effective heating length of 165 mm. However, a large amount of the area of these bulbs is at the back and radiates away from the heat pipe. Therefore, a good reflector around the setup is needed, so that most of this radiation is reflected to the heat pipe.

This calculation is expanded by replacing the outer cylinder by small cylinders with a diameter of 10 mm. The actual bulbs that are used have a diameter of 12 mm, but the wall of a quartz bulb does not deliver heat, only the gas inside the bulb does. Hence, only the volume of the gas is used for the calculation of the radiative heat transfer. Also, a reflector is placed around the bulbs, so that the radiation at the back side of the bulbs is reflected to the heat pipe as well. The reflector has an outer diameter of 150 mm with a wall thickness of 2 mm. In this case the calculation is performed by assuming the use of 6 bulbs. The calculation is also performed with the use of 5 bulbs and the use of 7 bulbs. These results can be found in Appendix B. Again, a 10 mm safety margin is kept between the bulbs surface and the heat pipe. As the glass wall of the bulb is neglected in the radius of the bulb, this 1 mm wall thickness is added to the safety margin, so that the overall geometry does not change while the radius of the bulb is assumed smaller. This means that the safety margin used in the calculation is 11 mm, so that the safety margin in the actual setup remains 10 mm.

In this situation, the bulb radiates to four surfaces, to one of its two neighbour bulbs, to the heat pipe and to the reflector. It is assumed that the reflector has perfect reflection. Also, the view factors are calculated in a 2 dimensional situation with infinitely long tubes again. In Figure 2.10, a picture of this configuration can be seen. It can be seen that 81.41° of the bulb perimeter views the heat pipe and 12.48° of the bulb perimeter sees a neighbouring bulb. Now, the view factor from the bulb can be calculated by dividing this angle by the total angle of a bulb perimeter which is 360° . The total sum of view factors is equal to one [14], so the view factor from the bulb to the reflector can be calculated by:

$$F_{bulb \rightarrow reflector} = 1 - F_{bulb \rightarrow heatpipe} - 2 \cdot F_{bulb \rightarrow bulb} \quad (2.12)$$

The calculated view factors are shown in Table 2. It looks like these view factors are calculated in a graphical way, but this is not the case. All the angles can be calculated by using basic geometric equations. These equations are programmed in Matlab, so that the program is robust for changes in the design and the size and number of bulbs used. This Matlab file can be found in Appendix B.

Table 2: View factors for a configuration with six bulbs

View factor	Value
$F_{bulb \rightarrow heatpipe}$	0.226
$F_{bulb \rightarrow bulb}$	0.035
$F_{bulb \rightarrow reflector}$	0.705

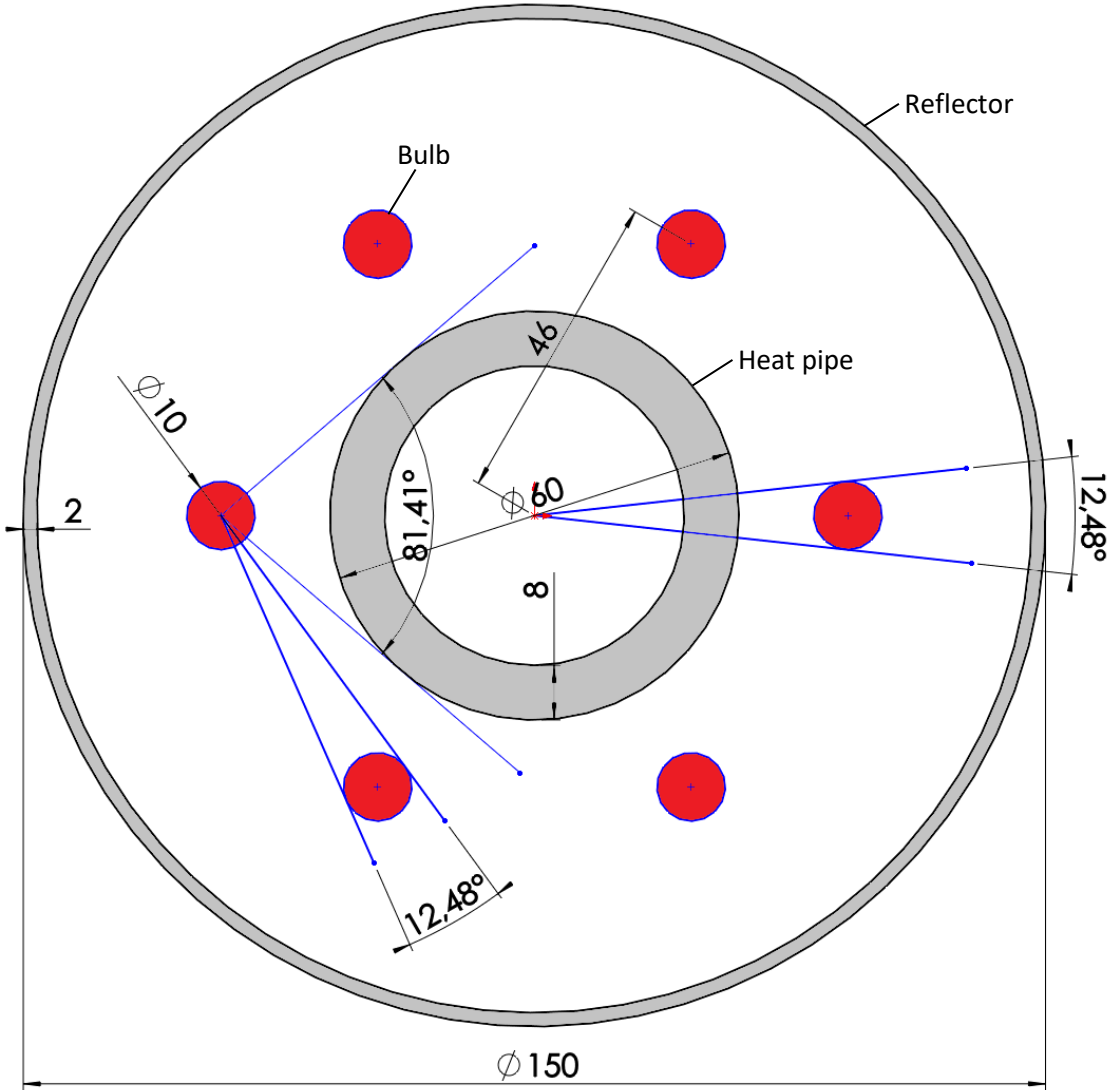


Figure 2.10: Geometry with 6 quartz bulbs and the reflector

The heat transfer from the bulb to the heat pipe can go in multiple ways. Only the three main paths are taken in account in this calculation; directly from the bulb to the heat pipe, from the bulb via the reflector to the heat pipe and from the bulb via the reflector to the reflector again and then to the heat pipe. This means that the view factor from the reflector to the heat pipe needs to be calculated. This is calculated by using the reciprocity rule, because the view factor from the heat pipe to the reflector can be calculated in a similar way as before. Therefore, the view factor from the heat pipe to the reflector is equal to:

$$F_{\text{heatpipe} \rightarrow \text{reflector}} = 1 - 6 \cdot F_{\text{heatpipe} \rightarrow \text{bulb}}$$

$$F_{\text{heatpipe} \rightarrow \text{reflector}} = 1 - 6 \cdot \frac{12.48}{360} = 0.792$$

Using the reciprocity rule gives:

$$F_{\text{reflector} \rightarrow \text{heatpipe}} = \frac{A_{\text{heatpipe}}}{A_{\text{reflector}}} \cdot F_{\text{heatpipe} \rightarrow \text{reflector}}$$

$$F_{\text{reflector} \rightarrow \text{heatpipe}} = \frac{2\pi \cdot r_{\text{heatpipe}} \cdot L_{\text{heatpipe}}}{2\pi \cdot r_{\text{reflector}} \cdot L_{\text{reflector}}} \cdot F_{\text{heatpipe} \rightarrow \text{reflector}}$$

$$F_{\text{reflector} \rightarrow \text{heatpipe}} = \frac{0.03}{0.073} \cdot 0.792 = 0.3255$$

For the calculation of the view factor $F_{\text{reflector} \rightarrow \text{reflector}}$ the view factor $F_{\text{reflector} \rightarrow \text{bulb}}$ has to be calculated first. This can be calculated with the rule of reciprocity:

$$F_{\text{reflector} \rightarrow \text{bulb}} = \frac{A_{\text{bulb}}}{A_{\text{reflector}}} \cdot F_{\text{bulb} \rightarrow \text{reflector}}$$

$$F_{\text{reflector} \rightarrow \text{bulb}} = \frac{0.005}{0.073} \cdot 0.705 = 0.0483$$

Then $F_{\text{reflector} \rightarrow \text{reflector}}$ can be calculated as:

$$F_{\text{reflector} \rightarrow \text{reflector}} = 1 - F_{\text{reflector} \rightarrow \text{heatpipe}} - 6 \cdot F_{\text{reflector} \rightarrow \text{bulb}}$$

$$F_{\text{reflector} \rightarrow \text{reflector}} = 1 - 0.3255 - 6 \cdot 0.0483 = 0.385$$

Now that every view factor is known, the heat transfer can be calculated as [14]:

$$\begin{aligned} \dot{Q}_{\text{bulb} \rightarrow \text{heatpipe}} = & \frac{\sigma(T_{\text{bulb}}^4 - T_{\text{heatpipe}}^4)}{\frac{1 - \epsilon_{\text{bulb}}}{\epsilon_{\text{bulb}} A_{\text{bulb}}} + \frac{1}{n_{\text{bulbs}} A_{\text{bulb}} F_{\text{bulb} \rightarrow \text{heatpipe}}} + \frac{1 - \epsilon_{\text{heatpipe}}}{\epsilon_{\text{heatpipe}} A_{\text{heatpipe}}}} \\ & + \frac{\sigma(T_{\text{bulb}}^4 - T_{\text{heatpipe}}^4)}{\frac{1 - \epsilon_{\text{bulb}}}{\epsilon_{\text{bulb}} A_{\text{bulb}}} + \frac{1}{n_{\text{bulbs}} A_{\text{bulb}} F_{\text{bulb} \rightarrow \text{reflector}} F_{\text{reflector} \rightarrow \text{heatpipe}}} + \frac{1 - \epsilon_{\text{heatpipe}}}{\epsilon_{\text{heatpipe}} A_{\text{heatpipe}}}} \\ & + \frac{\sigma(T_{\text{bulb}}^4 - T_{\text{heatpipe}}^4)}{\frac{1 - \epsilon_{\text{bulb}}}{\epsilon_{\text{bulb}} A_{\text{bulb}}} + \frac{1}{n_{\text{bulbs}} A_{\text{bulb}} F_{\text{bulb} \rightarrow \text{reflector}} F_{\text{reflector} \rightarrow \text{reflector}} F_{\text{reflector} \rightarrow \text{heatpipe}}} + \frac{1 - \epsilon_{\text{heatpipe}}}{\epsilon_{\text{heatpipe}} A_{\text{heatpipe}}}} \end{aligned} \quad (2.13)$$

When this is calculated with values for ϵ_{bulb} and $\epsilon_{heatpipe}$ of 0.9 and a bulb temperature of 1173 K again, the total heat transfer from the bulbs to the heat pipe is equal to 1357.6 W. This is higher than the required heat input of 1155 W. However, it is assumed that the reflector has perfect reflection. This is not the case in reality, so there could be some extra losses.

2.3.2 Thermal simulations with Solidworks

To check the analytical calculations, two thermal simulations are performed with Solidworks. Simulations are performed for the use of six bulbs. For these simulations, it is assumed that the bulbs have a diameter of only 10 mm again. This is because the wall of a quartz bulb does not deliver heat, but only the gas inside the bulb does. So, only the volume of the gas is set at 1173 K. Also, the emissivity of the bulbs and the heat pipe are set to 0.9 again and the emissivity of the reflector is set to 0.074, which is equal to the emissivity of polished stainless steel [15]. An overview of this simulation can be seen in Figure 2.11. The red cylinders represent the bulbs, the small pipe with the thick wall represents the heat pipe and the big pipe around represents the shell. There are also two end plates to reflect the radiation at the side of the bulbs to the heat pipe as well. The end plate at the front end is removed in this figure, otherwise the interior could not be seen.

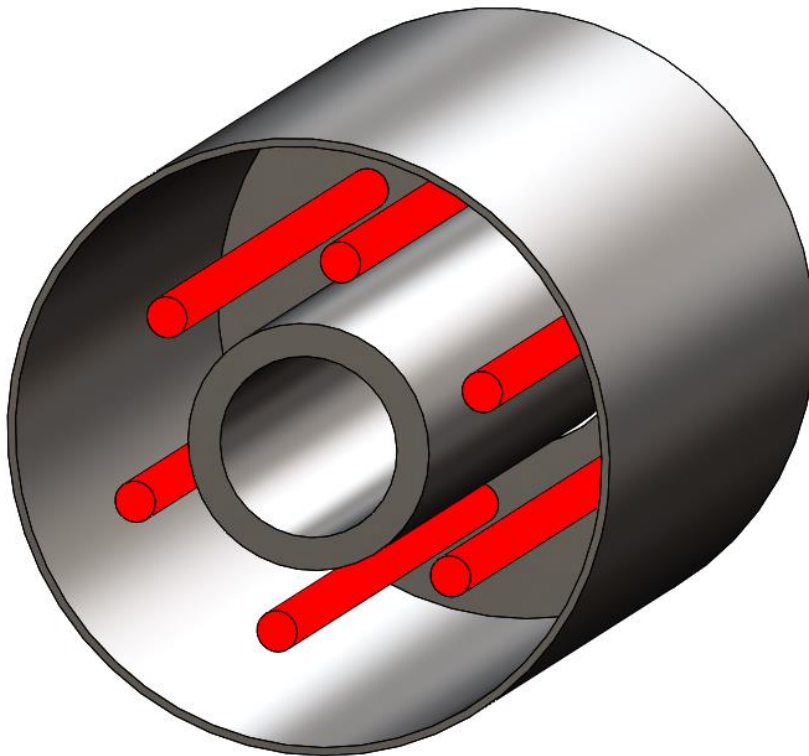


Figure 2.11: Overview of the thermal simulation

In the analytical calculation in Section 2.3.1, the heat transfer from the bulb to the heat pipe is the outcome of the calculation and the wall temperature of the heat pipe is a variable that could be adjusted. The simulations will be done in two different ways. In the first one, the temperatures are set like in the analytical calculation and the heat transfer from the bulb to the heat pipe is calculated. In the second one, the calculation is done the other way around. The outcome of the hand calculation will be used for the heat dissipation on the inside of the heat pipe, while the wall temperature of the heat pipe is the result of the simulation. The total heat dissipation is rounded off to 1200 W. There is a heat dissipation of 1033 W at the inside of the heat pipe and a heat dissipation of 167 W at the reflector, similar to the heat input calculation results.

The use of six bulbs will be simulated in the same geometry as in the hand calculation. The bulb temperature is set to 1173 K and the inside of the heat pipe is set at 723 K. The material of all elements is set to 316 stainless steel, which will also be the material in the actual test setup.

Solidworks Simulation is a finite element method. Solidworks Simulation uses the governing equations for conduction, radiation and convection. First, it calculates all the view factors for every element to other elements it views and the conduction matrix for every element. Next, it calculates the energy transfer to all the elements where it has energy transfer with. Then, depending on the solver used, it calculates the result. The iterative FFEplus solver or the direct Direct Sparse solver can be used. For thermal studies, it is recommended to use the iterative FFEplus solver. First, the simulations are performed with a coarse triangular mesh. This mesh consists of 11473 elements. After that, the simulations are performed with a fine mesh. The fine mesh consists of 38148 elements. For the results, the simulations performed with the fine mesh are shown. A picture of the fine mesh can be seen in Figure 2.12.

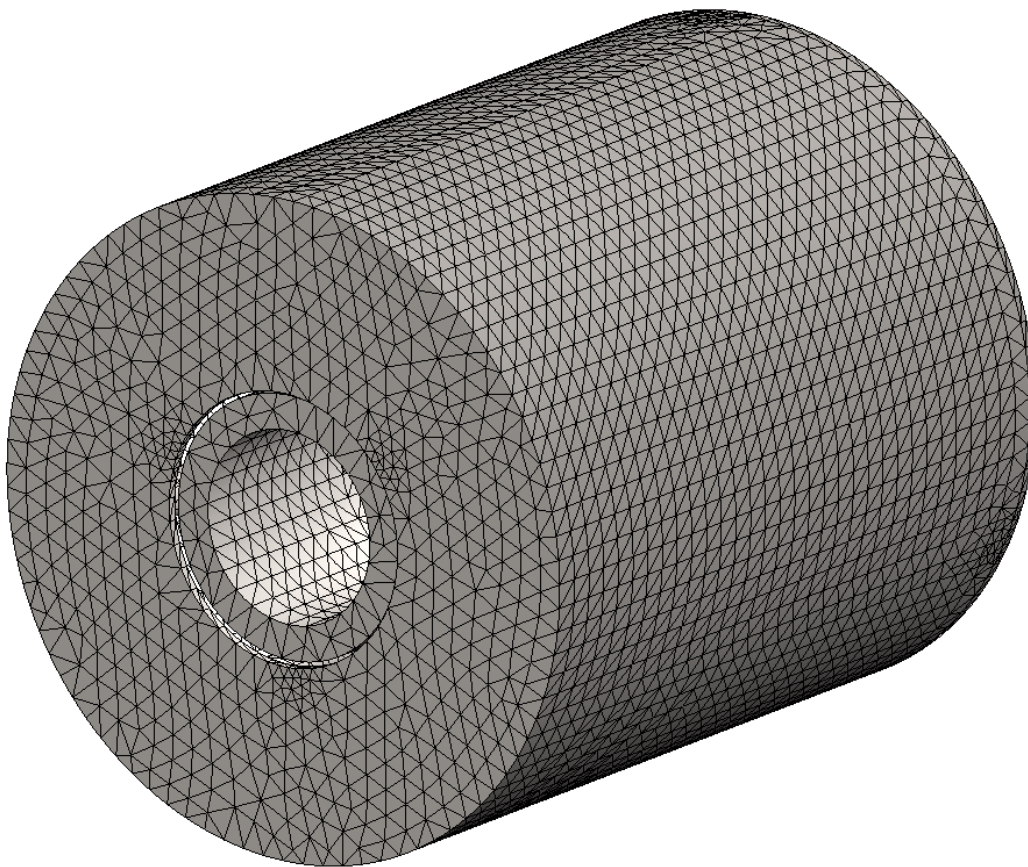


Figure 2.12: Overview of the mesh

In Figure 2.13 and Figure 2.14, the result of the first simulation is shown. In Figure 2.13, the heat flux in the radial direction is plotted. When a heat dissipation of 1033 W is divided by the area the resulting heat flux is 44750 W/m^2 . In Figure 2.13 the heat flux is higher than this required heat flux at every point. In Figure 2.14, the heat flux in the radial direction can be seen at the middle of the heat pipe. It can be seen that the heat flux in the radial direction has an equal distribution in the angular direction. It should be noted that the heat pipe is not rotating in the simulation, so this result will improve when the heat pipe is rotating. In Figure 2.14, the heat flux is slightly higher close to the bulbs. When the heat pipe rotates, the peaks will flatten out.

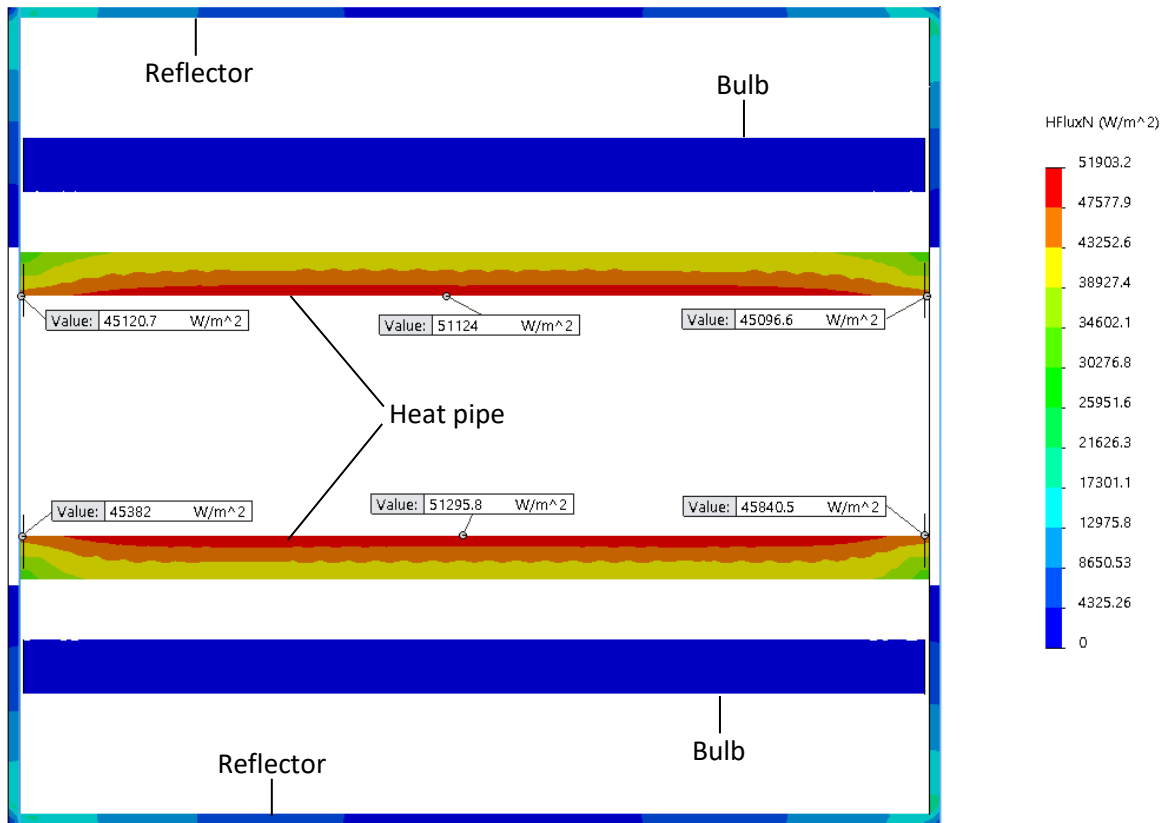


Figure 2.13: Heat flux with constant temperatures, side section cut

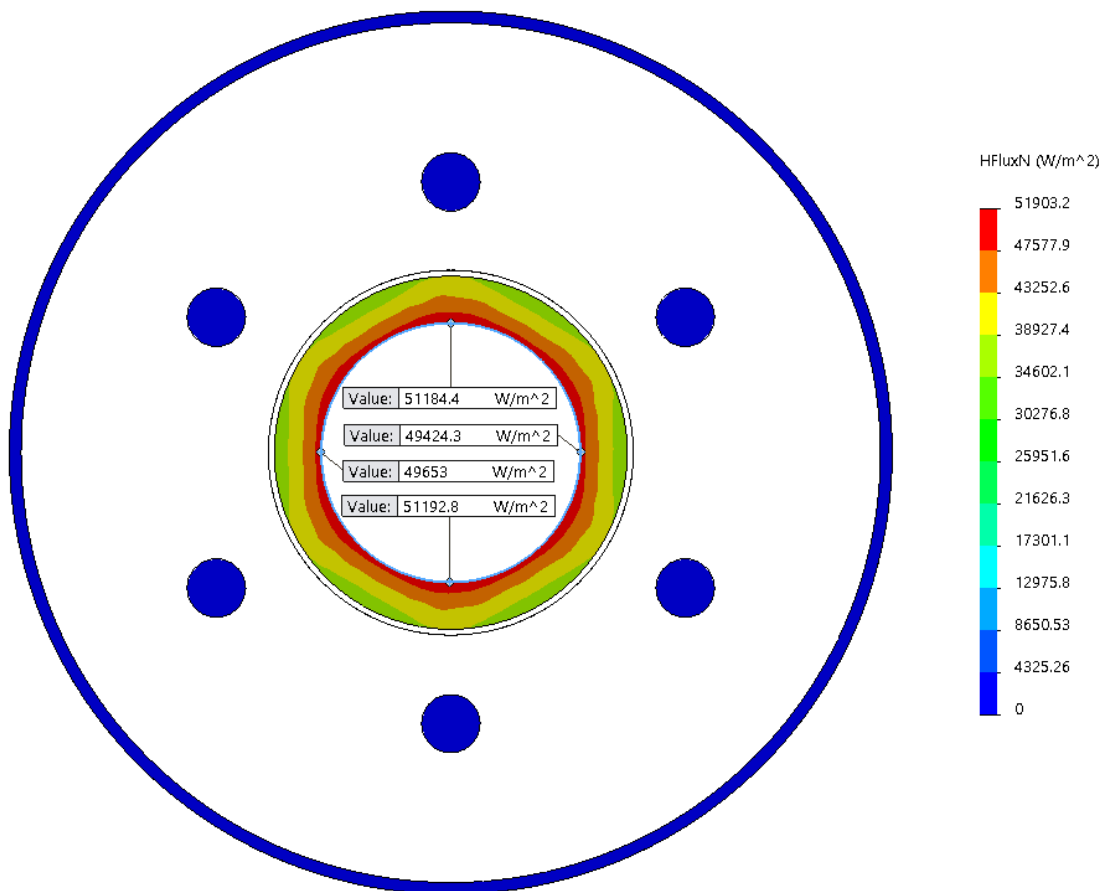


Figure 2.14: Heat flux with constant temperatures, front section cut

Next, a simulation is done where the heat output at the inside of the heat pipe wall is controlled. The wall temperature is now the variable. The same mesh and solver are used as in the first simulation. Again, at the outside of the reflector a heat output of 167 W is set. At the inside of the heat pipe wall the heat output is set at 1033 W. This means that the total heat output is equal to 1200 W again. The results of this simulation can be seen in Figure 2.16 and Figure 2.17. In the previous simulation the temperature at the inside of the heat pipe wall was set at 723 K. In Figure 2.16, it can be seen that the temperature is higher at every point at the inside of the heat pipe wall. In Figure 2.17, it can be seen that the temperature profile in the radial direction is uniform in the angular direction. Again, rotation will only improve the result. It can also be seen that the temperature drop over the wall is 19.1 K. This is equal to a heat flow of 1157 W.

In Figure 2.16, it can also be seen that the temperature at the outside of the reflector wall is lower than the temperature used in Chapter 2.2. This is because the temperature decreases when a heat loss is included in the simulation. A lower temperature only means a lower heat loss at the evaporator. So, some extra losses are included in the simulation.

In this section, the heat input is calculated in three different ways, which all give a positive result. So, it can be concluded that six bulbs are enough to provide the heating for the Delft heat pipe setup. Therefore, the heater unit is built by DEMO. A picture of the final heater unit is shown in Figure 2.15.

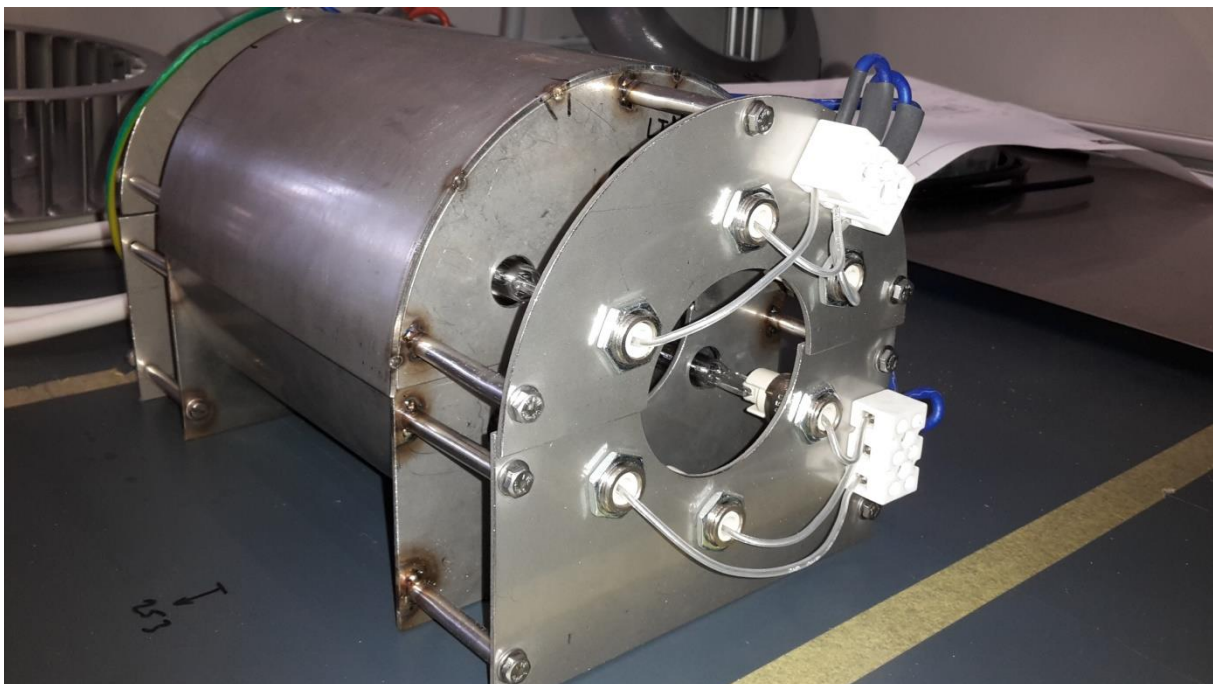


Figure 2.15: Heater unit



Figure 2.16: Temperature profile with constant heat flux, side section cut

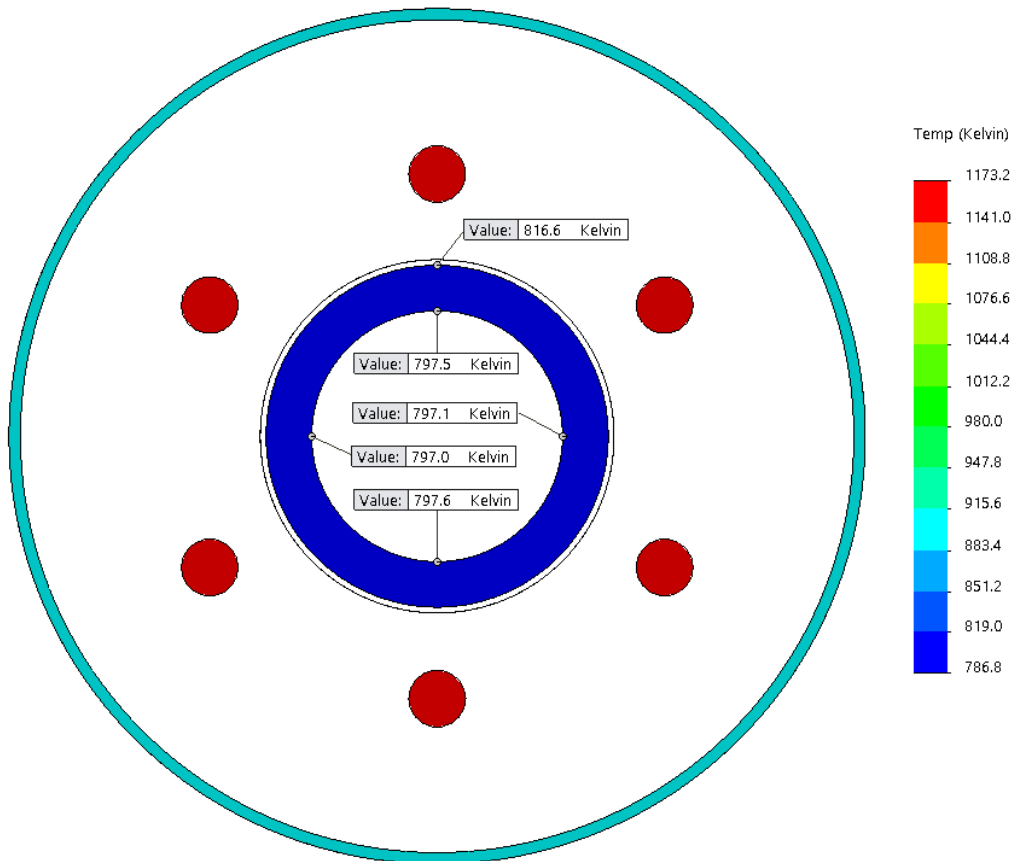


Figure 2.17: Temperature profile with constant heat flux, front section cut

2.4 Thermal heat transfer from condenser section

It should be calculated how much water is needed for the cooling of the heat pipe during operation. The required maximum heat flow out of the heat pipe is 900 W. The losses in the heat pipe should be compensated by the heat input, so it is safe to assume that the heat flow removed by the cooling is 900 W.

From [8], it can be read that the fan provides enough cooling when operating at high temperatures. This is not the case when operating at the lower side of the temperature range, for instance at 423 K. This is because the heat flow could still be 900 W and the temperature difference between the heat pipe and cooling is smaller than when the heat pipe is operating at 623 K. Furthermore, the theory does not always match practice, so mist cooling is implemented as extra cooling backup. Because this is a design calculation, the worst case scenario is considered. Also, it is unknown how the fan cooling interacts with mist cooling, so it is assumed that if mist cooling is used the effect of fan cooling is negligible.

The energy balance used to calculate how much energy is needed to evaporate a certain amount of fluid is [14]:

$$Q = \dot{m} \cdot \Delta h_{fg} \quad (2.14)$$

Where Δh_{fg} stands for the enthalpy of vaporization of the fluid and \dot{m} for the mass flow. The fluid used for the mist cooling is tap water. The evaporation energy of water at 100 °C is equal to 2257 kJ/kg [14]. This gives a water mass flow of:

$$\dot{m} = \frac{Q}{\Delta h_{fg}} = 0.399 \text{ g/s}$$

Although the tap water is not at 100 °C, using a higher value of Δh_{fg} at 20 °C will only reduce the amount of water needed, so this lower value can be assumed as a compensation for losses that are not included. One of those losses could be the assumption that 100% of the mist supplied to the heat pipe evaporates. The tap water could also cause some fouling on the heat pipe after a certain operating time, but the heat pipe can be cleaned easily by removing the top of the cooling duct.

There is certainly some error in the calculated value, as the cooling of the fan is not negligible, the evaporation rate is not 100% and the evaporation enthalpy differs at 20 °C, but this value gives an order to the expected value.

Because in [8] it is calculated that the cooling provided by the fan is enough at high temperatures, it is useful to know the temperature difference between the incoming and outgoing air flow. This can be calculated by using Eq. 2.14 again and replacing Δh by $c_p \cdot \Delta T$. This gives:

$$Q = \dot{m} \cdot c_p \cdot \Delta T \quad (2.15)$$

This translation can only be done if c_p is constant. Because the pressure of air is constant at a small ΔT and the pressure drop in the cooling channel is small, c_p can be assumed constant at 1.005 kJ/kg.K [14]. The mass flow can be calculated by:

$$\dot{m} = v \cdot A \cdot \rho \quad (2.16)$$

The density of air at 20 °C is equal to 1.204 kg/m³ [14]. From [8] it can also be read what the minimum required free air stream velocity should be to have sufficient cooling capacity. This is a minimum of around 10 m/s and the air cooling duct has an area of 125 mm x 180 mm. So ΔT can be calculated as:

$$\Delta T = \frac{Q}{v \cdot A \cdot \rho \cdot c_p} \quad (2.17)$$

$$\Delta T = \frac{900}{10 \cdot 0.125 \cdot 0.180 \cdot 1.204 \cdot 1006} = 3.3 \text{ } ^\circ\text{C}$$

So, the maximum expected temperature increase over the cooling duct is equal to 3.3 °C. When the air flow increases, this temperature difference will get smaller. Although the outgoing airflow should be handled with care, the temperature of the outgoing airflow will not be hot.

2.5 Flow pattern and fill ratio

The fluid distribution in the rotating heat pipe is very important for the performance of the heat pipe. For a better performance, a thin liquid layer is preferred. However, the layer should be thick enough to keep the entire wall wetted when evaporation takes place. Otherwise a burn-out takes place and the performance of the heat pipe drops significantly, because there is less surface for evaporation.

In a rotating heat pipe, one could have two flow regimes. There could be annular flow and non-annular flow. The different types of flow can be seen in Figure 2.18. In picture (a) there is no rotation at all, there is a pool of liquid on the bottom of the heat pipe. When the heat pipe starts rotating the liquid is pulled along the wall. The larger the rotational speed becomes, the thicker the liquid layer at the top of the heat pipe gets.

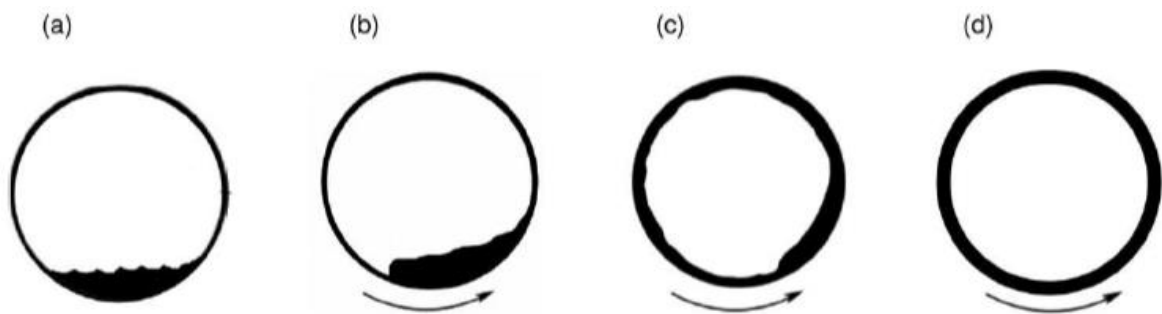


Figure 2.18: Flow regimes: from no rotation(a) to annular flow(d) [17]

To ensure a low resistance, a thin layer of liquid is preferred. Therefore, operating with non-annular flow is preferred over annular flow. Because with the same amount of fluid the liquid layer is thinner with non-annular flow than with annular flow. Operating in annular flow with the same layer thickness as in non-annular flow should give better results. Because there is no pool with annular flow, there is more area available for evaporation. However, the risk of a burn-out at the evaporator side is too large. Also, the head between the condenser and evaporator should be large to prevent a burn-out. So the gain in the evaporator is lost in the condenser section due to the large layer thickness resistance in the condenser. This means that the overall resistance of the heat pipe will become larger and thus the energy savings decrease. A pool of liquid prevents a burn-out in the evaporator section and keeps the layer thickness in the condenser thin as well. Therefore, a future heat pipe assisted annealing line will operate with non-annular flow.

It could be difficult to understand that the liquid layer resistance is smaller when there is non-annular flow than when there is annular flow. Therefore, the liquid layer resistance is calculated. In Figure 2.19 two possible flow patterns are shown. The left figure represents annular flow with a liquid layer thickness of 1 mm everywhere. In the right figure the liquid layer consist of a pool at the bottom with a liquid layer thickness of 1.512 mm. At the top there is a liquid layer thickness of 0.5 mm. In both cases the liquid area is the same. The heat pipe has an inner diameter of 44 mm, like the actual heat pipe. For both flow patterns the overall liquid layer resistance is calculated.

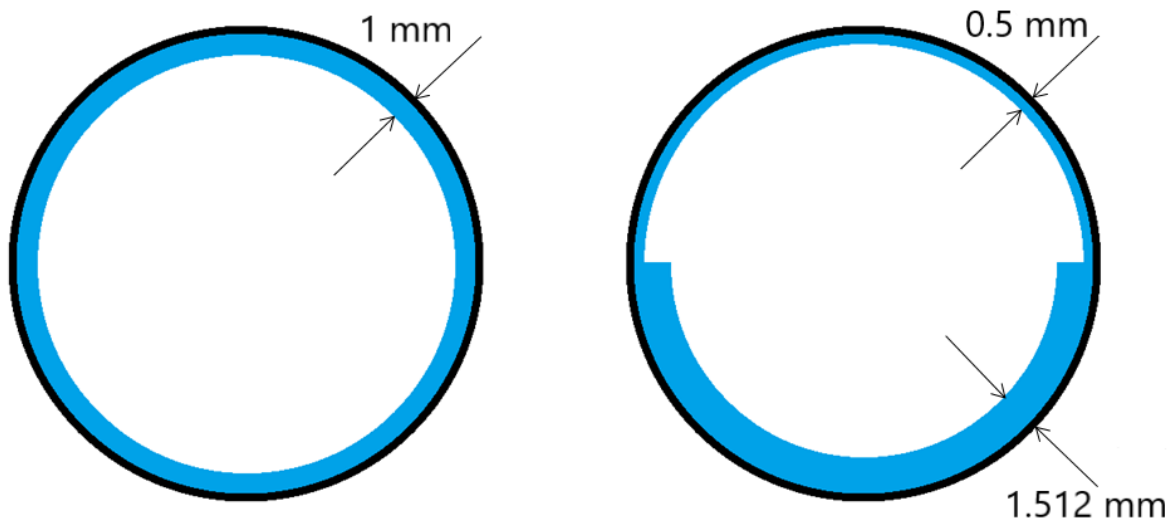


Figure 2.19: Schematic overview of annular flow and non-annular flow

The equation for the liquid layer thermal resistance is:

$$R = \frac{\ln\left(\frac{r_o}{r_i}\right)}{k \cdot 2\pi \cdot L} \quad (2.18)$$

The thermal conductivity k and the length L are the same for both situations. The liquid layer thickness for annular flow is 1 mm. This gives a liquid layer resistance of:

$$R_{annular} = \frac{\ln\left(\frac{22}{21}\right)}{k \cdot 2\pi \cdot L} = \frac{0.007404}{k \cdot L}$$

For the non-annular flow situation the overall resistance should be calculated as a parallel resistance. The equation for the total parallel resistance is:

$$R_{total} = \frac{R_{top} \cdot R_{bottom}}{R_{top} + R_{bottom}} \quad (2.19)$$

First the individual resistances are calculated:

$$R_{top} = \frac{\ln\left(\frac{22}{21.5}\right)}{k \cdot \pi \cdot L} = \frac{0.007318}{k \cdot L}$$

$$R_{bottom} = \frac{\ln\left(\frac{22}{20.488}\right)}{k \cdot \pi \cdot L} = \frac{0.02267}{k \cdot L}$$

Filling in the individual resistances in Eq. 2.19 gives:

$$R_{non-annular} = \frac{\frac{0.007318}{k \cdot L} \cdot \frac{0.02267}{k \cdot L}}{\frac{0.007318}{k \cdot L} + \frac{0.02267}{k \cdot L}}$$

$$R_{non-annular} = \frac{0.005532}{k \cdot L}$$

$$R_{non-annular} = 0.747 \cdot R_{annular}$$

So with the same amount of fluid the overall liquid layer resistance is lower when operating with non-annular flow.

In [18] a study has been done to find a correlation for which fill ratio and rotational speed annular flow occurs. In Figure 2.20 the result from this study is shown. Above the grey line annular flow occurs, below the line there is non-annular flow. This result is found with a literature study and checked with a CFD simulation for multiple cases. It should be noted that there is hysteresis between the formation and collapse of annular flow. This is because of a secondary flow in the pool of liquid which prevents the formation of annular flow [32].

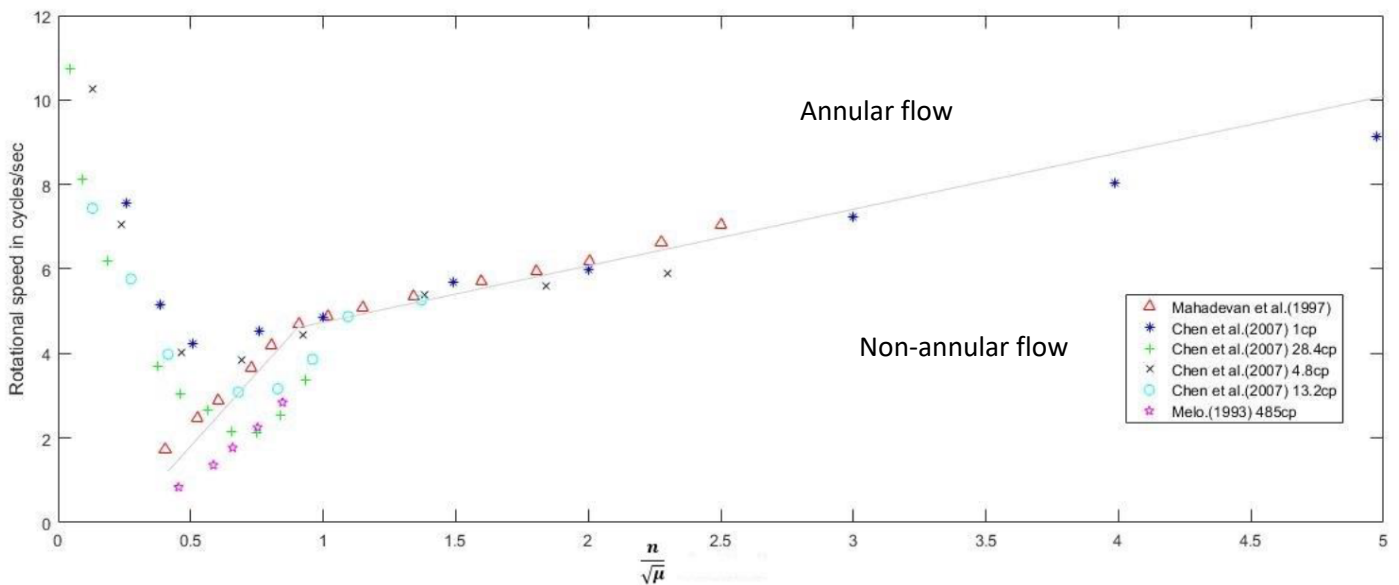


Figure 2.20: Annular flow correlation from rotational speed vs fill ratio/sqrt(viscosity) [18]

Because the heat pipe is used for research, it should be filled with an amount of fluid which makes it possible to operate in both flow regimes over the whole operating range. The heat pipe setup can be operated from 150 rpm to 1000 rpm. The Dowtherm A in the heat pipe has a temperature range from 423 K to 623 K. A calculation is made for several points within this range. For the temperature the whole range is covered with steps of 50 K. The rotational speed is taken at 150 rpm, 400 rpm, 700 rpm and 1000 rpm. The calculation is made for a filling amount of Dowtherm A from 10 gram to 50 gram with steps of 5 gram. The fill ratio is calculated as the volume of the liquid inside the heat pipe divided by the total volume of the heat pipe. This is:

$$Fill\ ratio = \frac{V_{liquid}}{V_{heatpipe}} \quad (2.20)$$

However, part of the liquid is evaporated during operation of the heat pipe. The heat pipe is at saturated conditions during operation, so the liquid volume can be calculated by solving the next set of equations:

$$f_{liquid} \cdot m_{dowthermA} \cdot \frac{1}{\rho_{liquid}} = V_{liquid} \quad (2.21)$$

$$f_{vapour} \cdot m_{dowthermA} \cdot \frac{1}{\rho_{vapour}} = V_{vapour} \quad (2.22)$$

$$V_{liquid} + V_{vapour} = V_{heatpipe} \quad (2.23)$$

$$f_{liquid} + f_{vapour} = 1 \quad (2.24)$$

When the equations are solved, Eq. 2.20 can be used to calculate the fill ratio. At last, the fill ratio is divided by the square root of the viscosity. The unit of the viscosity is mPa·s.

In Figure 2.21 the result is shown for three temperatures; the lower limit, the upper limit and the temperature in the middle of the temperature range. It can be seen that if the heat pipe is filled with less than 35 grams the heat pipe can be used in both flow regimes over the whole temperature range. Because a heat pipe assisted annealing line will operate in the non-annular flow regime, it is decided to fill the heat pipe with the largest amount of liquid where it is still possible to operate in both flow regimes. Therefore, it is decided to fill the heat pipe with 35 grams of Dowtherm A.

The code used for this calculation and to make these figures can be found in Appendix C.

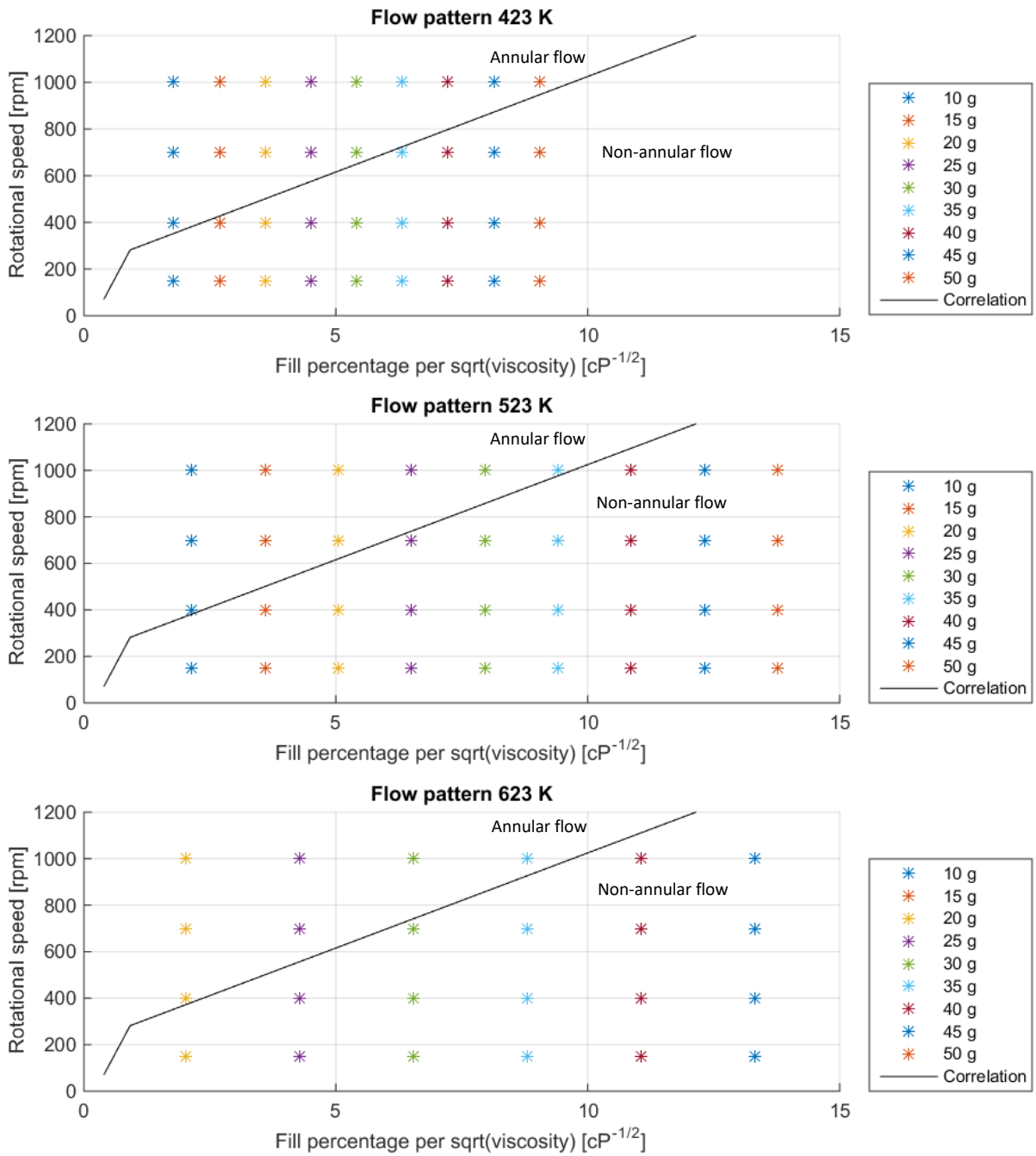


Figure 2.21: Flow pattern at various temperature levels

2.6 Slip ring error

The resistance of the slip ring will influence the temperature measurement. In this section, the influence of this resistance on the temperature measurement is calculated.

From [19], it follows that the contact resistance of the slip ring is smaller than 100 mΩ. Because this is a worst case scenario calculation, it is assumed that this resistance is 100 mΩ.

Voltage measurement is performed by putting a very large resistance in the electric scheme and measure the voltage across this resistance. For the measurement of the voltage coming from the thermocouples in the heat pipe, the Temperature Input Module NI 9213 is used [20]. This module measures the voltage across the thermocouple by putting a large resistance in between and amplify the measured voltage. In Figure 2.22, the input resistance of the NI 9213 can be seen. This figure has been adopted from [21] and adjusted for the NI 9213 Temperature Input Module. The overall resistance is equal to 78 MΩ.

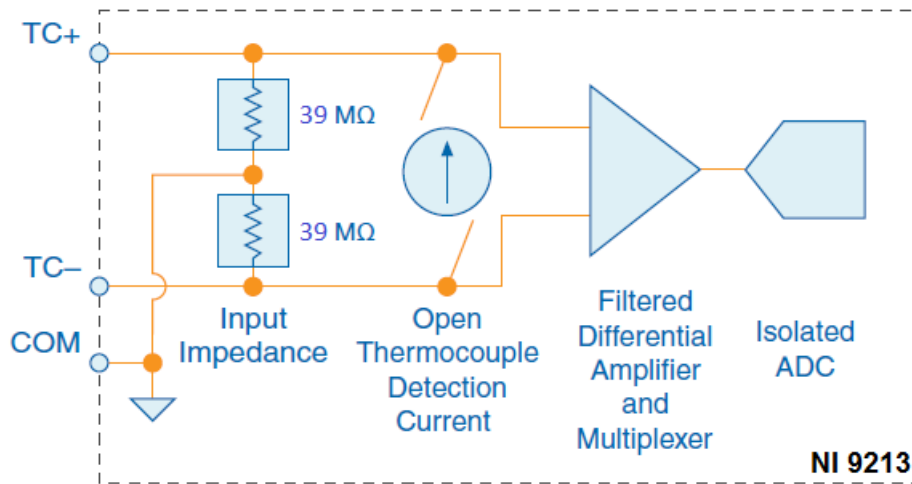


Figure 2.22: NI 9213 temperature input module

The resulting electric diagram can be seen in Figure 2.23. From this diagram the difference between the input and output voltage can be calculated. This is equal to:

$$U_{out} = \frac{R_{Impedance}}{R_{slipring} + R_{Impedance} + R_{slipring}} \cdot U_{in} \quad (2.25)$$

$$U_{out} = 0.99999744 \cdot U_{in}$$

This means that the error is equal to $2.56 \cdot 10^{-6}$. If the actual temperature measured by the thermocouple is 350.0 °C the error is equal to $8.96 \cdot 10^{-4}$ °C.

Therefore, the error related to the measurement of the temperature coming from the slip ring resistance is expected to be negligible.

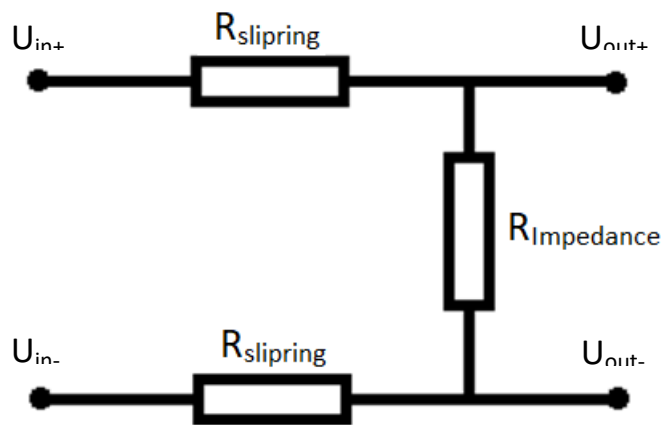


Figure 2.23: Electric diagram

2.7 Bearing cooling

In this part the need for bearing cooling is calculated. Because the bearing can only be heated up to a certain temperature it is important to know whether the bearings will heat up above or below this temperature.

In Figure 2.24 the bearing configuration can be seen. The heat pipe is supported by three bearings with the dimensions of an SKF type 6302 bearing. The actual bearings are made by the company Ceratec located in Geldermalsen, The Netherlands. The bearing rings are made of zirconium dioxide with silicon nitride balls. These materials are chosen because of their high thermal resistance and high operating temperature. In Figure 2.24, it looks like the heat pipe is bigger than the circle between the bearings. This has to do with the fact that the bearing runs in a groove. The bearing block is clamped by two M14 bolts, with a spring ring under the nut to guarantee a certain amount of clamping while radial thermal expansion of the tube and the bearings is possible. The radial thermal expansion of the tube is about 0.5 mm for the worst case scenario [8].

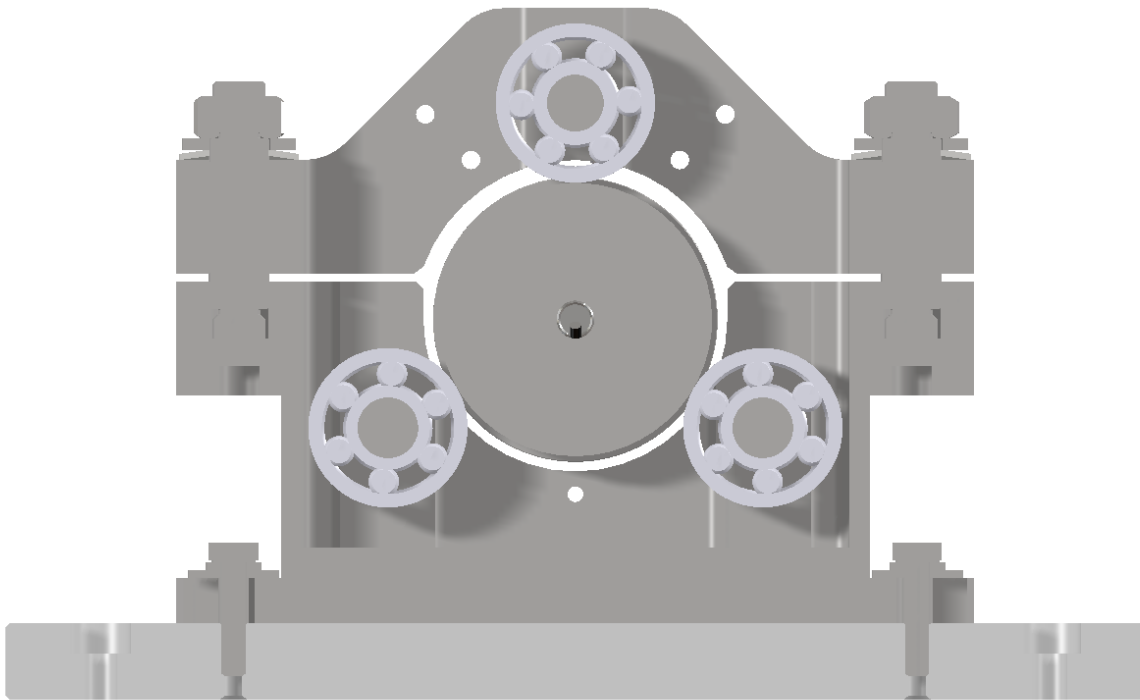


Figure 2.24: Bearing configuration

The SKF type 6302 bearing has a contact width of 13 mm. Ideally, the contact area of the bearings is a line contact but in reality, there is a certain contact area. For this calculation, this area is estimated as 13 mm by 5 mm. The purpose of this calculation is to estimate how much heat is transferred from the heat pipe to the bearing. It is assumed that the heat pipe has a temperature of 723 K. The Delft setup will be used for experiments with phenanthrene as working fluid in the future. When the vapour pressure of phenanthrene reaches 5 bar, the temperature will be about 723 K. Therefore, a heat pipe temperature of 723 K is used in this calculation. The supplier of the bearings gives a maximum operation temperature of 623 K [22]. For the zirconium dioxide and silicon nitride similar

values are found. It is assumed that the balls of the bearing should not heat up to above 573 K and the outer ring of zirconium dioxide will then be between 573 K and 723 K.

Now the heat transfer from the heat pipe to the bearing balls by contact can be calculated by using the equation for conductive heat transfer [14]:

$$Q_{cond} = -k \cdot A \cdot \frac{T_b - T_h}{\Delta x} \quad (2.26)$$

For zirconium dioxide the thermal conductivity is 3 W/(m.K) [23]. The cross-sectional area for this calculation is specified as 13 mm by 5 mm, the temperature difference between the heat pipe and the bearing balls is 723 K – 573 K and the minimum distance between these two points is 2.68 mm [24]. Now, everything is specified to calculate the conductive heat transfer from the heat pipe to the bearing balls:

$$Q_{cond} = 3 \cdot 0.013 \cdot 0.005 \cdot \frac{723 - 573}{0.00268} = 10.9 \text{ W}$$

Of course, there is also some radiative heat transfer from the heat pipe to the bearings. The equation to calculate this is:

$$Q_{rad} = \epsilon \cdot \sigma \cdot A \cdot F_{12} \cdot (T_h^4 - T_b^4) \quad (2.27)$$

The radiation is calculated in the radial direction only, not in the axial direction. Therefore, the area is calculated as $\pi \cdot d_{bearinggroove} \cdot 0.013$. For the emissivity factor, 0.62 is used [15]. This is the emissivity factor for 316 stainless steel after several heating and cooling cycles. For the view factor the view factor for two equal external cylinders is used. When the two cylinders touch each other, the view factor is equal to 0.18 [16]. Of course, the diameter of the heat pipe and the bearings differ a bit, but it is the best approximation available. Calculating gives:

$$Q_{rad} = 0.62 \cdot 5.67 \cdot 10^{-8} \cdot \pi \cdot 0.072 \cdot 0.013 \cdot 0.18 \cdot (723^4 - 573^4) = 3.08 \text{ W}$$

So in total 14.0 W of heat is supplied from the heat pipe to one bearing.

Because the bearing is spinning at high speed, it is expected that some heat from the bearing flows to the surrounding air by convective heat transfer. If this value is in the same order as the heat flow from the heat pipe to the bearing, there is no need for bearing cooling.

In the worst case scenario the rotational speed of the heat pipe is 150 rpm. This means that the outer shell of the heat pipe has a velocity of 0.565 m/s. There is no transfer of torque by the bearings, so there is no slip between the heat pipe and the bearings. This means that the outer shell of the bearing also has a velocity of 0.4712 m/s. This gives a rotational speed of the bearing of 26.9 rad/s. The equation to calculate the convective heat transfer from the plate to the air is:

$$Q_{out_{conv}} = h_c \cdot A \cdot (T_s - T_a) \quad (2.28)$$

The convective heat transfer coefficient h_c can be calculated with the equation:

$$h_c = \frac{Nu_d \cdot k}{d} \quad (2.29)$$

Kreith et.al. [25] found an empirical correlation for the Nusselt number for a rotating disk. The equation is:

$$Nu_d = 0.36 \cdot (Re_\omega)^{\frac{1}{2}} \quad (2.30)$$

This correlation is valid for a rotating disk spinning in air for $Re_\omega < 10^6$. The Reynolds number is calculated as:

$$Re_\omega = \frac{\omega \cdot D^2}{\nu} \quad (2.31)$$

All properties used in these equations should be taken for air at an intermediate temperature between the surface temperature and ambient temperature. This intermediate temperature is calculated as:

$$T_{int} = \frac{T_s + T_\infty}{2} = \frac{623 + 293}{2} = 458 \text{ K} \quad (2.32)$$

All properties for air are taken from [14] and are listed in Table 3.

Table 3: Properties of air at 458 K and atmospheric pressure

Property	Value
ν (m ² /s)	$33.12 \cdot 10^{-6}$
k (W/mK)	0.0367

First the Reynolds number is calculated, this gives a Reynolds number of $1.433 \cdot 10^3$. This is below 10^6 , so Eq. 2.30 can be used to calculate the Nusselt number. Calculating the Nusselt number gives 12.87. The convective heat transfer coefficient h_c can now be calculated with Eq. 2.29. This gives a convective heat transfer coefficient h_c of 11.25 W/(m²K).

Now Eq. 2.28 can be used to calculate the heat transfer from the plate to the air, this gives:

$$Q_{out_{conv}} = h_c \cdot A \cdot (T_s - T_\infty) = 6.37 \text{ W}$$

There will also be some radiation from the bearing surface to the environment, the equation to calculate this is:

$$Q_{out_{rad}} = \epsilon \cdot \sigma \cdot 0.5 \cdot A \cdot (T_s^4 - T_\infty^4) \quad (2.33)$$

Only half of the area of the bearing is used, because approximately the other half views the hot heat pipe, so no radiative heat loss will take place here. The emissivity is assumed to be one. Calculating gives:

$$Q_{out_{rad}} = \sigma \cdot 0.5 \cdot A \cdot (T_s^4 - T_\infty^4) = 6.97 \text{ W}$$

So the total heat transfer from the plate to the surroundings is:

$$Q_{out} = Q_{out_{conv}} + Q_{out_{rad}} = 13.34 \text{ W}$$

The total heat transfer is lower than the heat input, which was 14.0 W. So, extra cooling will be needed to prevent overheating. This will especially be the case when the setup is running for a long time. Extra cooling can be provided by blowing air in counter flow over the bearing.

3 Measurement and control in Delft setup

In this part the measurements will be described. This includes the sensors that are used and the hardware and software used for data acquisition.

3.1 Temperature measurements inside the heat pipe

Inside the wall of the heat pipe, there are six locations in axial direction where temperature and temperature gradient are measured. This is done by placing four K type thermocouples in series. The configuration can be seen in Figure 3.1. The purpose of using four thermocouples is to increase the precision of the measurement. For the temperature measurement the thermocouple in the bottom-left corner (MHF3) is used. For the temperature gradient measurement, all four thermocouples are used instead of using only two. This doubles the voltage, so if one of the temperature gradients is measured wrong, the error is only half.

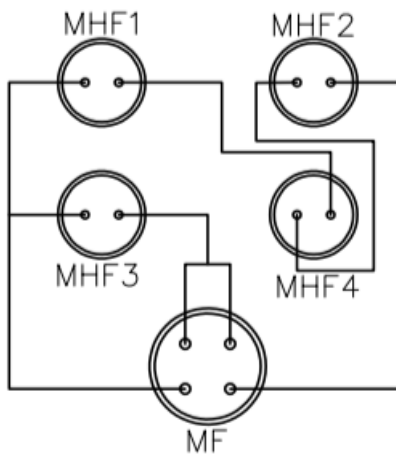


Figure 3.1: Configuration of the four thermocouples

Furthermore, there are five thermocouples placed in the vapour channel of the heat pipe. One of them is placed in the evaporator zone, another one is placed in the adiabatic zone and the other three are placed in the condenser zone. This is done because it is expected that the largest temperature gradient will be in the condensation zone. There is also a thermocouple at the outside of the wire tube, to check if the wires will not get too hot.

All those temperature signals are transported through the slip ring to two NI 9213 temperature input modules. This module has 16 channels, but there are 17 temperature inputs from the heat pipe, so two of them are needed. This will also make it possible to place more thermocouples in a new heat pipe that could be made in the future. Furthermore, another three thermocouples are placed inside the cabinet. The first one measures the temperature of the heating unit. The second one measures the air temperature inside the cabinet. The last one measures the temperature at the outlet of the cooling duct.

3.2 Data acquisition hardware

For the data acquisition several hardware components from National Instruments are used. First, a compactRIO 9066 is selected. This is a programmable controller where all the modules can be placed in. There are two NI 9213 temperature input modules, which can handle 16 temperature inputs per module. There is also a NI 9421 8 channel digital input module. This module is used for safety, for

instance to check if the doors are closed before the heat pipe can start rotating. Furthermore, there is a NI 9482 4 channel relay output, which is used to turn the motor or the fan on. Next, a NI 9201 8 channel analog input module is installed. This module measures different analog signals, for instance the air velocity in the fan channel or the pressure inside the heat pipe. The compactRIO processes these signals to make a calculation of the heat removed by the fan or shut off the heating unit in case the pressure becomes above 5 bar. Last, there is a NI 9265 4 channel analog output module, which controls the various frequency controllers. Those frequency controllers control the speed of the motor and the fan. There is also a controller for the lamps attached to this analog output module.

3.3 LabVIEW

All the signals that are acquired by the compactRIO should be processed. Therefore, a LabVIEW file is programmed. First, a list of requirements for the program is made:

- The program must show all temperatures and heat fluxes.
- The motor, the fan and the lamps must be controlled with the program.
- The pressurized air valve and the mist cooling must be turned on and off.
- The heat pipe should rotate before the cooling can be turned on and the cooling should be turned on before the lamps can be turned on.
- If the pressure inside the heat pipe exceeds 5 bar absolute, the heating should be turned off.
- If the wires of the thermocouples inside the heat pipe get hotter than 200 °C the heat should be turned off.
- If the emergency stop is pushed, the doors or heater unit are not closed or the temperature alarm is high, the motor, the fan, the lamps, the pressurized air and the mist cooling should be turned off.
- When the stop button is pressed, the motor, the fan, the lamps, the pressurized air and the mist cooling should be turned off.
- Data should be logged after every x seconds, x should be adjustable.

Furthermore, DEMO made an IO list. In the IO list, it is specified which signal is measured by which channel from the compactRIO. In this way it is possible to connect the inputs to the corresponding indicators. With a number of AND and OR blocks the required safety procedures are programmed. After that, a sequence structure is included. This sequence structures reinitialises the control buttons for the motor, the fan, the lamps, the pressurized air and the mist cooling to their default value, which is off. It reinitialises them when the program is executed and after the stop button is pushed. This guarantees that everything should be turned on by hand at the start of the program and everything is turned off again when the program is stopped.

Last, the data logging is programmed. The compactRIO has its own memory, where the program is saved and executed. Therefore, the data is stored on the memory of the compactRIO as well. On the front panel of the program there is a button 'Datafile' in the upper left corner. With this button one can choose what should happen with the datafile. Its default value is 'create or replace'. The benefit of this value is that it will delete the old datafile, by doing this it will prevent that the memory overflows. One can also choose to use the 'open or create' value. This will add the data at the end of the existing data set or create a new file if it does not exist. The logged data can be accessed with the File Transfer Protocol. It can be accessed by following the path: <ftp://169.254.127.72/home/lvuser/> when the compactRIO is connected. 169.254.127.72 is the IP address of the compactRIO. The IP

address of the compactRIO can be checked with NI MAX. If the IP address in NI MAX is different than 169.254.127.72 the number shown in NI MAX should be used in the path. The default name of the logged data is 'Data.TDMS'. When the path is followed and this file is clicked, the file is downloaded to your computer. This file can be opened with several programs. It is possible to open it with notepad, but also with Microsoft Excel. The name of this file can be changed in the block diagram.

A picture of the front panel of the program can be seen in Figure 3.2. Also, in Appendix D a larger picture of the front panel can be seen and the block diagram of the program. The program is tested with some dummy signals and a slightly different version of the program is tested during a leakage test of the heat pipe. In both situations the programs worked as expected. It is recommended to test all the safety procedures during commissioning of the setup.

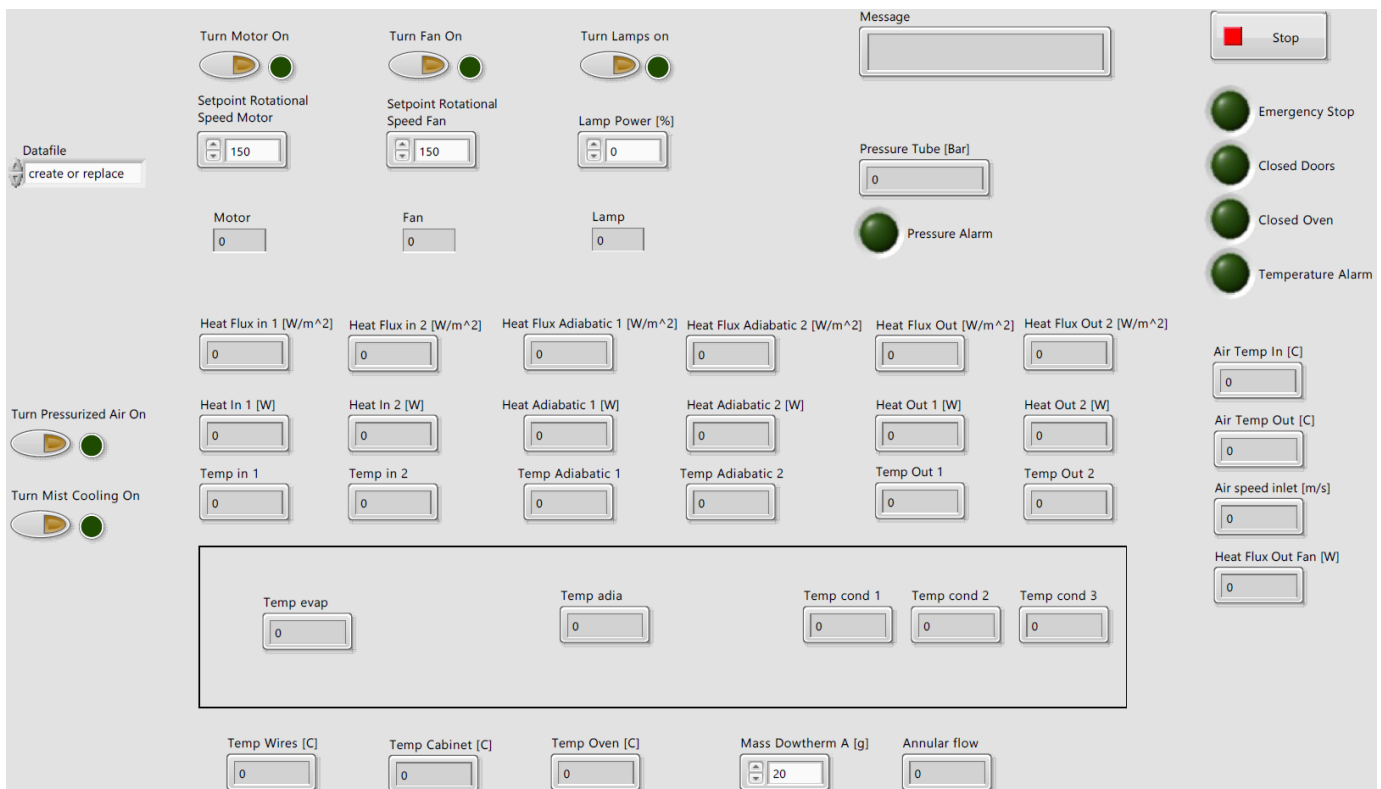


Figure 3.2: Picture of the front panel of the LabVIEW program

4 Model of the Delft setup

For the prediction of the behaviour of the experimental setup and to interpret the data of the setup a model has been developed. In this model, the parameters can be adjusted according to the setup. In this chapter, a description of this model and its validation with the data from literature is given.

4.1 Rotating heat pipe model

In the literature, there are a lot of papers about modelling a heat pipe. Some of the papers contain data of experiments, which could be used for model validation. The report of Xie et al. [26] contains data for a rotating heat pipe and most variables are described. However, the data can only be used for the steady state behaviour of the heat pipe, because the transient data is not reliable. It gives the impression that there is less heat input at the start of the experiment. Another report that is interesting for modelling and model validation is the report of Ferrandi et al. [27]. Although this report contains a non-rotating heat pipe, it contains accurate data for validation, especially for transient behaviour. Because the heat pipe contains a wick it can be regarded as a rotating heat pipe in annular flow. Also, the report gives a very clear description of how the heat capacity and conductivity of the wick should be calculated.

In [28], it is shown that a network model can provide a reasonably accurate and practically simple way to model a transient heat pipe. For steady state analysis the network model is very accurate, because the interior of the heat pipe does not change anymore. Therefore, the resistances can be calculated very accurate. Furthermore, using a CFD model would require a lot more computing time and the extra information it provides is of low value for the commissioning of the heat pipe setup. Therefore, it is chosen to create a network model.

A network model consists of several resistances. In Figure 4.1, an overview of the heat transfer network as reported in [28] is shown. This will be similar for the model presented in this paper. The dotted lines of number three and six are very small resistances that can be neglected. Resistance number 3 is the vapour channel resistance. If the adiabatic zone of the heat pipe has perfect insulation, this resistance is zero. Resistance number 6 is an important flow for the liquid to return to the evaporator. However, if there is no heat exchange between the liquid and vapour flow in the adiabatic zone, this resistance is zero. Also the Delft setup does not have a wick, but there is a liquid layer. In the network model the liquid layer is nearly the same as the wick. It is also a resistance through which the heat has to flow. The only difference is the conductivity of the layer, because the wick material is in general a better conductor than the liquid.

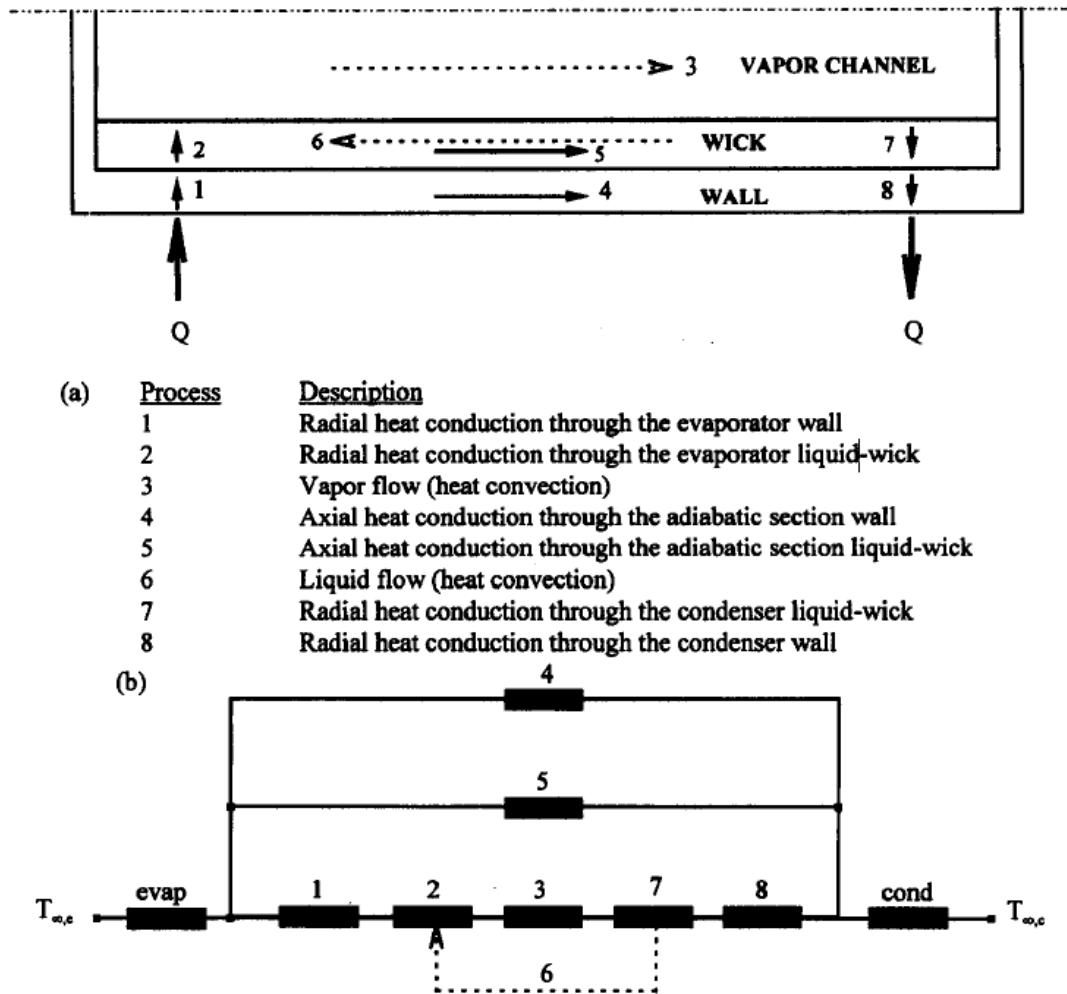


Figure 4.1: An overview of the heat transfer network and the corresponding resistances as reported in [28]

The resistances used for the Delft setup network model are shown in Figure 4.2. The model consists of seven nodes which are connected via the resistances. There are nodes for the evaporator section, the adiabatic section and the condenser section. Every section has two nodes for both the wall and the liquid inside the heat pipe. In the Delft setup all the sections have an equal length of 166 mm, so this has been used for the model as well. The vapour channel has only one node, because the vapour channel resistance is neglected. The resistance for the vapour flow is considerably smaller than other resistances [28]. Therefore, this assumption does not create significant errors.

All the nodes have a lumped mass, except for the vapour channel node. The mass of the vapour is very small, especially at low temperatures. When the time step is taken too large and the heat flux is high, this causes the model to diverge. Using a small time step can solve this, but it would make the model very slow. Therefore, it is chosen to use a node without mass. The temperature of the vapour channel depends then directly from the heat input and heat output.

Furthermore, there are two resistances which connect the heat pipe to the source and sink temperature. For the source resistance, it is the radiation resistance from the lamps to the heat pipe. For the sink resistance, it is the convective cooling resistance between the heat pipe and the duct temperature. For the radiative resistance the equations from the analytical calculation of Chapter 2.2 are used. For the convective cooling the equations from Chapter 4.3 of [8] are used.

4.2 Modelling approach

In Figure 4.3 an arbitrary node with one input and one output is shown. For any arbitrary node, an energy balance can be written as:

$$\frac{d}{dt}(m_i c_{p,i} T_i) = \sum Q_{i,in} - \sum Q_{i,out} \quad (4.1)$$

The node in Figure 4.3 only has one heat input and one heat output, so the sigma is not necessary, but Figure 4.2 shows that every node has at least three connections.

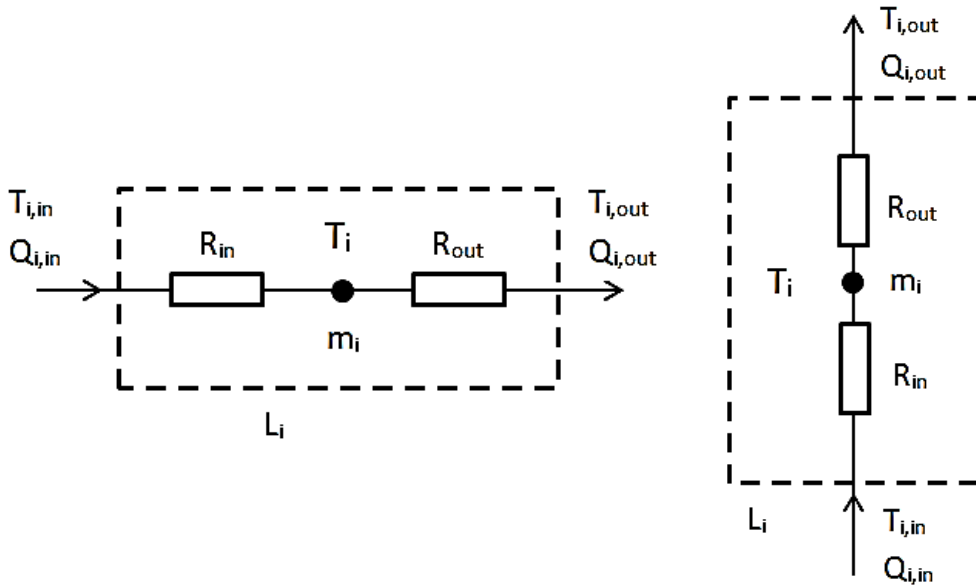


Figure 4.3: Arbitrary node in axial direction (left) and radial direction (right)

Because the mass and heat capacity are assumed to be constant for a given time step, Eq. 4.1 can be rewritten as:

$$\rho_i A_i L_i c_{p,i} \cdot \frac{dT_i}{dt} = Q_{i,in} - Q_{i,out} \quad (4.2)$$

Where $Q_{i,in}$ and $Q_{i,out}$ can be defined as: (4.3)

$$Q_{i,in} = \frac{T_{i,in} - T_i}{R_{in}}$$

$$Q_{i,out} = \frac{T_i - T_{i,out}}{R_{out}} \quad (4.4)$$

Because the heat pipe has a uniform cylindrical shape, cylindrical coordinates are used. This means that the equation of the resistance differs for the axial and radial direction. In axial direction the equation for R_{in} is:

$$R_{in} = \frac{L_i}{k_i \cdot A_i} \quad (4.5)$$

And the equation for R_{in} in radial direction is:

$$R_{in} = \frac{\ln \frac{r_{i,in}}{r_i}}{k_i \cdot 2\pi \cdot L_i} \quad (4.6)$$

Next, the temperatures $T_{i,in}$ and $T_{i,out}$ have to be specified. These temperatures can be calculated by using the neighbouring node, because $Q_{i,in}$ is equal to $Q_{i-1,out}$. Derivation of this gives that $T_{i,in}$ can be specified as:

$$T_{i,in} = \frac{T_i \cdot R_{in} + T_{i-1} \cdot R_{out}}{R_{in} + R_{out}} \quad (4.7)$$

Please note that R_{out} in this case is the resistance of the previous node. When specifying this resistance for $T_{i,in}$ in axial direction, this gives:

$$T_{i,in} = \frac{T_i \cdot \left(\frac{k_i A_i}{L_i}\right) + T_{i-1} \cdot \left(\frac{k_{i-1} A_{i-1}}{L_{i-1}}\right)}{\left(\frac{k_i A_i}{L_i}\right) + \left(\frac{k_{i-1} A_{i-1}}{L_{i-1}}\right)} \quad (4.8)$$

The equations for $T_{i,in}$ and $T_{i,out}$ can then be substituted in Eq. 4.3 and Eq. 4.4. After that, Eq. 4.3 and Eq. 4.4 can be substituted in Eq. 4.2.

Non-annular flow

As calculated in Chapter 2.5, non-annular flow lowers the resistance compared to annular flow when operating with the same amount of fluid. Therefore, this has to be implemented in the model. Similar to the calculation in Chapter 2.5, the fill factor per square root viscosity is calculated. The amount of liquid that evaporates is calculated with Eq. 2.17 till Eq. 2.20. With the mass of liquid, the thickness of the liquid layer at every node can be calculated, assuming annular flow. In the model the head difference between the evaporator and condenser is not calculated. To compensate for the head between the evaporator and condenser, the parameter 'reducedm' can be adjusted. When this parameter is one, the liquid layer thickness is equal at every node. When this parameter is below one, for instance 0.8, 20 percent of the liquid mass is replaced from the evaporator to the condenser. At the adiabatic section the liquid layer thickness is kept the same.

The head can be calculated with the Darcy-Weisbach equation [34]:

$$\frac{\Delta p}{L} = f_D \cdot \frac{\rho}{2} \cdot \frac{\bar{v}}{d_h} \quad (4.9)$$

Where the pressure difference Δp can be described as:

$$\Delta p = \rho \cdot g \cdot \Delta h \quad (4.10)$$

This equation relates the pressure difference, and thus the head, between the condenser liquid layer and evaporator liquid layer to the friction in the liquid layer flow. The length of the liquid layer channel is described as: $L = \frac{1}{2} \cdot L_e + L_a + \frac{1}{2} \cdot L_c$

Because the head calculation is only valid when there is annular flow inside the heat pipe, the heat pipe is rotating with high rotational speed. Therefore, the centripetal acceleration will be much larger

than the gravitational acceleration, so the gravitational acceleration in Eq. 4.10 can be replaced by the centripetal acceleration. The centripetal acceleration is equal to:

$$a_c = \omega^2 \cdot r \quad (4.11)$$

When there is laminar flow inside the heat pipe, the Darcy friction factor f_d can be calculated with [34]:

$$f_d = \frac{64}{Re_d} \quad (4.12)$$

Re_d can be calculated with Eq. 2.8. Eq. 4.12 is valid if $Re_d < 2300$.

Substituting Eq. 4.10 and Eq. 4.12 in Eq. 4.9 gives:

$$\Delta h = \frac{L}{\rho} \cdot a_c \cdot \frac{32\mu \cdot \bar{v}}{d_h^2} \quad (4.13)$$

The average velocity \bar{v} is calculated as:

$$\bar{v} = \frac{\dot{m}}{\rho_l \cdot A_{La}} \quad (4.14)$$

The mass flow can be calculated by:

$$\dot{m} = \frac{Q}{\Delta h_{fg}} \quad (4.15)$$

In the worst case scenario the heat flow is 900 W and the temperature inside the heat pipe is 623 K. Then the Reynolds number is 667.1, so Eq. 4.12 can be used to calculate the Darcy friction factor.

A Matlab program has been written to calculate the head. This program also gives a suggestion for the parameter 'reducedm', based on the head calculation. It should be noted that this is only valid for annular flow. For non-annular flow it is suggested to set the parameter 'reducedm' to one. This Matlab program can be found in Appendix E.

The mass of liquid can also be used to calculate the fill factor per square root of viscosity. This factor is used to calculate the rotational speed at which annular flow occurs. Next, a gain is introduced to lower the resistance of the liquid layer when there is non-annular flow. When the rotational speed is equal or greater than the annular flow rotational speed the gain is one. Below the annular flow rotational speed the gain is calculated as:

$$Resistance\ gain = \frac{\omega_{annular}}{\omega_{heatpipe}} \quad (4.16)$$

In this equation $\omega_{annular}$ is the rotational speed at which complete annular flow would occur and $\omega_{heatpipe}$ is the actual rotational speed of the heat pipe. A graphical representation of this equation can be seen in Figure 4.4.

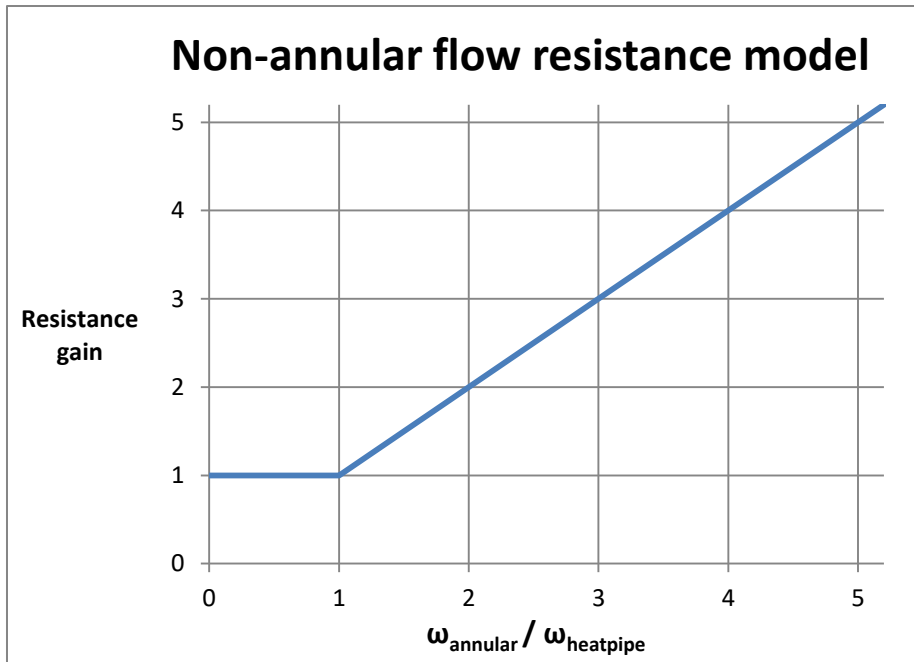


Figure 4.4: Resistance gain model for non-annular flow

The properties of Dowtherm A and 316 stainless steel are dependent of the temperature. Therefore, their properties are calculated for each node by using the previous temperature at that node. For Dowtherm A the properties supplied by The Dow Chemical Company are used [29]. For 316 stainless steel the correlations found in [30] are used. If a correlation is available, the equation is implemented in Simulink, otherwise a lookup table is used. It uses linear interpolation between two tabulated values.

Next, the model can be programmed. This has been done in Simulink. Simulink is a block diagram based programming environment. In the model, all the nodes are programmed and connected with each other. The differential equations are solved with the explicit fourth order Runge-Kutta solver with a fixed time step of 0.1 s. This time step is chosen to keep the simulation fast and stable. In combination with the Simulink model there is a Matlab file which contains all the fixed variables. An overview of this file and the Simulink file can be found in Appendix F.

4.3 Literature based validation

As described in the introduction, there are two papers available for validation of this model. The first one [26] is a stainless steel rotating heat pipe filled with ammonia. It is filled with a large amount of ammonia. This paper is used to check the steady state behaviour. The second one [27] is a copper heat pipe with a wick, which is non-rotating. The heat pipe is filled with water. Due to the wick the heat pipe can be regarded as a rotating heat pipe with annular flow. Also, this paper contains very precise data for both transient and steady state behaviour.

4.3.1 Rotating ammonia heat pipe

For this validation, the current model is adjusted slightly. First, the heat pipe is filled with ammonia instead of Dowtherm A, so the correct fluid properties are implemented. The heat pipe has a fill factor per square root of viscosity of $59.9 \text{ cP}^{-1/2}$ and the rotational speed is 400 rpm. From Figure 2.21, it can be seen there is definitely non-annular flow behaviour. Therefore, non-annular flow compensation is used. Also, the heating and cooling of the heat pipe is done in another way. For the heating, a constant heat supply of 100 W is applied. For the cooling a fan has been used, but the condenser has fins to increase the cooling area. In [31], it is stated that a convective heat transfer coefficient of $335 \text{ W/m}^2\text{K}$ is applicable and an area increase factor of 1.5 to account for the fins is considered. For consistency, these values are also used for this validation. All the other parameters that specify the heat pipe can be found in Table 4. Most of them are found in [26], but some values are not specified. For instance, the adiabatic zone diameter and wall thickness are not specified. These values are estimated from the schematic overview of the setup.

Table 4: Parameters used for validation of ammonia heat pipe [26]

Parameter	Value
Overall Length	600 mm
Evaporator section length	300 mm
Adiabatic section length	200 mm
Condenser section length	100 mm
Heat pipe material	Steel
Material of fins	Aluminium
Evaporator outer diameter	42 mm
Adiabatic outer diameter	37 mm
Condenser outer diameter	28 mm
Evaporator wall thickness	6 mm
Adiabatic wall thickness	6 mm
Condenser wall thickness	1.5 mm
Working fluid	Ammonia
Working fluid loading	40 g
Heat input to the evaporator	100 W
Cooling air temperature	20 °C
Experiment time	45 minutes

Also, the heat pipe material is specified as steel. Due to corrosion between carbon steel and ammonia, it is expected that stainless steel has been used, so the properties of 316 stainless steel are used in this validation.

In Figure 4.5 the results of the experiment in the paper and the simulation are shown. As stated before, only the steady state behaviour can be validated with this experiment, because the transient of the experiment has a different shape than expected. It could be that the constant heat supply is not constant, due to start up time of the heater. Also, it could be that there is extra mass that has to be heated, for instance the supports of the heat pipe. This will also increase the time to reach steady state. Nevertheless, the steady state behaviour of the model is close to the steady state behaviour in the experiment. After 45 minutes, the temperature difference between the model prediction and the experiments at the evaporator is 0.34 K and at the condenser it is 0.96 K. The differences could have to do with the experiment results as well, because the measurements are done with several thermistors with an accuracy of ± 0.25 K. Furthermore, the result at steady state was given without decimals, which means that there could be a rounding error of up to 0.5 K. So, the heat pipe model is validated at steady state with non-annular flow.

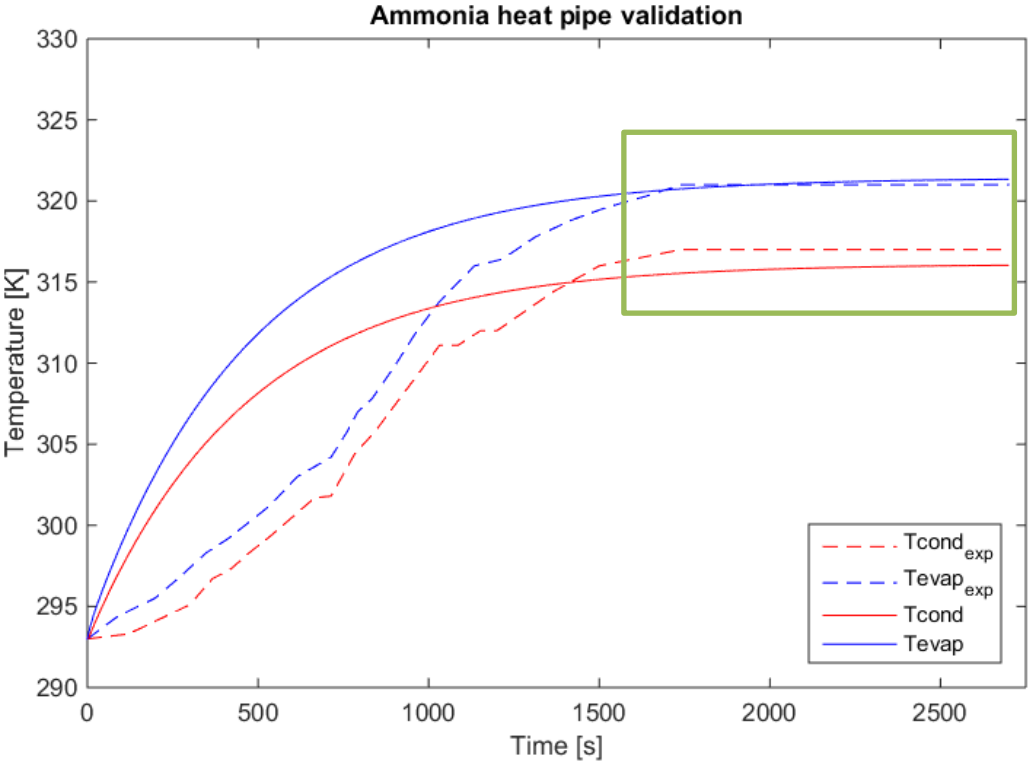


Figure 4.5: Comparison between ammonia heat pipe experiment and simulation

4.3.2 Non rotating water-copper heat pipe

The water-copper heat pipe is used to check the transient behaviour of the heat pipe model. The major difference with this heat pipe compared to the heat pipe model is that this heat pipe has a wick. This is translated to an annular flow for a rotating heat pipe. Furthermore, in the paper it is specified how thermal resistance of the wick/liquid layer should be modelled. Also, the heating profile and the convective heat transfer coefficient are specified in the paper. In addition to the graph with the results, there is also a table with the temperatures after certain times. These temperatures are very precise and can be used for the comparison.

Table 5: Parameters used for validation of water-copper heat pipe [27]

Parameter	Value
External tube diameter	19.1 mm
Internal tube diameter	18.8 mm
Internal wick diameter	17.3 mm
Evaporator length	600 mm
Adiabatic length	90 mm
Condenser length	200 mm
Wick porosity	0.5
Initial temperature	296.2 K
Cooling water temperature	294.5 K
Cooling water mass flow	0.01133 kg/s
Copper thermal conductivity	390 W/(mK)

The result of the simulation is shown in Figure 4.6. Also, the temperatures of the experiment and the simulation at the different times are shown in Table 6 and Table 7. The temperatures of the simulation are slightly higher at every time step. The maximum difference is for the temperature at the evaporator after 66 seconds. The temperature difference is then 0.63 K. The root-mean-square error is 0.3625 K.

Table 6: Temperatures of the experiment at different times

Temperature [K]	66 s	130 s	225 s	1000 s
Tevap	315.72	331.43	337.68	341.59
Tvapor	313.20	327.46	333.11	336.62
Tcond	306.34	315.62	319.28	321.55

Table 7: Temperatures of the simulation at different times

Temperature [K]	66 s	130 s	225 s	1000 s
Tevap	316.35	331.93	337.92	341.80
Tvapor	313.64	327.91	333.34	336.85
Tcond	306.57	315.97	319.54	321.85

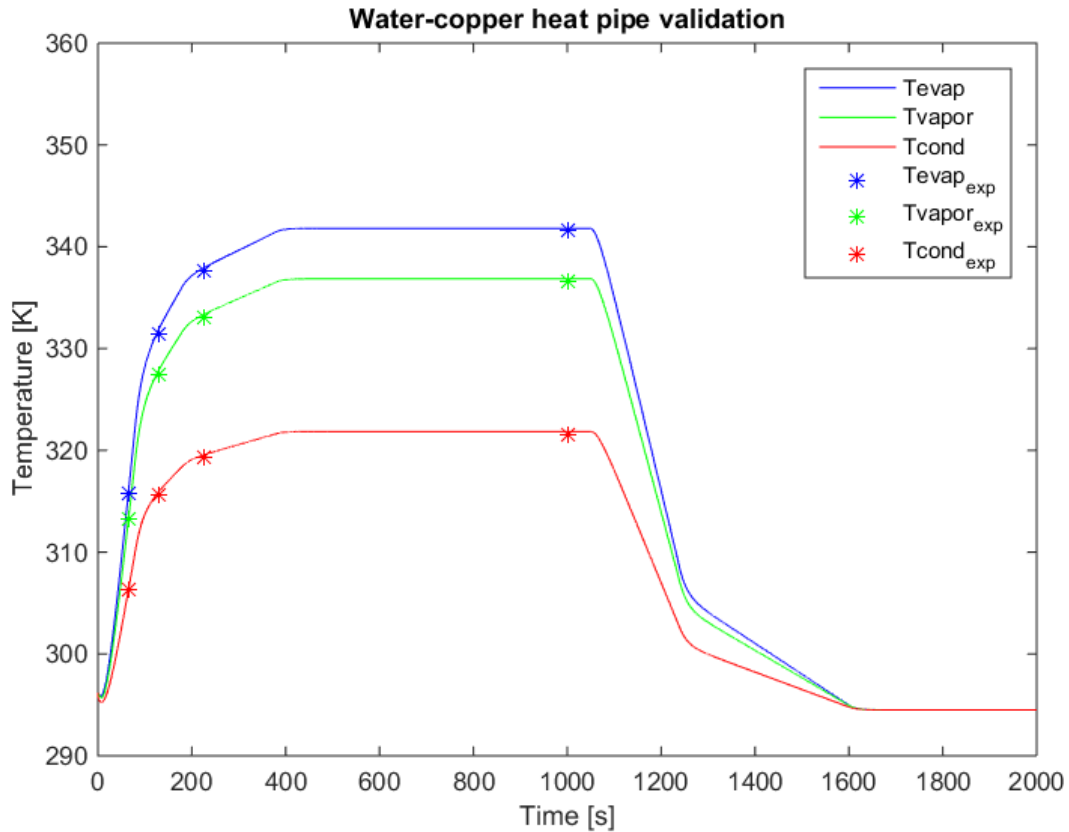


Figure 4.6: Comparison between water-copper heat pipe experiment and simulation

4.3.3 Conclusion

A network model can provide a simple model which can be used for both steady state and transient behaviour. The validations look promising, so the network model can be used to compare the simulations with the experiments. Of course, the model could be improved, so there are some recommendations as well. First, the head calculation could be included in the program, so that the parameter 'reducedm' is calculated during the simulation, depending on the rotational speed and heat flux. However, this calculation is only valid for annular flow. Furthermore, it could be better to calculate the resistance gain for non-annular flow per node instead of for the whole pipe. When the head calculation is programmed, the fill factor per square root viscosity could be calculated for all three nodes. Then, the gain factor would be more accurate for both the evaporator and the condenser. This might improve the validation with the ammonia heat pipe.

5 Commissioning of the Delft setup

In this chapter an update of the latest status for the Delft rotating heat pipe setup is given.

The heat pipe itself is finished. The end parts have been welded to the heat pipe. Now, the electrical connections from the heat pipe to the slip ring are connected by Thermo Electra. The cabinet is almost finished. The heater unit and the cooling channel are finished. The electrical connections are also connected. They can be controlled with the LabVIEW program. The LabVIEW program has been tested during a leakage test with the actual heat pipe. The goal of this test was to check if the seal of pressure sensor does not leak. During this test the LabVIEW program functioned as it should be. The bearing cooling is also finished.

For the filling of the heat pipe with Dowtherm A, a procedure has been written. The required equipment for the squeezing of the valve is available. This procedure has been tested. It seals the heat pipe completely. When the heat pipe returns from Thermo Electra it will be filled with 35 gram of Dowtherm A, vacuumed and sealed with the squeeze tube.

Then, the heat pipe will be placed inside the cabinet. It should be checked that all the safety procedures work before any experiments are conducted. When the safety procedures work, experiments can be done with the heat pipe.

6 Conclusion

In this chapter a conclusive summary of this thesis is given. After that, some recommendations are given for further research with the Delft setup.

6.1 Conclusive summary

In the introduction, the goal of this thesis is described as: finishing the development of the TU Delft rotating heat pipe setup and using this test setup to validate the developed model. This goal was divided into several objectives.

After the description of the setup and its changes compared to the setup described in [8], an investigation of what has to be done before the commissioning of the setup was made. It was discovered that the heat input calculation in [8] is overestimated, because insulation is not taken into account. Therefore, a new calculation was made. It is concluded that at the highest temperature 1155 W of heat input is needed. Also, the available band heaters could not be used, therefore IR heating with quartz lamps has been considered. A calculation was made to confirm if they will provide enough power to meet the requirements of the setup. It is concluded that six quartz bulbs with an effective heating length of 165 mm will provide enough power. In the filling amount calculation, it is learned that non-annular flow is beneficial for the heat transfer compared to annular flow. This conclusion is only valid when the heat pipe is filled with the same amount of fluid. Also, it was decided to fill the heat pipe with 35 grams of Dowtherm A as a start. With this amount of fluid, it is possible to operate the heat in annular and non-annular flow over the whole temperature range. The slip ring will not cause large deviations when measuring the temperature. Last, it is concluded that bearing cooling is needed.

Another objective was to select the required data acquisition hardware and program the required software for control and data acquisition. A compactRIO 9066 is selected together with two temperature input modules, a 8 channel digital input module, a 4 channel relay module, a 8 channel analog input module and a 4 channel analog output module. This configuration is able to process all the signals and has extra capacity to handle more signals in the future. A LabVIEW program was designed to control the Delft setup. This program meets all the requirements. It has been tested with dummy signals and during a leakage test with the actual heat pipe. During these tests everything worked as it should be.

A model which represents the actual Delft rotating heat pipe setup has been made. The same inputs as in the Delft setup can be adjusted. This model has been developed as a network model. These types of models are often used because of their reasonably accurate and practically simple way to model transient heat pipe analysis. This model was validated with two different papers. In the first paper, an experiment is performed with a stainless steel ammonia heat pipe, which operates in non-annular flow. The data of this paper is only useful for steady state. At the steady state part, the maximum deviation is 0.96 K. In the second paper, a copper-water heat pipe is used. This heat pipe is not rotating, but has a wick. This means its behavior is similar to a rotating heat pipe with annular flow. The data of this paper is very precise and shown in a graph and in a table at three different points at 4 time stamps. The root-mean-square error between the experiment and the model at all data points is 0.36 K.

The commissioning of the heat pipe is in progress now. When all the safety procedures are checked, the experiments can be conducted.

6.2 Recommendations

Based on the experiences during this thesis, some recommendations are given for the experiments with the Delft setup and for the manufacturing of a new heat pipe in the future.

6.2.1 Recommendations for the experiment

During the leakage test it was discovered that the reading of the pressure sensor in the heat pipe is influenced by the temperature. Therefore, it is recommended to use some of the temperature readings at the inside of the heat pipe for the measurement of the pressure inside the heat pipe. However, the pressure sensor can be used for vacuum reading when the heat pipe is at room temperature.

Also, it is recommended to use the forced convection bearing cooling all the time. The bearings might not get too hot, but the electronics are also sensible for high temperatures and could eventually be damaged by the high temperatures of the heat pipe.

When starting with experiments, it is recommended to start with low temperatures and low heat fluxes. When these experiments go well, these variables can be increased slowly. When something happens with the heat pipe at high temperature, at least some data at lower temperatures is gathered then already.

Furthermore, it could be useful to validate the annular flow correlation found by Krishnan [18]. Together with that it could be investigated if there is hysteresis in the annular flow correlation.

Last, the non-annular flow resistance model proposed in Chapter 4.2 could be validated.

6.2.2 Recommendations for manufacturing a new heat pipe

It is recommended to change the design of the end parts. Because the end part is welded over the pressure sensor, the pressure sensor can never be reached without damaging the heat pipe. A leakage test is performed to check if the pressure sensor is not leaking, but this is no guarantee this will never happen after a certain amount of experiments. In a future heat pipe it would be better to be able to reach the pressure sensor without damaging the heat pipe.

References

- [1] G. Paulussen. (2010). *Heat pipe assisted strip heat treatment*. Tata Steel. Patent No. WO2011012257A1
- [2] M.F. Ashby et al. (2009) *Materials engineering, science, processing and design*. Second edition, pp. 479–493
- [3] G. Grover. (1963) *Evaporation-condensation heat transfer device*. Patent No. US3229759A
- [4] V. Gray. (1969) *The rotating heat pipe—a wickless hollow shaft for transferring high heat fluxes*. Proc. of ASME/AIChE Heat Transfer Conference. ASME paper 69-HT-19.
- [5] O. Ramos jr. *Inspired Heat-Pipe Technology*. (7 September 2017)
http://www.lanl.gov/science/NSS/issue1_2011/story6full.shtml
- [6] *The 'liquid cooling' system from the Galaxy S7 explained*. (7 September 2017)
<https://www.sammobile.com/2016/03/07/the-liquid-cooling-system-from-the-galaxy-s7-explained/>
- [7] G. Paulussen. (2009) *Continuous Heat Treatment using Heat Pipes*. Tata Steel. Internal document, Reference Source no.: 145630
- [8] B. Meltzer. (2016) *High Temperature Rotating Heat Pipe Setup for the Heat Pipe Assisted Annealing Project*. Delft University of Technology. MSc thesis,
<http://resolver.tudelft.nl/uuid:528b3a9c-21a7-4010-827f-311c5df180d3>
- [9] M. Celik, M. Patki, G. Paulussen, W. de Jong and B.J. Boersma. (2018) *Dynamic modelling of the Heat Pipe Assisted Annealing Line*. Submitted to Joint 19th IHPC and 13th IHPS, Pisa, Italy, 10-14 June 2018
- [10] M. Celik et al. (2018) *Experimental and numerical investigation of contact heat transfer between a rotating heat pipe and a steel strip*. International Journal of Heat and Mass Transfer. Vol. 122, pp. 529–538
- [11] *Rotex Torsionally flexible coupling*. (16 January 2018)
<https://eriks.nl/documentatie/mechanische-aandrijftechniek/Askoppelingen/ktr-rotex.pdf>
- [12] *Kulite High Temperature High Bandwidth Amplified Gas Turbine Pressure Transducer ETL-GTS-X-312 (M) Series*. (2014) <http://www.kulite.com/docs/products/ETL-GTS-312.pdf>
- [13] T.W. Uhlmann, M.B.H. Mantelli, M. Manzoni, M. Marengo and P. Eskilson. (2016) *Experimental Tests on Sodium Thermosyphons*. Proc. of the 18th IHPC and 12th IHPS, Jeju, Korea, 12-16 June 2016
- [14] A.F. Mills. (2013) *Basic Heat and Mass Transfer*. Pearson New International Edition, Second edition.
- [15] M.F. Modest. (2003) *Radiative Heat Transfer*. Academic Press, Second edition, pp. 745–758

- [16] I. Martínez. (8 March 2017) *Radiative view factors*.
<http://webserver.dmt.upm.es/~isidoro/tc3/Radiation%20View%20factors.pdf>
- [17] S. Suppiah Singaram, H. Lodha & R.J. Jachuck. (2014) *Experimental investigation of continuous single-phase rimming flow in a horizontal rotating cylinder*. *AIChE Journal*, Vol. 60 (11), pp. 3939-3950. doi:10.1002/aic.14569
- [18] V. Krishnan. (2016) *Study of flow patterns inside a rotating heat pipe*. Tata Steel. Internship report, Reference Source no.: 166078
- [19] *Slip ring datasheet SRH2578 series* (13 April 2017) <http://www.penlink.se/docs/SRH2578en.pdf>
- [20] *NI 9213 datasheet* (13 April 2017) http://www.ni.com/pdf/manuals/374916a_02.pdf
- [21] *NI 9214 and TB-9214 datasheet* (13 April 2017)
http://www.ni.com/pdf/manuals/375138a_02.pdf
- [22] *Kogellager*. (21 September 2017) https://ceratec-ceramic-bearings.com/kogellager.html#kogellager_pagina
- [23] *Information of Zirconia (Zirconium Oxide, ZrO₂)*. (21 September 2017)
<http://global.kyocera.com/prdct/fc/list/material/zirconia/zirconia.html>
- [24] *Deep Groove Ball Bearings 6302*. (25 April 2017) <http://www.skf.com/group/products/bearings-units-housings/ball-bearings/deep-groove-ball-bearings/deep-groove-ball-bearings/index.html?designation=6302&nfp=NFP-6302>
- [25] F. Keith, R.M. Manglik and M.S. Bohn. (2011) *Principles of heat transfer*. Cengage, Seventh Edition, p. 337
- [26] M. Xie, Z. Xue, W. Qu, and W. Li. (2015) *Experimental investigation of heat transfer performance of rotating heat pipe*. *Procedia Engineering*. Vol. 99, pp. 746-751.
- [27] C. Ferrandi, F. Lorizzo, M. Mameli S. Zinna and M. Marengo. (2010) *Lumped parameter model of sintered heat pipe: Transient numerical analysis and validation*. *Applied Thermal Engineering*. Vol. 50(1), pp. 1280-1290.
- [28] Z.J. Zuo and A. Faghri. (1998) *A network thermodynamic analysis of the heat pipe*. *International Journal of Heat and Mass Transfer*. Vol.41 (11), pp.1473-1484.
- [29] *Dowtherm A Product Technical Data*. (6 June 2017)
http://msdssearch.dow.com/PublishedLiteratureDOWCOM/dh_0030/0901b803800303cd.pdf
- [30] *AUSTENITIC STAINLESS STEEL (316)*. (8 November 2017)
<http://www-ferp.ucsd.edu/LIB/PROPS/PANOS/ss.html>
- [31] M. Patki. (2017) *Dynamic Behaviour of Heat Pipe Assisted Annealing*. Delft University of Technology. MSc Thesis No. 2758
- [32] L. Lin and A. Faghri. (1998) *Condensation in Rotating Stepped Wall Heat Pipes with Hysteretic Annular Flow*. *Journal of Thermophysics and Heat Transfer*. Vol.12 (1), pp.94-99.

[33] J. T. Anderson and O. A. Saunders. (1953) *Convection from an Isolated Heated Horizontal Cylinder Rotating about Its Axis*. Proceedings of the Royal Society A: Mathematical, Physical and Engineering Sciences, Vol.217 (1131), pp.555-562.

[34] F.M. White. (2011) *Fluid Mechanics*. McGraw-Hill, Seventh edition in SI units.

List of symbols

Latin symbols

A	Area	$[m^2]$
a_c	Centripetal acceleration	$\left[\frac{m}{s^2}\right]$
c_p	Specific heat capacity at constant pressure	$\left[\frac{J}{kg \cdot K}\right]$
d	Diameter	$[m]$
d_h	Hydraulic diameter	$[m]$
F	View factor	$[-]$
f	Fraction	$[-]$
f_d	Darcy friction factor	$[-]$
g	Gravitational acceleration	$\left[\frac{m}{s^2}\right]$
h_c	Convective heat transfer coefficient	$\left[\frac{W}{m^2 \cdot K}\right]$
h_{fg}	Specific enthalpy of evaporation	$\left[\frac{J}{kg}\right]$
k	Thermal conductivity	$\left[\frac{W}{m \cdot K}\right]$
L	Length	$[m]$
m	Mass	$[kg]$
\dot{m}	Mass flow rate	$\left[\frac{kg}{s}\right]$
p	Pressure	$[Pa]$
Q	Heat flow	$[W]$
q	Heat flux	$\left[\frac{W}{m^2}\right]$
R	Thermal resistance	$\left[\frac{K}{W}\right]$
R	Electrical resistance	$[\Omega]$
r	Radius	$[m]$
T	Temperature	$[K]$
t	Time	$[s]$

U	Voltage	[V]
V	Volume	[m ³]
v	Velocity	$\left[\frac{m}{s}\right]$
\bar{v}	Average velocity	$\left[\frac{m}{s}\right]$

Greek symbols

β	Thermal expansion coefficient	$\left[\frac{1}{K}\right]$
ε	Emissivity coefficient	[-]
ρ	Density	$\left[\frac{kg}{m^3}\right]$
σ	Stefan-Boltzmann constant	$\left[\frac{W}{m^2 \cdot K^4}\right]$
ν	Kinematic viscosity	$\left[\frac{m^2}{s}\right]$
μ	Dynamic viscosity	[Pa · s]
ω	Rotational speed	[RPM]

Dimensionless numbers

Gr _d	Grashof number	$\frac{g \cdot \beta \cdot \Delta T \cdot d^3}{\nu^2}$
Nu _d	Nusselt number	$\frac{h_c \cdot d}{k}$
Re _d	Reynolds number	$\frac{\rho \cdot v \cdot d}{\mu}$
Re _{ω}	Reynolds number	$\frac{\omega \cdot d^2}{\nu}$
Pr	Prandtl number	$\frac{c_p \cdot \mu}{k}$

Abbreviations

a	Adiabatic section
axial	Axial direction of the heat pipe
air	Air
b	Bearing
c	Condenser section
cond	Condensation
conv	Convection

d	Diameter
e	Evaporator section
eps	ϵ
evap	Evaporation
h	Heat pipe
i	Heat pipe inner shell
in	In-flowing
inf	∞
ins	Insulation
l	Liquid
La	Liquid in the adiabatic section
Lc	Liquid in the condenser section
Le	Liquid in the evaporator section
o	Heat pipe outer shell
out	Out-flowing
p	Pressure
r	Reflector
rad	Radiation
s	Surface
ssa	Stainless steel at the adiabatic section
ssc	Stainless steel at the condenser section
sse	Stainless steel at the evaporator section
v	Vapour
W	Heat pipe wall
Wa	Heat pipe wall at the adiabatic section
Wc	Heat pipe wall at the condenser section
We	Heat pipe wall at the evaporator section
∞	Ambient

Appendix A

Required heat input

Constants

```
clear all
close all

Ts = 298:25:773;           %Temperature range heat pipe surface [K]
Tins = 298:1:773;         %Temperature range inside insulation [K]
Tinf = 293;                %Ambient temperature [K]

Tr = 1039;                 %Temperature reflector [K]

do = 0.060;                %outer diameter hp [m]
L = 166e-3;                %Length adiabatic zone or evaporator zone[m]
A = pi*do*L;               %area adiabatic zone [m^2]

omega = 1000;              %rpm
v = omega*2*pi/60*do/2;    %tangential speed heat pipe surface [m/s]

sigma = 5.670367*10^-8;    %Stefan Boltzmann constant [W*m^-2*K^-4]
eps = 0.62;                %emissivity coefficient (M.F. Modest - Radiative heat transfer)

do_ins = 250e-3;           %outer diameter insulation [m]
di_ins = 150e-3;           %inner diameter insulation [m]
k = 0.11;                  %conductivity insulation adiabatic zone and evaporator zone
                             [W/(mK)]
```

Iteration for temperature Tins

```
for j=1:length(Ts)

    for i=1:length(Tins)

        Tfilm = (Ts(j)+Tins(i))/2;

        lambda = refpropm('L','T',Tfilm,'P',101.325,'air.mix');
        rho = refpropm('D','T',Tfilm,'P',101.325,'air.mix');
        mu = refpropm('V','T',Tfilm,'P',101.325,'air.mix');

        Re_d(j) = rho*v*do/mu;

        Nu_d = 0.10*Re_d(j)^(2/3);
        hconv = Nu_d*lambda/do;

        Qzero(i) = eps*sigma*A*(Ts(j)^4-Tins(i)^4)+ hconv*A*(Ts(j)-Tins(i))-2*pi*k*L*(Tins(i)-Tinf)/log(do_ins/di_ins);
    end

[M,n] = min(abs(Qzero));
```

```

Qevap(j) = 2*pi*k*L*(Tr-Tinf)/log(do_ins/di_ins);

Qload(j) = 900;
Qlossrad(j) = eps*sigma*A*(Ts(j)^4-Tins(n)^4);
Qlossconv(j) = hconv*A*(Ts(j)-Tins(n));
Qloss1(j) = Qlossrad(j) + Qlossconv(j);
Qloss2(j) = 2*pi*k*L*(Tins(n)-Tinf)/log(do_ins/di_ins);
Qtotall(j) = Qlossrad(j) + Qlossconv(j) + Qload(j) + Qevap(j);

T(j) = Tins(n);
Re(j) =
refpropm('D','T',(T(j)+Ts(j))/2,'P',101.325,'air.mix')*v*do/refpropm('V','T',(T(j)+Ts(j))/2,'P',101.325,'air.mix');
Re_c(j) = 0.93*sqrt((9.81*refpropm('B','T',(T(j)+Ts(j))/2,'P',101.325,'air.mix')*(Ts(j)-T(j))*do^3/(refpropm('$','T',(T(j)+Ts(j))/2,'P',101.325,'air.mix')/10000)^2)/refpropm('^','T',(T(j)+Ts(j))/2,'P',101.325,'air.mix'));
end

```

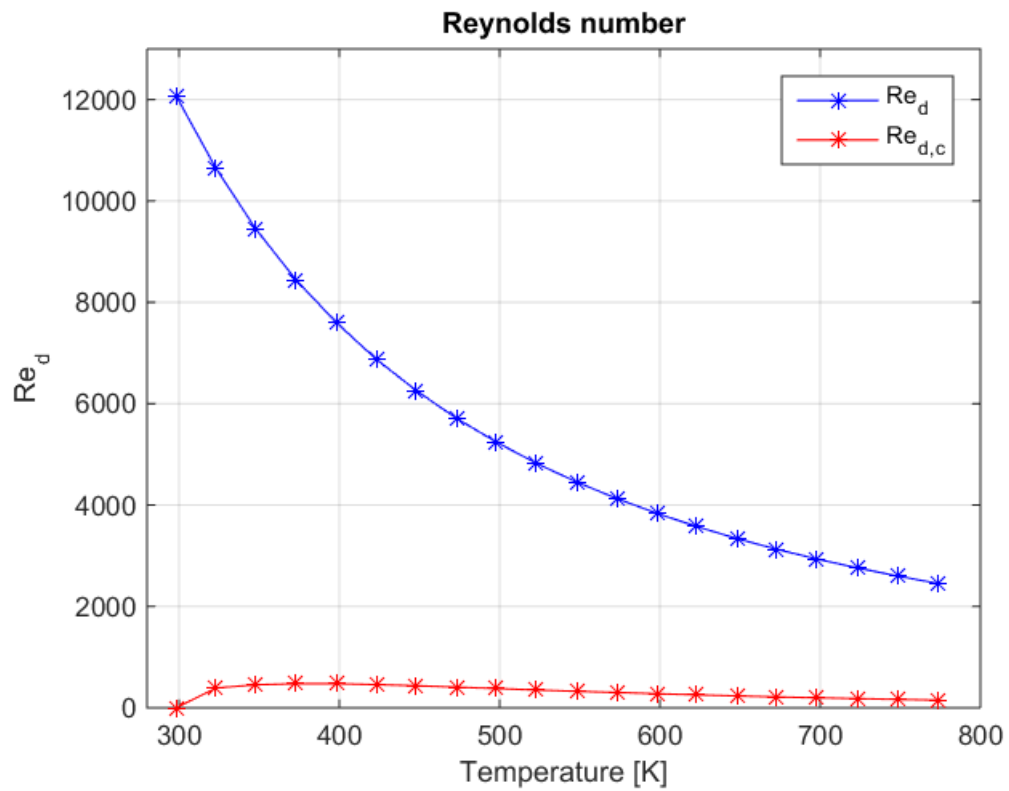
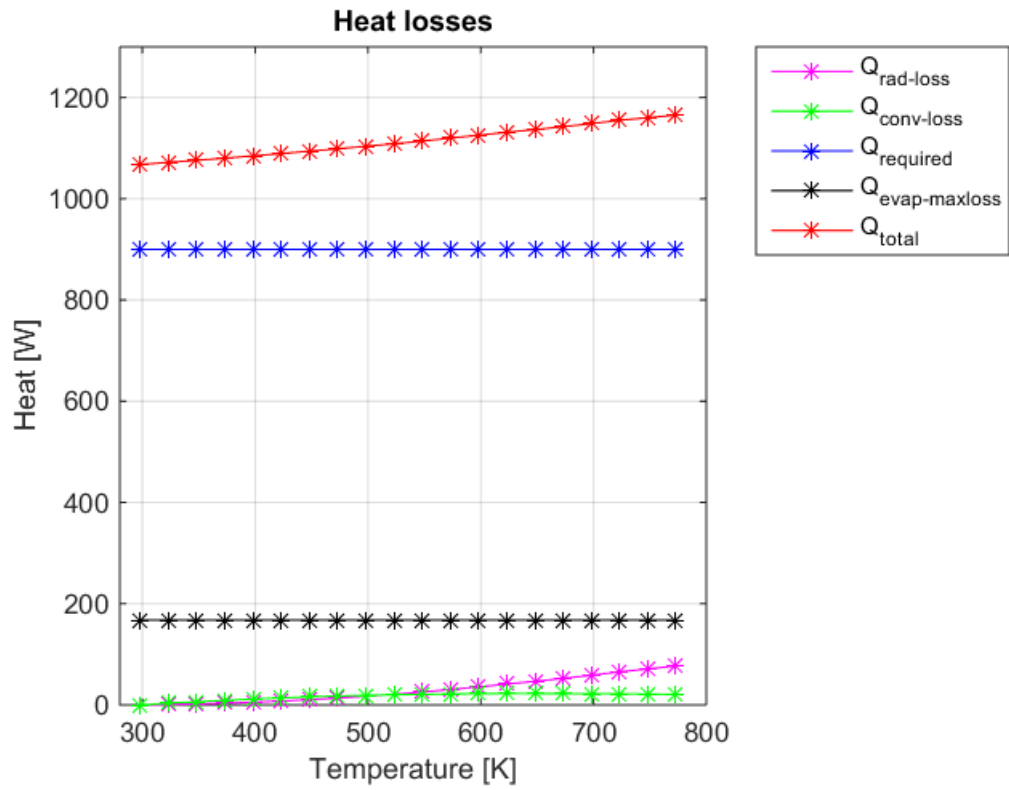
Figures

```

figure
plot(Ts,Qlossrad,'m*-')
hold on
plot(Ts,Qlossconv,'g*-')
plot(Ts,Qload,'b*-')
plot(Ts,Qevap,'k*-')
plot(Ts,Qtotall,'r*-')
grid on
axis([280 800 0 1300])
xlabel('Temperature [K]')
ylabel('Heat [W]')
title('Heat losses')
legend('Q_r_a_d_-_l_o_s_s','Q_c_o_n_v_-_l_o_s_s','Q_r_e_q_u_i_r_e_d','Q_e_v_a_p_-_m_a_x_l_o_s_s','Q_t_o_t_a_l','Location','northeastoutside')

figure
plot(Ts,Re,'b*-')
hold on
plot(Ts,Re_c,'r*-')
grid on
xlabel('Temperature [K]')
ylabel('Re_d')
legend('Re_d','Re_d,_c')
axis([280 800 0 13000])
title('Reynolds number')

```

Appendix B

Radiation calculation

constants

```
rbulb = 0.005;           %radius bulb [m]
rheatpipe = 0.030;      %radius heat pipe [m]
rreflector = 0.073;     %radius reflector [m]
safetymargin = 0.011;   %safety margin between heatpipe and bulb (10mm and 1mm wall
thickness of bulb);
L = 0.167;              %length of tubes [m]
Lbulb = 0.167;         %length of bulbs [m]
sigma = 5.670367*10^-8; %Stefan Boltzmann constant [W*m^2*K^4]
T1 = 1173;             %Temperature outer shell [K]
T2 = 723;              %Temperature inner shell [K]
eps1 = 0.9;            %Emmissivity bulb [-]
eps2 = 0.9;            %Emmissivity heatpipe [-]

nbulb = [5 6 7];       %number of bulbs used [-]
```

view factor calculations

```
for i=1:length(nbulb)

    anglebulb_origin = 360/nbulb(i);           % angle between bulb relative to
origin [deg]
    dbulb_origin = rheatpipe+safetymargin+rbulb; %distance between bulbs and origin
[m]
    dbulb_bulb = 2*dbulb_origin*sin(anglebulb_origin*pi/(2*180)); %distance between two
bulbs [m]

    anglebulb_bulb = 2*asin(rbulb/dbulb_bulb)*180/pi; %angle of view factor bulb to
other bulb [deg]
    Fbulb_bulb = anglebulb_bulb/360;           %view factor bulb to other bulb

    anglebulb_heatpipe = 2*asin(rheatpipe/dbulb_origin)*180/pi; %angle of view factor bulb to
heatpipe [deg]
    Fbulb_heatpipe = anglebulb_heatpipe/360;   %view factor bulb to heatpipe

    Fbulb_reflector = 1-Fbulb_heatpipe-2*Fbulb_bulb; %view factor bulb to reflector

    angleheatpipe_bulb = 2*asin(rbulb/dbulb_origin)*180/pi; %angle of view factor heatpipe
to bulb [deg]
    Fheatpipe_bulb = angleheatpipe_bulb/360;  %view factor heatpipe to bulb

    Fheatpipe_reflector = 1- nbulb(i)*Fheatpipe_bulb; %view factor heatpipe to
reflector

    Abulb = 2*pi*rbulb*Lbulb;                 %Area of bulb [m^2]
    Aheatpipe = 2*pi*rheatpipe*L;             %Area of heat pipe [m^2]
    Areflector = 2*pi*(rreflector)*L;        %Area of reflector [m^2]

    Freflector_bulb = Abulb/Areflector*Fbulb_reflector;
    Freflector_heatpipe = Aheatpipe/Areflector*Fheatpipe_reflector; %view factor reflector to
```

heatpipe by using reciprocity

```
Freflector_reflector = 1-Freflector_heatpipe-6*Freflector_bulb;
```

```
%Heat input into surface A2:
```

```
Qdirect = sigma*(T1^4-T2^4)/((1-eps1)/(eps1*Abulb)+1/(nbulb(i)*Abulb*Fbulb_heatpipe)+(1-eps2)/(eps2*Aheatpipe)); %[W]
```

```
Qreflected = sigma*(T1^4-T2^4)/((1-eps1)/(eps1*Abulb)+1/(nbulb(i)*Abulb*Fbulb_reflector*Freflector_heatpipe)+(1-eps2)/(eps2*Aheatpipe)); %[W]
```

```
Q2reflected = sigma*(T1^4-T2^4)/((1-eps1)/(eps1*Abulb)+1/(nbulb(i)*Abulb*Fbulb_reflector*Freflector_reflector*Freflector_heatpipe)+(1-eps2)/(eps2*Aheatpipe)); %[W]
```

```
Qttotal(i) = Qdirect+Qreflected +Q2reflected; %Total heat from bulb to heatpipe is the sum of direct and reflected heat
```

```
end
```

```
disp(['Qttotal with 5 bulbs = ' num2str(Qttotal(1), '%.1f') ' W'])
```

```
disp(['Qttotal with 6 bulbs = ' num2str(Qttotal(2), '%.1f') ' W'])
```

```
disp(['Qttotal with 7 bulbs = ' num2str(Qttotal(3), '%.1f') ' W'])
```

Qttotal with 5 bulbs = 1183.7 w

Qttotal with 6 bulbs = 1357.6 w

Qttotal with 7 bulbs = 1514.6 w

Appendix C

Filling amount Dowtherm A

Constants

```
T = [293 423 473 523 573 623];           %Temperature range [K]
rho_l = [1059.6 952.2 907.1 859.0 806.8 748.6]; %Liquid density [kg/m^3]
rho_v = [0.00022 0.2165 1.031 3.446 9.071 20.43]; %Vapour density [kg/m^3]
mu = [4.290 0.580 0.390 0.280 0.210 0.160]; %Dynamic viscosity [mPa s]

L = 0.5; %Length heatpipe[m]
di = 0.044; %Inner diameter heatpipe[m]
Volume = L*pi/4*di^2; %Volume heatpipe [m^3]
rpm = [150 400 700 1000]; %Rotational speed heat pipe [rpm]
m = [10 15 20 25 30 35 40 45 50]; %Filling ammount [g]
```

Iteration of m_l

```
for i = 1:length(m)
    for j = 1:length(T)

        Volume_v(j,i) = Volume - m(i)/rho_l(j)/1000;
        m_v(j,i) = Volume_v(j,i)*rho_v(j)*1000;
        m_l(j,i) = m(i) - m_v(j,i);

    end
end

for n = 1:3
    for i = 1:length(m)
        for j = 1:length(T)

            volume_v(j,i) = volume - m_l(j,i)/rho_l(j)/1000;
            m_v(j,i) = volume_v(j,i)*rho_v(j)*1000;
            m_l(j,i) = m(i) - m_v(j,i);

        end
    end
end
```

Calculating all fill ratios

```
for i = 1:length(m)
    for j = 1:length(T)

        delta_l(j,i) = m_l(j,i)/(rho_l(j)*1000)/(pi*di*L)*1000; %Layer thickness annular
        flow [mm]
        fillratio(j,i) = m_l(j,i)/(rho_l(j)*1000)/Volume*100;
        fillpersqrtvis(j,i) = fillratio(j,i)/sqrt(mu(j));

    end
end
```

Plotting figures

```
% figure          %293K
% hold on
% for i=1:9
%     plot([fillpersqrtvis(1,i) fillpersqrtvis(1,i) fillpersqrtvis(1,i)
fillpersqrtvis(1,i)],rpm, '*')
% end
% plot([0.402 0.917 5 10 15],[73.02 281.8 615.7 1025 1433], 'k-')
% xlabel('Fill percentage per sqrt(viscosity) [cP-1/√2]')
% ylabel('Rotational speed [rpm]')
% title('Flow pattern 293 K')
% legend('10 g', '15 g', '20 g', '25 g', '30 g', '35 g', '40 g', '45 g', '50
g', 'Correlation', 'Location', 'southeast')
```

```
figure          %423K
subplot(3,1,1)
hold on
for i=1:9
    plot([fillpersqrtvis(2,i) fillpersqrtvis(2,i) fillpersqrtvis(2,i)
fillpersqrtvis(2,i)],rpm, '*')
end
plot([0.402 0.917 5 10 15],[73.02 281.8 615.7 1025 1433], 'k-')
xlabel('Fill percentage per sqrt(viscosity) [cP-1/√2]')
ylabel('Rotational speed [rpm]')
title('Flow pattern 423 K')
legend('10 g', '15 g', '20 g', '25 g', '30 g', '35 g', '40 g', '45 g', '50
g', 'Correlation', 'Location', 'southeastoutside')
grid on
axis([0 15 0 1200])
```

```
% figure          %473K
% hold on

% for i=1:9
%     plot([fillpersqrtvis(3,i) fillpersqrtvis(3,i) fillpersqrtvis(3,i)
fillpersqrtvis(3,i)],rpm, '*')
% end
% plot([0.402 0.917 5 10 15],[73.02 281.8 615.7 1025 1433], 'k-')
% xlabel('Fill percentage per sqrt(viscosity) [cP-1/√2]')
% ylabel('Rotational speed [rpm]')
% title('Flow pattern 473 K')
% legend('10 g', '15 g', '20 g', '25 g', '30 g', '35 g', '40 g', '45 g', '50
g', 'Correlation', 'Location', 'southeast')
```

```
% figure          %523K
% hold on
subplot(3,1,2)
hold on
for i=1:9
    plot([fillpersqrtvis(4,i) fillpersqrtvis(4,i) fillpersqrtvis(4,i)
fillpersqrtvis(4,i)],rpm, '*')
end
plot([0.402 0.917 5 10 15],[73.02 281.8 615.7 1025 1433], 'k-')
xlabel('Fill percentage per sqrt(viscosity) [cP-1/√2]')
ylabel('Rotational speed [rpm]')
title('Flow pattern 523 K')
```

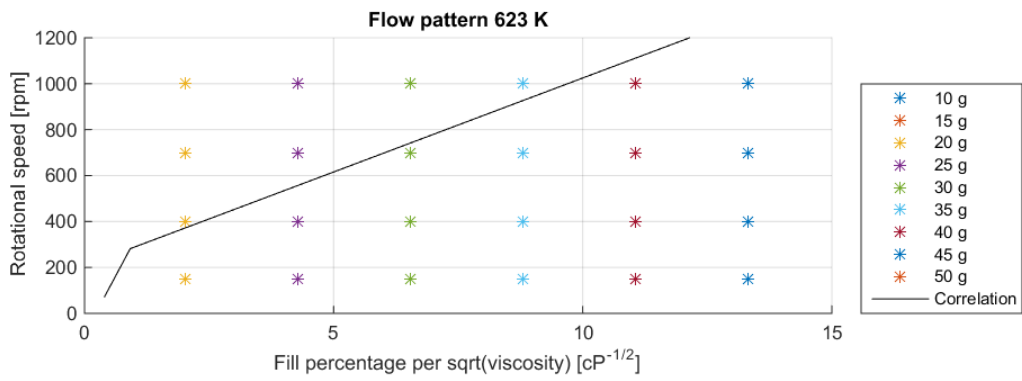
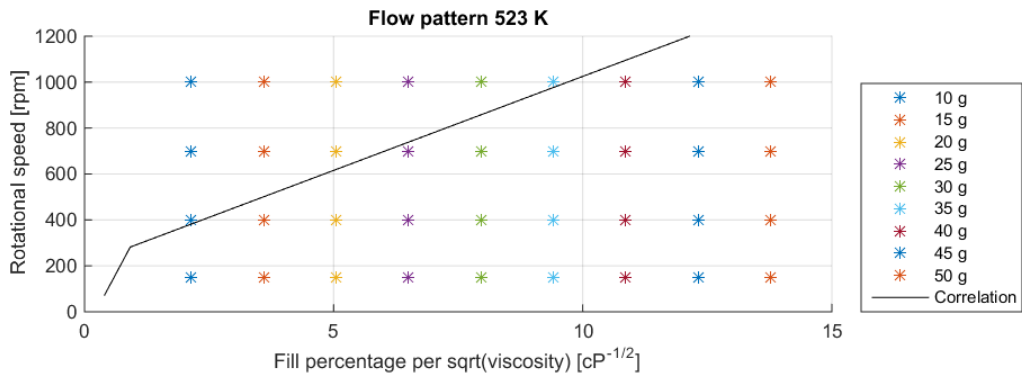
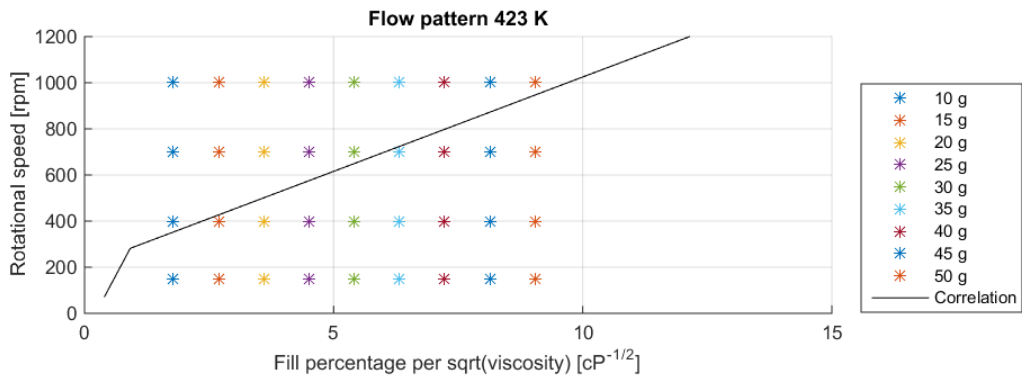
```

legend('10 g','15 g','20 g','25 g','30 g','35 g','40 g','45 g','50
g','Correlation','Location','southeastoutside')
grid on
axis([0 15 0 1200])

% figure          %573K
% hold on
% for i=1:9
%   plot([fillpersqrtvis(5,i) fillpersqrtvis(5,i) fillpersqrtvis(5,i)
fillpersqrtvis(5,i)],rpm, '*')
% end
% plot([0.402 0.917 5 10 15],[73.02 281.8 615.7 1025 1433],'k-')
% xlabel('Fill percentage per sqrt(viscosity) [cP-1/1/2']')
% ylabel('Rotational speed [rpm]')
% title('Flow pattern 523 K')
% legend('10 g','15 g','20 g','25 g','30 g','35 g','40 g','45 g','50
g','Correlation','Location','southeast')

% figure          %623K
% hold on
subplot(3,1,3)
hold on
for i=1:9
    plot([fillpersqrtvis(6,i) fillpersqrtvis(6,i) fillpersqrtvis(6,i)
fillpersqrtvis(6,i)],rpm, '*')
end
plot([0.402 0.917 5 10 15],[73.02 281.8 615.7 1025 1433],'k-')
xlabel('Fill percentage per sqrt(viscosity) [cP-1/1/2']')
ylabel('Rotational speed [rpm]')
title('Flow pattern 623 K')
legend('10 g','15 g','20 g','25 g','30 g','35 g','40 g','45 g','50
g','Correlation','Location','southeastoutside')
grid on
axis([0 15 0 1200])

```

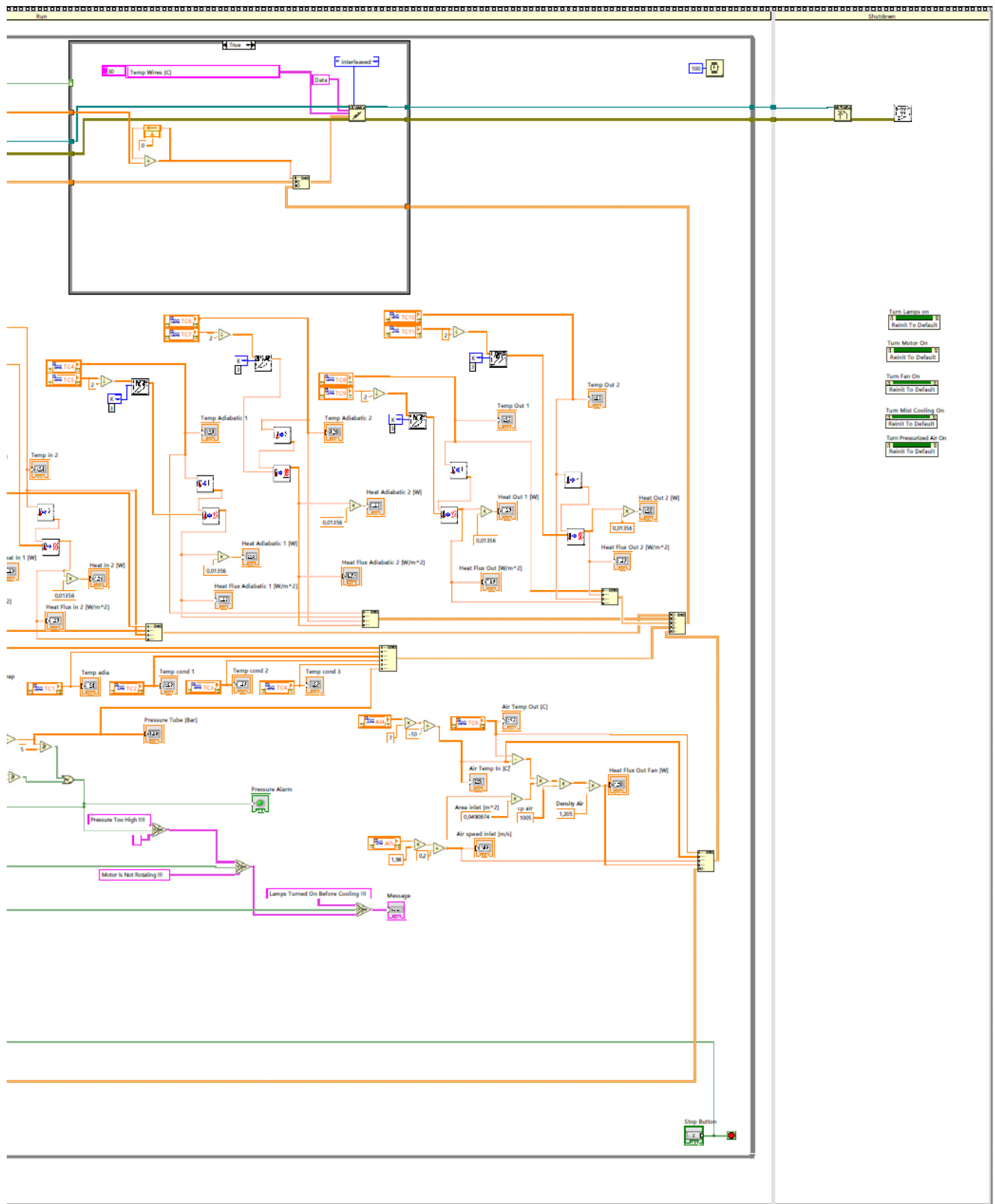


Appendix D

LabVIEW program

The LabVIEW program interface is organized into several functional sections:

- Control and Status:** Includes a 'Stop' button with a red indicator, and four green indicator lights for 'Emergency Stop', 'Closed Doors', 'Closed Oven', and 'Temperature Alarm'.
- Message and Pressure:** A 'Message' text box and a 'Pressure Tube [Bar]' numeric display (0) with a 'Pressure Alarm' indicator light.
- Actuator Controls:** Features 'Turn Motor On', 'Turn Fan On', and 'Turn Lamps on' buttons, each with a corresponding indicator light. Below these are 'Setpoint Rotational Speed Motor' (150) and 'Setpoint Rotational Speed Fan' (150) numeric displays, and 'Motor' (0) and 'Lamp' (0) numeric displays.
- Temperature and Heat Flux Data:** A grid of numeric displays for 'Heat Flux in 1 [W/m^2]', 'Heat Flux in 2 [W/m^2]', 'Heat Flux in 1 [W/m^2]', 'Heat Flux in 2 [W/m^2]', 'Heat Flux Adiabatic 1 [W/m^2]', 'Heat Flux Adiabatic 2 [W/m^2]', 'Heat Flux Out 1 [W/m^2]', 'Heat Flux Out 2 [W/m^2]', 'Heat Out 1 [W]', 'Heat Out 2 [W]', 'Temp in 1', 'Temp in 2', 'Temp Adiabatic 1', 'Temp Adiabatic 2', 'Temp Out 1', 'Temp Out 2', 'Air Temp In [C]', 'Air Temp Out [C]', 'Air speed inlet [m/s]', and 'Heat Flux Out Fan [W]'. All displays show a value of 0.
- Temperature and Mass Data:** A central box contains 'Temp evap', 'Temp adia', 'Temp cond 1', 'Temp cond 2', and 'Temp cond 3' displays, all showing 0. To the right are 'Temp Wires [C]', 'Temp Cabinet [C]', 'Temp Oven [C]', 'Mass Dowertherm A [g]' (20), and 'Annular flow' displays.
- Additional Controls:** 'Turn Pressurized Air On' and 'Turn Mist Cooling On' buttons with indicator lights.
- Utility:** A 'Datafile create or replace' button.



Appendix E

Head calculation

Variables

```
i = 5; %Temperature and corresponding fluid properties (1 = 150C,
2 = 200C, 3 = 250C, 4 = 300C, 5 = 350C)
Q = 500; %Heat input [W]
rpm = 1000; %Rotational speed heat pipe [rpm]
```

Constants

```
T = [423 473 523 573 623]; %Temperature range [K]
rho_l = [952.2 907.1 859.0 806.8 748.6]; %Liquid density [kg/m^3]
rho_v = [0.2165 1.031 3.446 9.071 20.43]; %Vapour density [kg/m^3]
mu = [0.580 0.390 0.280 0.210 0.160]/1000; %Dynamic viscosity [Pa s]
h_fg = [343.6 322.4 299.8 274.2 244.0]*1000; %Latent heat [J/kg]

L = 0.5; %Length heatpipe[m]
di = 0.044; %Inner diameter heatpipe[m]
Volume = L*pi/4*di^2; %Volume heatpipe[m^3]
m = 35; %Filling ammount [g]

d_l = [0.535971327 0.553342244 0.554583905 0.515769202 0.390283734]/1000; %layer thickness
annular flow [m]
```

Calculation

```
m_flow = Q/h_fg(i); %Flow of evaporation [kg/s]
A_l = pi/4*(di^2-(di-2*d_l(i))^2); %Crosssectional area liquid layer [m^2]
U_l = m_flow/(rho_l(i)*A_l); %Average speed in liquid layer [m/s]
dh = 4*A_l/(pi*di); %Hydraulic diameter [m]
rot_acc = (rpm*2*pi/60)^2*(di/2); %Rotational acceleration [m/s^2]
L_eff = 2/3*L; %Effective length liquid channel [m]

head = (32*mu(i)*U_l)/(dh^2)/(rho_l(i)*rot_acc/L_eff)*1000; %[mm]

Re = rho_l(i)*U_l*dh/mu(i);

d_evap = d_l(i)*1000-head/2; %[mm]
d_adia = d_l(i)*1000; %[mm]
d_cond = d_l(i)*1000+head/2; %[mm]

reducedm = d_evap/d_adia;

disp(['head = ' num2str(head) ' mm'])
disp(['reducedm = ' num2str(reducedm)])
```

```
head = 0.20207 mm
reducedm = 0.74113
```

Appendix F

Network model

Variables

```
omega = 150;           %rot speed (150-1000) [RPM]
fan = 3000;           %fan capacity (750-3000) [m^3/h]
lamppower = 0.8;     %lamp power variable [0-1] (1 is full power)
mistgain = 1;       %gain in cooling by using mist cooling
```

Constants

```
m = 35e-3;           %Mass liquid [kg]

reducedm = 0.8;     %reduced mass in evaporator section, added to condenser zone

do = 60e-3;         %outer diameter [m]
di = 44e-3;         %inner diameter [m]
dm = (di+do)/2;    %middle diameter [m]
ro = do/2;         %outer radius [m]
ri = di/2;         %inner radius [m]
rm = (ri+ro)/2;    %middle radius [m]

Le = 166e-3;       %evaporator section length [m]
La = 166e-3;       %adiabatic section length [m]
Lc = 166e-3;       %condenser section length [m]

vtube = pi/4*di^2*(Le+La+Lc); %Volume tube [m^3]

%http://www-ferp.ucsd.edu/LIB/PROPS/PANOS/ss.html is used for conductivity and heat capacity
of stainless steel depending of temperature

%k_sse = 18;       %conductivity stainless steel evaporator [W/(mK)] *values from mills at
600K
rho_sse = 8238;    %density stainless steel evaporator [kg/m^3]
%cp_sse = 550;     %specific heat capacity stainless steel evaporator [J/(kgK)]

%k_ssa = 18;       %conductivity stainless steel adiabatic [W/(mK)]
rho_ssa = 8238;    %density stainless steel adiabatic [kg/m^3]
%cp_ssa = 550;     %specific heat capacity stainless steel adiabatic [J/(kgK)]

%k_ssc = 18;       %conductivity stainless steel condenser [W/(mK)]
rho_ssc = 8238;    %density stainless steel condenser [kg/m^3]
%cp_ssc = 550;     %specific heat capacity stainless steel condenser [J/(kgK)]

evapgain = 1;      %increased conductivity of dowtherm when evaporation takes place
condgain = 1;      %increased conductivity of dowtherm when condensation takes place

A_axial = pi/4*(do^2-di^2); %area in axial direction [m^2]
```

Convective cooling

```
A_fan = 0.0225;           %Area fan duct [m^2]
v_inf = fan/3600/A_fan;   %free stream speed
Pr = 0.69;                %Prantl number air
T_inf = 293;              %Free stream air temp [K]
k_inf = 26.24*10^-3;      %free stream thermal cond [W/mK]
nu_inf = 1.568*10^-5;     %free stream kinematic viscosity [m^2/s]

Re_inf = v_inf*do/nu_inf;
Nu_o =
0.3+(0.62*(Re_inf)^0.5*Pr^(1/3))/((1+(0.4/Pr)^(2/3))^0.25)*(1+(Re_inf/282000)^(5/8))^0.8;
Nu_rot = (1+0.019*Re_inf^0.221)*Nu_o;
h_rot = Nu_rot*k_inf*do;
```

Radiative heat transfer

```
rbulb = 0.005;           %radius bulb [m]
safetymargin = 0.011;    %safety margin between heatpipe and bulb (10mm and 1mm wall thickness
of bulb);
Lbulb = 0.165;           %length of bulbs [m]
sigma = 5.670367*10^-8;  %Stefan Boltzmann constant [W*m^2*K^4]
eps1 = 0.9;              %Emmisivity bulb
eps2 = 0.9;              %Emmisivity heatpipe
nbulb = 6;               %number of bulbs used

% view factor calculations
anglebulb_origin = 360/nbulb;           % angle between bulb relative to
origin [deg]
dbulb_origin = ro+safetymargin+rbulb;    %distance between bulbs and origin
dbulb_bulb = 2*dbulb_origin*sin(anglebulb_origin*pi/(2*180)); %distance between two bulbs

anglebulb_bulb = 2*asin(rbulb/dbulb_bulb)*180/pi; %angle of view factor bulb to other
bulb [deg]
Fbulb_bulb = anglebulb_bulb/360;         %view factor bulb to other bulb

anglebulb_heatpipe = 2*asin(ro/dbulb_origin)*180/pi; %angle of view factor bulb to heatpipe
[deg]
Fbulb_heatpipe = anglebulb_heatpipe/360; %view factor bulb to heatpipe

Fbulb_reflector = 1-Fbulb_heatpipe-2*Fbulb_bulb; %view factor bulb to reflector

angleheatpipe_bulb = 2*asin(rbulb/dbulb_origin)*180/pi; %angle of view factor heatpipe to bulb
[deg]
Fheatpipe_bulb = angleheatpipe_bulb/360; %view factor heatpipe to bulb

Fheatpipe_reflector = 1- nbulb*Fheatpipe_bulb; %view factor heatpipe to reflector

Abulb = 2*pi*rbulb*Lbulb; %Area of bulb
Aheatpipe = 2*pi*ro*Le; %Area of heat pipe
Areflector = 2*pi*(ro+2*rbulb+2*safetymargin)*Le; %Area of reflector

Freflector_heatpipe = Aheatpipe/Areflector*Fheatpipe_reflector; %view factor reflector to
heatpipe by using reciprocity
```

